University of Alberta

Miscibility Studies of Engineering Thermoplastic Polymer Blends

By

Mingzong Zhang 

A thesis submitted to the Faculty of Graduate Studies and Research in partial fulfillment

of the requirements for the degree of Doctor of Philosophy

in

Chemical Engineering

Department of Chemical and Materials Engineering

Edmonton, Alberta
Spring, 2005

Abstract

Engineering thermoplastic polymer blends constitute a large part of polymer consumption. To optimize the design of such blends, a great deal of attention has been focused on predicting and characterizing the miscibility of these blends. In this thesis, both experimental and molecular dynamics (MD) simulation methods have been used to address miscibility of three kinds of engineering thermoplastic polymer blends. In particular, the heats of mixing and Flory-Huggins interaction parameters of poly(etherimide) (PEI)/polycarbonate (PC), PEI/ Poly(butylene terephthalate) (PBT) and PC/PBT blends at different compositions were calculated from MD simulation. For the PEI/PC blend, both differential scanning calorimetry (DSC) and MD simulation showed that they are immiscible. However, the degree of compatibility of a 80:20 PEI/PC blend is higher than that of a PC rich blend. This anomalous thermodynamic behavior was found to be due mainly to intermolecular interactions. Transmission electron microscopy (TEM) results confirmed this observation.

The inherent miscibility of PEI/PBT blends was also successfully predicted from MD simulation. At concentrations used in the simulations, the heats of mixing were found to be negative. The miscibility between PEI and PBT is attributed to favorable van der Waals interaction. The morphology of as-quenched PEI/PBT blend samples and annealed samples was also investigated. MD simulation was also applied to PC/PBT blends to study their inherent miscibility in the melt state, and the results indicate that PC/PBT blends are completely immiscible in the absence of transesterification reactions.

The quantitative disagreement between the MD simulated and experimentally determined interaction parameters was also addressed.

A new approach to predict glass transition temperatures (T_g) of polymers was developed. In particular, the intensities of peaks of the radial distribution function (RDF) at different temperatures obtained from MD simulation were employed to predict the T_g. Compared with traditionally used specific volume-temperature method, the accuracy of the prediction was significantly improved. This is because within the capacity of current computational power, it is impossible for the bulk specific volume to reach equilibrium below T_g; however, the local specific volume at a shorter length scale related to the intensity of peaks of the RDF can reach equilibrium.

Acknowledgements

I would like to take this opportunity to express my special gratitude to my supervisors Dr. Phillip Choi and Dr. Uttandaraman Sundararaj for their unfailing encouragement, and constructive, patient and invaluable guidance both during my research work and in my daily life.

I would like to thank the polymer group members for the help with various equipment and for helpful discussions.

My sincere thanks also go to Dr. Ming Chen from the Surgical Medical Research Institute at the University of Alberta for teaching me how to perform the TEM experiments and Mr. Bob Barton from Chemical and Materials Engineering Department for his computer support.

The financial support provided by Natural Science and Engineering Research Council of Canada (NSERC) is greatly acknowledged.

Thanks also go to my parents; their love and encouragement always surround me even though we are far apart.

Last, but certainly not least, I would like to thank my wife, Yan Yu, who showed her great patience, understanding and love during the course of this thesis work.

TABLE OF CONTENTS

LIST OF TABLES

LIST OF FIGURES

Nomenclature

e_h Energy density originates from specific interactions

D_0 Van der Waals energy well depth

E_b Total bond stretching energy kcal/mol

E_θ Total bond bending energy kcal/mol

E_ϕ Total bond torsional energy kcal/mol

E_ψ Total inversion energy kcal/mol

E_{vdw} Total interaction energy for van der Waals

E_Q Total interaction energy for electrostatics

$\tilde{g}$ Reduced radial distribution function

ΔG Gibbs free energy change upon mixing

$\Delta \overline{G}_m$ Gibbs free energy change upon mixing per lattice site

ΔH Enthalpy change upon mixing

ΔH_f Latent heat of fusion per repeating unit

$\Delta \overline{H}_m$ Enthalpy change upon mixing per lattice site

k_B Boltzamann constant, 1.38065×10^{-23} J/K

l Bond length

l_0 Equilibrium bond length

n Total number of lattice sites

N_i Degree of polymerization of component i

R Gas constant

R_0 Van der Waals bond length

S(0) Scattering function at zero wavevector

ΔS Entropy change upon mixng

$\Delta \bar{S}_m$ Entropy change upon mixing per lattice site

T Absolute temperature, K

V_s Reference molar volume

Greek Symbols

α Thermal expansion coefficient

σ Standard deviation

δ Hilderbrand solubility parameter

ϕ_i Molar volume concentration of component i

Φ Torsional angle

Φ_0 Equilibrium torsional angle

ε Dielectric constant

χ Flory-Huggins interaction parameter

θ Bond angle

θ_0 Equilibrium bond angle

ψ Plane angle

ψ_0 Equilibrium plane angle and defines as zero for a planar molecule

Abbreviations

CUT	Continuous use temperature
DMTA	Dynamic mechanical thermal analysis
DSC	Differential scanning calorimetry
MD	Molecular dynamics
LCT	Lattice cluster theory
LCST	Low critical solution temperature
PA	Polyamides
PAI	Poly (amide imide)
PBT	Poly (butylenes terephalate)
PC	Polycarbonate
PE	Polyethylene
PEEK	Poly (ether ether ketone)
PEI	Poly (ether imide)
PEK	Poly (ether ketone)
PEKK	Poly (ether ketone ketone)
PES	Poly (ether sulphone)
PEST	Thermoplastics polyesters
PI	Polyimide
PMMA	Poly (methyl methacrylate)
POM	Polyoxymethylene
PP	Polypropylene
PPE	Poly (phenylene ether)

PPS	Poly (phenyl sulfide)
PPSS	Poly (phenyl sulfide sulphone)
PS	Polystyrene
PSF	Polysulfone
PVC	Poly (vinyl chloride)
RDF	Radial distribution function
SANS	Small angle neutron scattering
TEM	Transmission electron microscope
T_g	Glass transition temperature
T_m	Melting temperature
T_c	Crystalline temperature
UCST	Upper critical solution temperature

Chapter 1

Introduction

1.1 Introduction to polymer blends

Polymer blends constitute a multibillion-euros business per year [Wilkinson and Ryan 1998]. They constitute ca. 36wt% of the total polymer consumption and their importance continues to increase [Utracki 2002]. We can obtain new materials with enhanced properties from a limited number of palettes at low cost by blending different polymers and yet preserve their individual properties in the final mixture. This method is extremely attractive due to low cost and fast development. For example, most common polymers cannot satisfy high stiffness and resistance to fracture simultaneously because increase in stiffness is usually associated with increased brittleness. However, polymer blends offer such a chance to obtain both properties. The mixture of polystyrene and polybutadiene, i.e., high impact polystyrene, is a well-known example with such properties. The advantages of polymer blending on performance, economy and processing have accelerated R&D activities in the field of polymer blends in both scientific and industrial communities.

According to Utracki [2002], synthetic polymers can be classified as commodity resins, engineering resins and special resins. Commodity resins constitute 71% by volume of all consumed plastics; they include five large-volume commonly used polymers: polyethylene (PE), polypropylene (PP), polystyrene (PS), poly(methyl methacrylate) (PMMA) and poly(vinyl chloride) (PVC). Engineering polymers refer to

those polymers having high performance at continuous use temperature (CUT)>100 ^{0}C and a tensile strength >40MPa.

Polymers such as polyamides (PA), thermoplastics polyesters (PEST), poly (phenylene ether) (PPE), polycarbonate (PC) and poly (oxymethylene) (POM) belong to this category. They constitute 13% by volume and 34% by the dollar value of the total polymers consumption. Special polymers refer to those polymers with glass transition temperature (T_g) > 200 ^{0}C, and modulus > 3GPa. They are produced in a small volume for special applications and usually very expensive. Poly (etherkeones) (PEK, PEEK, and PEKK), polyimides (PI, PEI, and PAI) and sulfur-containing polymers (PPS, PPSS, PES, and PSF) belong to this category. In this study, we focus on engineering and specialty polymer blends.

Most commercial polymer blends are melting compounded through extrusion or injection molding. However, the application of pressure could induce melt-like behavior at temperatures below the glass transition temperature as reported by Gonzalez-Leon *et al.* recently [2003].

1.2 Miscibility of polymer blends

The macroscopic properties of polymer blends are determined by the microstructure of the system, which depends primarily on the miscibility of the components. Miscibility is not only important for polymer blends, but also determines the physical properties for copolymers and interpenetrating networks [Olabisi *et al.* 1979]. Based on their miscibility, polymer blends can be classified as miscible blends, compatible blends and immiscible blends. Most polymer blends are immiscible because of the low contribution of the mixing entropy to the free energy of mixing when

compared to small molecule analogs. Polymer blends that are partially miscible yet offer attractive mechanical properties are classified as compatible polymer blends. Some degree of microheterogeneity is usually desirable to preserve the individual properties of respective polymer components [Hess *et al.* 1993]. In miscible polymer blends, chains of different polymers are mixed at the segmental level. It is well known that in order to form miscible polymer blends, specific interactions between polymer pairs, such as hydrogen bonding, which can result in a negative heat of mixing, or a negative change in volume upon mixing, are generally required. Although miscibility is not a prerequisite for the usefulness of polymer blends, a better understanding of the miscibility and those factors influencing miscibility is essential for the design of new polymer blend systems.

There exist many methods to determine the miscibility of polymer blends. Direct visual observation through a microscope has been used more often than other methods as a preliminary study of the degree of miscibility. Generally speaking, for immiscible and partially miscible polymer blends, opacity will be observed when the size of heterogeneity is larger than 100 nm and the difference of refractive index between the two polymers are greater than 0.01. For miscible polymer blends, homogeneous phase structure is observed and they are transparent. The most widely used method to determine miscibility is by measuring the glass transition temperatures of the blends. The T_g method is relatively simple, but some inherent uncertainties of the measurements need to be examined. First, it can only be used for blends where the T_g difference between the constituent polymers is greater than 10 ^{0}C. Secondly, T_g is insensitive when one of the components is less than 10 wt%. For immiscible polymer blends, generally two distinct glass transition temperatures that are exactly the same as the T_g's of the constituent

components would be observed. In compatible polymer blends, the two T_g's of the pure polymers shift towards each other but do not coincide. For miscible polymer blends, they exhibit a single glass transition between the T_g's of the components with a sharpness of transition similar to that of the pure components [Weber 2002; Olabisi *et al.* 1979; Paul and Bucknall 2000]. Such observation implies miscibility on the order of 20-40 nm [Kuo, 2001].

Whether or not a polymer blend can be regarded as being miscible on the segmental level when a broad single glass transition is observed is still a matter of debate. The glass transition temperature is a macroscopic property. Therefore, it is still not clear how large the domain size of compositional difference is required to yield a single T_g. The glass transition temperature is usually determined from differential scanning calorimetry (DSC); the domain size that DSC can resolve is on the order of 20-30 nm [Wu, 2002]. A very broad single glass transition does not guarantee that the blend is miscible on the segmental level. For example, only one single T_g is observed for PS/PMMA/SMMA blends; however, transmission electron microscope (TEM) shows that the blend exhibits two-phase structures with domain size of 1 μm [Winey *et al.* 1996]. Dynamic mechanical thermal analysis (DMTA) is believed to be more sensitive than DSC in determining the T_g of polymer blends because it can detect segmental relaxation behavior of molecules [Stoeltin *et al.* 1970]. The domain size that DMTA can resolve is on the order of 5-10 nm [Molnar and Eisenber 1992]. Other less common methods for the determination of glass transition temperature include dilatometry and dielectric spectroscopy. Some researchers argue that T_g is not sensitive to the thermodynamic miscibility of the components but rather to the degree of dispersion

[Schultz and Young 1980]. Despite such debates, T_g is still widely used as an important parameter for characterizing miscibility of polymer blends. Other methods which are commonly used to characterize miscibility of polymer blends, such as the Hildebrand solubility parameter approach, melting point depression method, small angle neutron scattering (SANS) method will be discussed in detail in Chapter 2. Molecular dynamics (MD) simulation method will be discussed in Chapter 3.

1.3 Objectives of the thesis

One of the major objectives of this research is to understand the miscibility of engineering thermoplastic polymer blends on a molecular level based on molecular dynamics simulation. It is well known that the chemical structure details and local packing behavior is essential to the understanding of the thermodynamics of polymer blends. The aim is to produce information that can be used as a guide for the relationship between miscibility and chemical structure for polymer blends. The binary polymer blends selected for this work are compatible polycarbonate (PC) /poly(ether imide) (PEI) blends, miscible PEI/PBT blends and immiscible polycarbonate (PC)/poly(butylenes terephalate) (PBT) blends. These polymer blends are commercially and scientifically important. The chemical structures of these polymers are shown in Figure 1.1. In this study, the MD simulation was used to calculate the heats of mixing and the corresponding Flory-Huggins interaction parameters for these binary blends. We attempt to provide molecular explanation for the different levels of miscibility of engineering thermoplastic polymer blends. The glass transition temperature is an important parameter that determines the type of application for which a polymer is suitable, and is related to

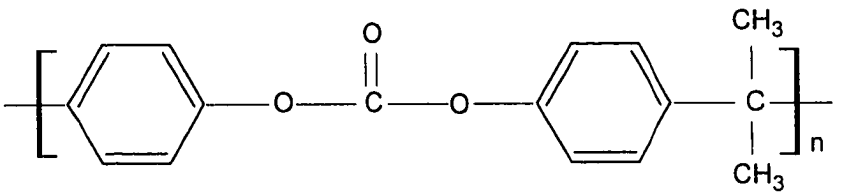

PC

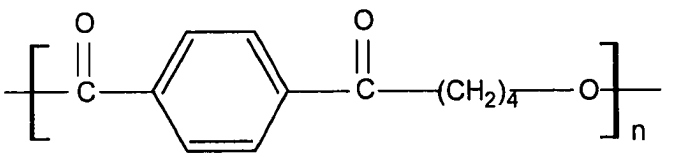

PBT

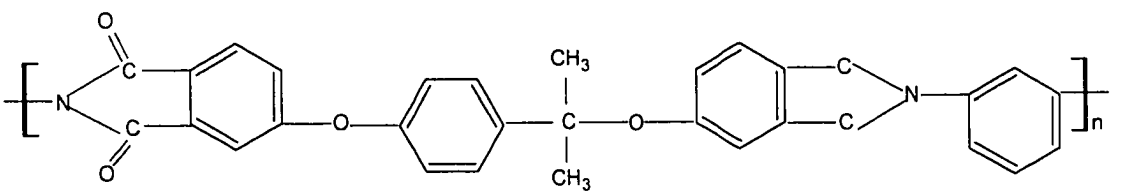

PEI

Figure 1.1 Chemical structures of PC, PBT and PEI repeating units

the miscibility of polymer blends. However, the glass transition is probably the least understood property of polymers. Another objective of this work is to develop a new, more accurate method to predict glass transition temperatures of polymers solely from their chemical structure based on molecular dynamics simulation.

1.4 Structure of the thesis

This thesis consists of eight chapters. In chapter 2, fundamentals of thermodynamics of polymer blends, solubility parameters and Flory-Huggins interaction parameters are reviewed. First, the Flory-Huggins lattice theory of polymer blends will be introduced; then, the advantages and disadvantages of this theory will be discussed; and finally, the lattice cluster theory for polymer blends will be briefly introduced. Different methods to obtain the Flory-Huggins interaction parameter will be presented and compared in this chapter.

In chapter 3, molecular dynamics simulation techniques will be introduced. The force fields used in the simulation and the model construction methods will also be discussed in this chapter. In chapter 4, the MD simulation method as well as the experimental procedure associated with the miscibility study, such as DSC, TEM will be described first. These methods are used to characterize the miscibility of PEI/PC blends in the melt state. Anomalous thermodynamic behavior of this blend was observed by experiments and MD simulation. The reasons why PEI and PC are more miscible at 80% PEI will be discussed. In the subsequent two chapters (chapters 5 and 6), I will apply the methods described in chapter 4 to other engineering thermoplastic blends, namely PEI/PBT (Chapter 5) and PC/PBT (Chapter 6) blends. A completely miscible PEI/PBT

blend is investigated in chapter 5. Why they form a miscible blend on a molecular level will be discussed, and some experimental results of the PEI/PBT blend are also presented in this chapter. In chapter 6, MD simulation results of the PC/PBT blend are presented. The controversy in the literature about whether or not PC/PBT blends are miscible will be examined in the context of transesterification between PC and PBT. Chapter 7 describes a new method based on computed radial distribution functions from MD simulation to predict glass transition temperatures of polymers. All the major findings of this study and recommendations for future work are summarized in chapter 8.

1.5 References

Gonzalez-Leon, J.A.; Acar M.H.; Ryu, S.W.; Ruzette, A.V.G. and Mayes, A.M. (2003) Low-Temperature Processing of 'Baroplastics' by Pressure-induced Flow, *Nature*, 426 (6965): 424-428.

Hess, W. M.; Hred, C.R. and Vegvari P.C. (1993) Characterization of Immiscible Elastomer Blends, *Rubber. Chem. Technol.*, 66(3): 329-375.

Kuo, S.W. and Chang F.C. (2001) Effect of Copolymer Composition and Free Volume Change on the Miscibility of Poly(styrene-co-vinylphenol) with Poly(ε-caprolactone), *Macromolecules*, 34(22):7737-7743.

Molnar, A. and Eisenber, A. (1992) Miscibility of Polyamide-6 with Lithium or Sodium Sulfonated Polystyrene Ionomers, *Macromolecules*, 25(21): 5774-5782.

Olabisi, O.; Robeson, L.M. and Shaw M.T. (1979) *Polymer-Polymer Miscibility*, Academic Press, New York.

Paul D. R. and Bucknall C. B.(2000) *Polymer Blends*, John Wiley & Sons Inc., New York.

Schultz, A. R. and Young, A.L. (1980) DSC on Freeze-Dried Poly(methyl methacrylate)-Polystyrene Blends, *Macromolecules* , 13(3): 663-668.

Stoeltin, J.; Karasz, F.E. and Macknigh,W.J. (1970) Dynamic Mechanical Properties of Poly(2,6-dimethyl-1,4-phenylene ether)-Polystyrene Blends, *Polym. Eng. Sci.*, 10(3): 133.

Ultracki, L. A. (2002) *Polymer Blends Handbook*, Kluwer Academic Publishers, Dordrecht, The Netherlands.

Weber M. (2002) Engineering Polymer Alloys by Reactive Extrusion, *Macromol. Symp.*, 181:189-200.

Wilkinson, A.N. and Ryan, A.J. (1998) *Polymer Processing: Structure Development*, Kluwer Academic Publishers, Dordrecht, The Netherlands.

Winey, K.I.; Berba, M.L. and Galvin, M.E. (1996) Ternary Phase Diagrams of Poly(styrene-co-methyl methacrylate), Poly(methyl methacrylate), and Polystyrene: Monomer Sequence Distribution Effect and Encapsulation, *Macromolecules*, 29(8): 2868-2877.

Chapter 2

Thermodynamics of polymer blends

The thermodynamics of polymer blends is understood in the framework of the Gibbs free energy before and after mixing. The change of the Gibbs free energy upon mixing is given by the following equation:

$$\Delta G_m = \Delta H_m - T\Delta S_m \qquad (2\text{-}1)$$

where ΔH_m and ΔS_m represent the enthalpy and entropy changes upon mixing under constant pressure and temperature condition, respectively. Entropy always favors mixing, while enthalpy of interactions between the two components can either promote or inhibit mixing.

2.1 The Flory-Huggins lattice theory of polymer blends

2.1.1 The entropy change of mixing of polymer blends

In 1940's, a polymer solution theory was independently developed by Paul Flory and Maurice Huggins [Flory 1941; Huggins 1941]. It is probably the most widely used theory for the thermodynamics of polymer blends and concentrated solutions. The basic assumption of this theory is that each polymer chain is composed of series of segments, and each segment occupies one lattice site as shown in Figure 2.1.

Based on statistical thermodynamics, Flory and Huggins developed the expression for the entropy of mixing of binary polymer blends in equation (2-1), for a blend containing polymers A and B,

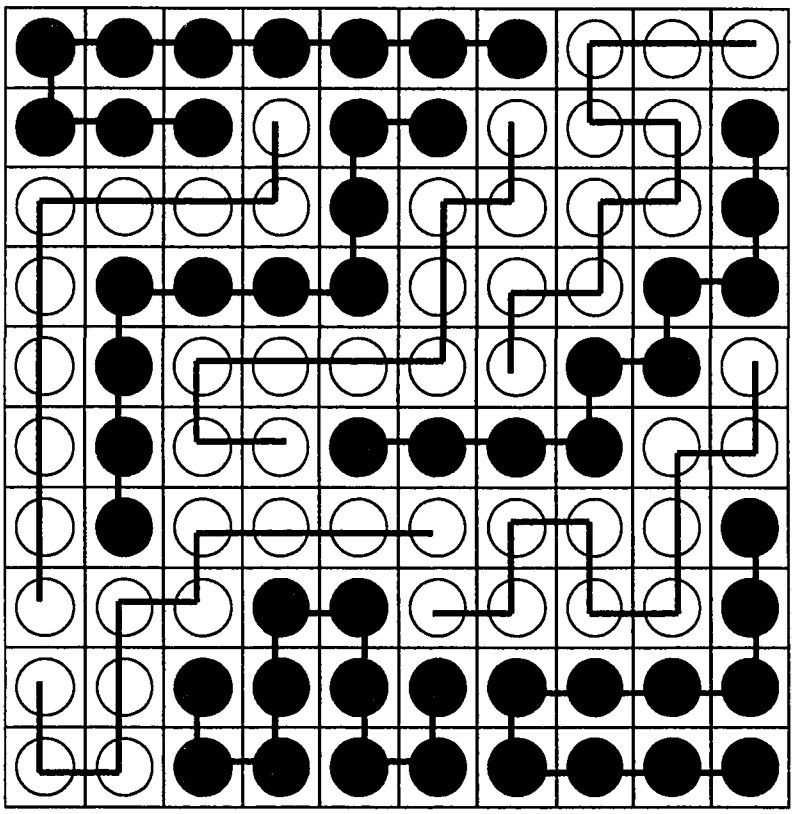

Figure 2.1 Schematic representation of a lattice model of a binary polymer blend with five white 10-ball chains and five black 10-ball chains.

$$\Delta\bar{S}_m = -k\left[\frac{\phi}{N_A}\ln\phi + \frac{1-\phi}{N_B}\ln(1-\phi)\right] \tag{2-2}$$

where $\Delta\bar{S}_m$ is the entropy of mixing per lattice site, i.e., $\frac{\Delta S_m}{n}$, where n is the total number of lattice sites; ϕ is the volume fraction of polymer A, N_A and N_B are essentially the degrees of polymerization or the number of lattice sites occupied by polymers A and B, and k_B is the Boltzmann constant with a value of 1.38065×10^{-23} J/K. This expression for the entropy of mixing is derived based on the assumption that the conformational entropy for a polymer chain in the mixed state is identical to that in its pure state. In other

words, only the translational entropy that is associated with the motion of centers of mass of polymers is included. This assumption is reasonable for non-polar polymer blends because chains in the melt state behave more or less like ideal chains [Flory 1953]. Another assumption is that all the lattice sites are occupied by polymeric segments; therefore, there is no volume change during mixing, which is not always true for polymer blends, even for those composed of non-polar components. For some blends, the compressibility is a crucial ingredient of a meaningful thermodynamic description of polymer blends [Sanchez and Lacombe 1978]. And this leads to the development of equation-of-state theories for describing the thermodynamics of polymer blends.

2.1.2 The enthalpy change of mixing of polymer blends

The energy of binary polymer blends per lattice site is given by equation (2-3) according to the Flory-Huggins lattice (FH) theory:

$$\Delta\overline{H}_m = \chi\phi(1-\phi)kT \qquad (2\text{-}3)$$

where χ is the Flory-Huggins interaction parameter. χ will be discussed in detail later in this chapter. It is defined as,

$$\chi \equiv \frac{z}{2}\frac{(2u_{AB} - u_{AA} - u_{BB})}{kT} \qquad (2\text{-}4)$$

where z is the coordination number of the lattice and u_{AB}, u_{AA} and u_{BB} are the pair-wise interaction energies between adjacent lattice sites occupied by the segments of polymers A and B. In deriving Equation (2-3), the local concentration fluctuation is not included to ensure that the polymer chains are completely randomly distributed. Therefore, Equation (2-3) is based on the mean field assumption that there is no local concentration fluctuation. The differences in chemical structures are also completely ignored; however,

the microstructure is important for determining miscibility. It has been reported that the miscibility of polyolefins are quite dependent on the local architecture [Londono *et al.* 1998]; the predeuterated and protonated polybutadienes are reported to be phase separated [Bates *et al.* 1985].

From equation (2-4), we can see that the FH interaction parameter in the FH theory is purely enthalpic and it decreases with increasing temperature. The miscibility of polymer blends can only be reached at high temperatures. With decreasing temperature, the resulting increase of χ will results in the termination of the miscibility window. The system will then go into a two-phase region, which is called the upper critical solution temperature (UCST) phase behavior; and the concept is shown in Figure 2.2a. However, experiments showed that some polymer blends will become immiscible with increasing temperature, i.e., the system show a lower critical solution temperature (LCST) phase behavior (Figure 2.2b). The experimentally observed LCST phase behavior cannot be predicted from the FH theory. There are two possible mechanisms for the explanation of LCST phase behavior [Strobl 1996]. One is that there is volume shrinkage for some polymer blends, which results in a decrease of the free volume available for the local motion of monomers, hence reducing the entropy. The effect usually increases with increasing temperature and finally overcompensates the initial attractive interaction. The second mechanism is that there is a competition between attractive forces between specific groups incorporated in the two polymers as well as repulsive interactions between the remaining units. The fraction of attractive groups decrease with increasing temperature and finally the repulsive forces dominate, which results in the system separating into two phases at high temperatures.

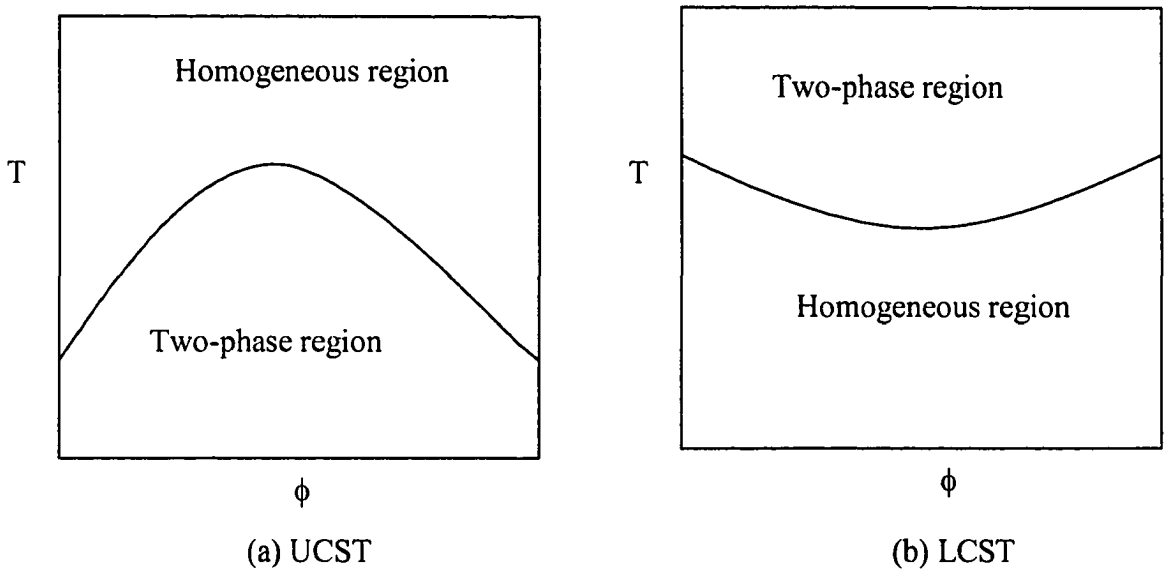

Figure 2.2: The UCST and LCST phase behavior of polymer blends

2.1.3 The Gibbs free energy change of mixing of polymer blends

Combining the expressions of entropy and enthalpy changes of mixing and substituting them into Equation (2-1) gives the Flory-Huggins equation for polymer blends. The Gibbs free energy change of mixing per lattice site is expressed as:

$$\Delta\overline{G}_m = kT\left[\frac{\phi}{N_A}\ln\phi + \frac{1-\phi}{N_B}\ln(1-\phi) + \chi\phi(1-\phi)\right] \qquad (2\text{-}5)$$

In this equation, the first two terms originate from the combinatorial entropy contribution, which always promote mixing. For polymer blends, the entropy change of mixing is usually negligible because it scales with N^{-1}, and the degree of polymerization is usually quite large. The last term comes from the enthalpic contribution, it can either promote or oppose mixing depending on the sign of the Flory-Huggins interaction parameter χ. For a negative χ, there is an net attractive interaction between the two polymers, i.e., they like

each other more than themselves. And such polymer blends tend to form a mixed single-phase structure. For most polymer blends, χ is positive, there is net repulsion between the two polymers, i.e., they like themselves more than each other.

Once the expression for the Gibbs free energy change upon mixing is obtained, the phase behavior of polymer blends can be determined. In general, the thermodynamic criteria for the miscibility of polymer blends are a negative Gibbs free energy change of mixing, which is a general requirement for any spontaneous process; and a positive second derivative of ΔG_m with respect to the concentration of one of the components, $\frac{\partial^2 \Delta G_m}{\partial \phi^2}$, which ensures the stability of the blends. Thermodynamic miscibility of polymer blends is fulfilled as long as the heterogeneity domain size is less than 10 nm [Ultracki, 2002]. The dependence of the Gibbs free energy change of mixing on concentration is illustrated in Figure 2.3 and Figure 2.4. Figure 2.3 shows the ΔG_m vs ϕ for a binary polymer blend that is miscible on the entire composition range, i.e., it satisfies the two requirements of thermodynamic criteria of miscibility at all concentrations. Figure 2.4 shows that although for the whole composition range the first criteria is satisfied (that is ΔG_m<0), in the range of $\phi'_{sp} < \phi < \phi''_{sp}$, since the second criteria is not satisfied, a small perturbation will cause the system to separate into two phases. The polymer blends in this composition range are unstable. In this figure, the ϕ'_b and ϕ''_b are referred to as the binodal compositions while ϕ'_{sp} and ϕ''_{sp} are the spinodal compositions.

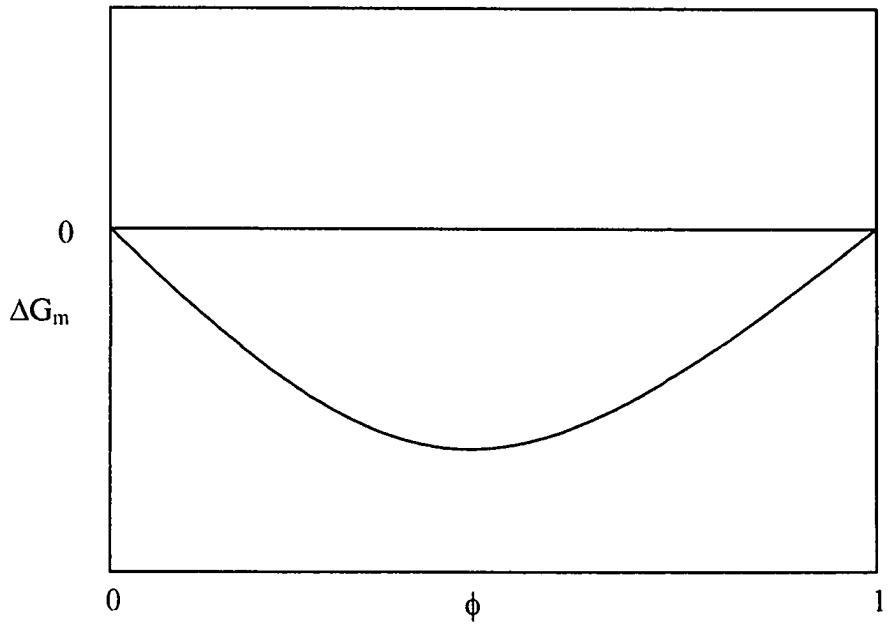

Figure 2.3: Gibbs free energy of mixing vs. volume concentration for a symmetric miscible binary polymer mixture (N_A=N_B=N)

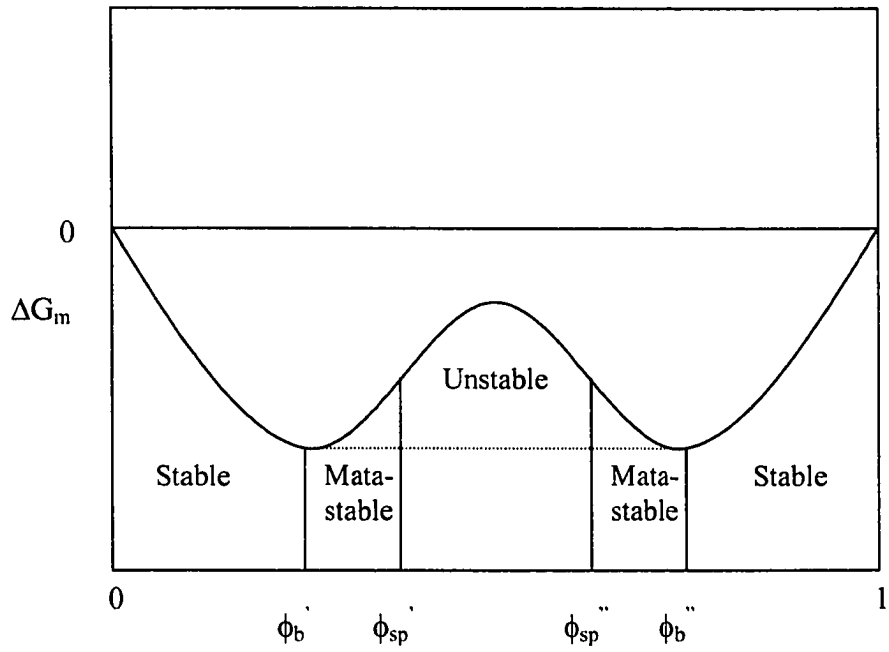

Figure 2.4: Gibbs free energy of mixing vs. volume concentration for a symmetric partially miscible binary polymer mixture (N_A=N_B=N)

2.2 The lattice cluster theory

The lattice cluster theory (LCT) was developed by Freed and coworkers in the 1990's [Dudowicz and Freed 1991]; it is an extension of the FH theory to describe the thermodynamics of polymer blends in the liquid state. The LCT has already provided a number of conceptual advances for the understanding of polymer blends [Freed and Dudiwicz 1995]. Compared with the FH theory, the LCT incorporates two major modifications. One is that it distinguishes different structures of the monomeric units by allowing the monomeric units to occupy several different adjacent lattice sites dictated by the actual monomer size and shape. Therefore, it more closely resembles the actual chain conformation than that found using the Flory-Huggins theory. Examples of polypropylene and polyisobutylene (PIB) using the lattice cluster model are given in Figure 2.5. The other modification is that it includes the local packing and interactions. Therefore, the effect of nonrandom mixing on the thermodynamic properties is taken into account. The FH interaction parameter, which is energetic origin in the FH theory, in the LCT also has an important entropic component arising from the differences in molecular size and shape of monomers.

The advantage of the LCT is that it can be used to investigate the effect of the monomer structure, composition and compressibility on miscibility, especially polyolefin miscibilities. The LCT has been widely used to explain the miscibility of polyolefin blends where the two resins differ in the type and size of short chain branching [Freed Dudowicz 1996; Freed and Dudowicz 1996]. The deficiencies of the LCT arise from the simplifications induced by the underlying lattice model [Utracki, 2002]. The applicable range of LCT theory is rather limited. It was found by Quinn and Gujrati that the LCT

predicts a spurious phase separation in the miscible region of incompressible polymer solutions or a blends [Quinn and Gujrati, 1999].

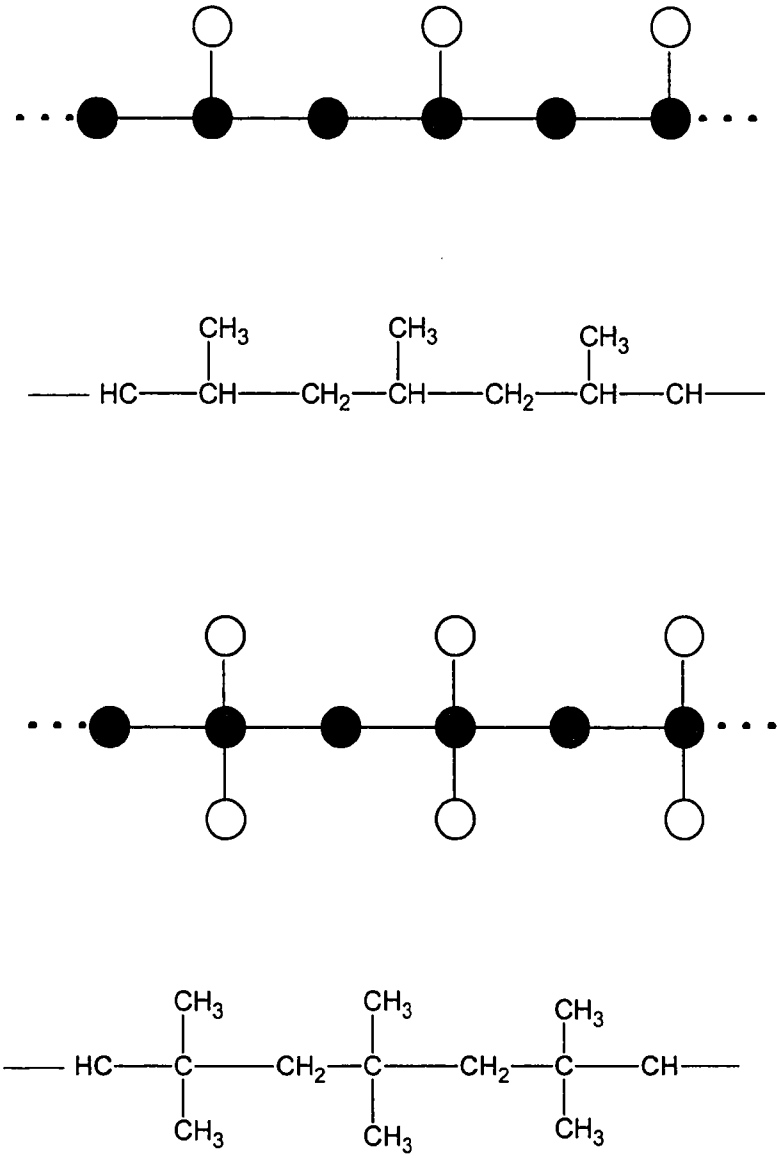

Figure 2.5: United atom models of PP and PIB used in the LCT. Circles denote CH_n (n=0-3) groups occupying single lattice sites. Filled circles indicate the backbone chain groups, while the open circles are for side groups.

2.3 The Flory-Huggins interaction parameter

By setting the second and third derivatives of Gibbs free energy change of mixing with respect to the volume concentration to zero, the critical Flory-Huggins interaction parameter can be obtained. It is given by

$$(\chi_{AB})_{cri} = \frac{1}{2}\left(\frac{1}{\sqrt{N_A}} + \frac{1}{\sqrt{N_B}}\right)^2 \qquad (2\text{-}6)$$

Polymer blends will be miscible if their χ values is less than $(\chi_{AB})_{cri}$, and they will be immiscible if their $\chi > \chi_{cri}$. For symmetric polymer blends, i.e., $N_A = N_B = N$, the critical χ_{cri} scales as $\chi_{cri}N = 2$. Because of the high molecular weight nature of polymers, $(\chi_{AB})_{cri}$ is fairly close to zero. Therefore, in order to form a miscible polymer blend, the Flory-Huggins interaction parameter between the polymers of interest should be negative.

In the original Flory-Huggins theory, the interaction parameter χ is purely enthalpic. However, experimental work has established that some additional parameters such as concentration fluctuation and pressure, which are not incorporated in the FH theory, can play an important role. Empirically, χ has been assumed to be composed of enthalpic χ_H and entropic parts χ_S, respectively,

$$\chi(\phi, T, N_1, N_2 \ldots) = \chi_S(\phi, N_1, N_2 \ldots) + \frac{\chi_H(\phi, N_1, N_2 \ldots)}{T} \qquad (2\text{-}7)$$

each of them being a function of concentration and molecular weight of both polymers and other parameters. There has been controversy about the relative contributions of χ_S and χ_H to the overall χ. For less miscible blends, χ is mostly enthalpic in origin, while for highly miscible blends, the entropic portion may dominate [Freed and Dudowicz 1996]. It is important to know the value of interaction parameter for a given polymer blend

because it determines the phase behavior of polymer blends. In the following section of this chapter, several experimental methods that have been commonly used to determine the interaction parameter will be discussed.

2.3.1 The melting point depression method

The melting point depression method is widely used to obtain the FH interaction parameter of amorphous/semi-crystalline polymer blends [Nishi *et al.* 1975; Wang and Nishi 1977],

$$\frac{1}{T_m} - \frac{1}{T_m^0} = -\frac{RV_1}{\Delta H_{f1} V_2} \chi_{12} \phi_2^2 \qquad (2\text{-}8)$$

where T_m and T_m^0 are the melting temperature and equilibrium melting temperature of the crystallizable polymer component in the mixture and in the corresponding pure state, respectively. ΔH_{f1} is the latent heat of fusion per repeating unit of the fully crystalline polymer. In this equation, subscripts 1 and 2 denote the crystalline and amorphous components, respectively.

The equilibrium melting point can be obtained by the Hoffman-Weeks expression [Hoffman and Weeks 1962], i.e., plot the T_m vs. T_c, and the intercept of the extrapolated data with T_m=T_c is taken as the equilibrium melting temperature. However, a curvature observed in the Hoffman-Weeks plot, especially at high T_c, makes the estimation of the equilibrium melting point difficult; and the extrapolated equilibrium melting temperature also varies with levels of crystallinity [Alamo *et al.* 1995]. Another method used to determine the equilibrium melting point is Gibbs-Thomson approach, which is believed to be more reliable. However, because this approach requires the determination of the

crystal thickness using TEM, it is not used as frequently as Hoffman-Weeks expression [Paul and Bucknall 2000].

The shortcoming of using this method to determine the FH interaction parameter is its unreliability. The equilibrium melting depression points for amorphous/crystalline polymer blends are usually in the order of 5 ^{0}C. However, the uncertainty of extrapolated equilibrium melting points is in the range of a few degrees up to 10 ^{0}C, which makes the estimated χ very unreliable [Runt and Gallaher 1991]. The χ obtained using this method should be confirmed by other techniques.

2.3.2 The small angle neutron scattering (SANS) method

The FH interaction parameter can also be obtained by measuring the composition fluctuations using SANS, the scattering function at zero wavevector $S(0)$ can be related to the second order derivative of the Gibbs free energy of mixing by the following equation:

$$S(0) = kT\left(\frac{\partial^2 \Delta G_{mix}}{\partial \phi^2}\right)^{-1} \qquad (2\text{-}9)$$

Using the FH expression for the Gibbs free energy change of mixing (equation 2-5) in the above equation, one obtains

$$\frac{1}{S(0)} = \frac{1}{N_A \phi} + \frac{1}{N_B (1-\phi)} - 2\chi \qquad (2\text{-}10)$$

From equation (2-10), we can see that by measuring the zero wavevector of the scattering function, the FH interaction parameter can be obtained thereof. This expression can also be extended to the nonzero wavevector by random-phase approximation [Rubinstein and Colby 2003]. The disadvantage of this method is that the discrimination is based on the atomic number; therefore, it requires that one of the components at least be partially

labeled with deuterium. The deuteration has an effect on the miscibility [Utracki, 1990]. SANS is an excellent method to determine the size and intermolecular interactions of polymer blends provided that the isotopic effect is absent or has been appropriately corrected.

2.3.3 The solubility parameter method

The Flory-Huggins interaction parameter can be obtained from the solubility parameters of the pure polymers. The solubility parameter is defined as the square root of the cohesive energy density. The cohesive energy density is defined as the ratio of molar energy of vaporization divided by the molar liquid volume, i.e.,

$$\delta = \sqrt{CED} = \sqrt{\left(\frac{\Delta E_v}{V}\right)} \qquad (2\text{-}11)$$

The closer the solubility parameter, the more compatible the components to be mixed. The relation between χ and solubility parameters of pure polymers are described in equation 2-11:

$$\chi = \frac{V_s}{RT}(\delta_A - \delta_B)^2 \qquad (2\text{-}12)$$

in which δ_A and δ_B are the Hilderbrand solubility parameters of polymers A and B, respectively and V_s is a reference molar volume. The choice of V_s is somewhat arbitrary and it is usually taken as the molar volume of the smaller monomer component among polymers A and B. Some researches take 100 ml/mol as the reference volume [Utracki, 2002; Rubenstein and Colby 2003].

The concept of solubility parameter originates from Hilderbrand's work on enthalpy change of mixing for regular solutions. Two assumptions are associated with this concept, one is that there are no specific interactions between the molecules, only van

der Waals forces; therefore, it is not suitable for mixtures with strong polar and specific intermolecular interactions, such as hydrogen bonding. Another assumption is that the intermolecular interaction between A and B, is the geometric mean of the intermolecular interactions, A-A and B-B of the pure components.

The main drawback of this approach is that equation 2-12 is limited to the enthalpic part of the FH interaction in equation 2-6; the entropic and specific interaction effects are omitted. Furthermore, only positive interaction parameters can be obtained and the composition dependence of χ cannot be investigated. Bush *et al.* modified the solubility parameters approach so that it can include negative ΔH_m, [Bush *at al.* 1996]

$$\frac{\Delta H_m}{V} = \phi(1-\phi)[(\delta_1 - \delta_2)^2 - e_h] \qquad (2\text{-}13)$$

where e_h is the energy density that originates from specific interactions. There are other modifications as well to include the specific interactions between the components of the polymer blends [Painter *et al.* 1988; 1989a; 1989b].

The comparison of the solubility parameters is usually conducted at room temperature. However, miscibility of polymer blends at 200-300 ^{0}C is often of interest. And it is well known that the solubility parameter decreases sharply with increasing temperature, and the dependence on temperature is different for different polymers [Utracki 2004]. Therefore, comparison of solubility parameters in the melt state should provide more realistic information on polymer-polymer miscibility. Therefore, one must practice caution when using this method to estimate the miscibility. Despite these drawbacks, the closely matched solubility parameter provides a necessary (but not necessarily sufficient) condition for miscibility. I will discuss this topic more in the later chapters.

There exist other less common methods such as 2D solid-state high resolution NMR [Guo 1996], IGC [Zhao 2002], infrared spectroscopy [Simon, 2003] etc. for the determination of miscibility in polymer blends. Practically, it is difficult to determine the Flory-Huggins interaction parameter by experiment. This is because the high viscosity of the polymers involved that makes the diffusion towards equilibrium rather slow. Molecular dynamics (MD) simulation provides another choice for the investigation of miscibility of polymer blends, and this will be presented in detail in the next chapter.

2.4 References

Alamo, R.G.; Viers, B.D. and Mandelkern, L. (1995) A Re-examination of the Relation between the Melting Temperature and the Crystallization Temperature: Linear Polyethylene, *Macromolecules*, 28(9): 3205-3213.

Bates, F.S.; Wignall, G.D. and Koehler, W.C. (1985) Critical-behavior of Binary-liquid Mixtures of Deuterated and Protonated Polymers, *Phys. Rev. Lett.* 55(22): 2425-2428.

Bush S.F.; Methven, J.M. and Blackburn, D.R. (1996) Partial Compatibility and Formation of Thickened, Shrinked, Shrink-resistant Thermoset Moulding Compounds, *High Perform. Polym.* 8(1): 67-82.

Dudowicz, J. and Freed, K. F. (1996) Influence of Monomer Structure and Interaction Asymmetries on the Miscibility and Interfacial Properties of Polyolefin Blends, Macromolecules, 29(27): 8960-8972.

Dudowicz, J. and Freed, K. F. (1991) Effect of Monomer Structure and Compressibility on the Properties of Multicomponent Polymer Blends and Solutions 1. Lattice Cluster Theory of Compressible Systems, *Macromolecules*, 24(18): 5076-5095.

Flory, P.J. (1953) *Principles of Polymer Chemistry*, Cornell University Press, New York.

Flory, P.J. (1941) Thermodynamics of High Polymer Solutions, *J. Chem. Phys.*, 9, 660.

Freed, K.F. and Dudowicz, J. (1996) Influence of Short Chain Branching on the Miscibility of Binary Polymer Blends: Application to polyolefin Mixtures, *Macromolecules*, 29(2): 625-636.

Freed, K. F. and Dudowicz, J. (1995) A Lattice-Model Molecular Theory for the Properties of Polymer Blends, *Trends Polym. Sci.* 3(8): 245-288.

Guo, M.M. (1996) Solid-state High-resolution NMR Studies on the Miscibility of Polymer Blends, *Trends Polym. Sci.*, 4(7): 238-244.

Hoffman, J.D. and Weeks, J.J. (1962) Melting Process and Equilibrium Melting Temperature of Polychlorotrifluoroethylene, *J. Res Natl Bur. Std. A*, 66: 13.

Huggins, M.L. (1941) Solutions of Long Chain Compounds, *J. Chem. Phys.*, 9, 440.

Londono, J.D.; Maranas, J.K.; Mondello, M.; Habenschuss A.; Grest, G.S.; Debenedetti, P.G.; Graessley, W.W. and Kumar, S.K. (1998) Chain-Packing Effects in the Thermodynamics of Polymers, *J. Poly. Sci.: Poly. Phys.* 36(16): 3001-3005.

Nishi, T, Wang, T.T. and Kwei, T.K. (1995) Thermally Induced Phase Separation Behavior of Compatible Polymer Mixtures, *Macromolecules*, 8(2): 227-234.

Painter, P.C.; Ainter, P.C. and Coleman, M.M (1989a) Thermodynamics of Hydrogen-bonding in Polymer Blends: 1. Application of Association Models, *Macromolecules*, 22(2): 570-579.

Painter, P.C.; Ainter, P.C. and Coleman, M.M (1989b) Thermodynamics of Hydrogen-bonding in Polymer Blends: 2. Phase Behavior, *Macromolecules*, 22(2): 580-585.

Painter, P.C.; Ainter, P.C. and Coleman, M.M (1988) Hydrogen-bonding in Polymer Blends:2. Theory, *Macromolecules*, 21(1):66-72.

Paul D. R. and Bucknall C. B.(2000) *Polymer Blends*, John Wiley & Sons Inc., New York.

Quinn, B. and Guirati, P.D. (1999) The Range of Validity of the Lattice Cluster Theory, *J. Chem. Phys.*, 110(2): 1299-1306.

Rubinstein, M. and Colby, R.H. (2003) *Polymer Physics*, Oxford University Press, New York.

Runt, J. and Gallaher K.P. (1991) Polymer Polymer Interaction Parameters Via Melting Point Depression- a Critical Analysis, *Polymer Communications*, 32(6):180-182.

Sanchez, I.C. and Lacombe, R. H. (1978) Statistical Thermodynamics of Polymer Solutions, *Macromolecules*, 11 (6): 1145-1156.

Simon, G.P. (2003) *Polymer Characterization Techniques and Their Application to Blends*, Oxford University Press, New York .

Strobl, G. (1996) *The Physics of Polymers: Concepts for Understanding Their Structures and Behavior*, Springer, New York.

Ultracki, L.A. (2004) Statistical Thermodynamics Evaluation of Polymer-Polymer Miscibility, *J. Poly. Sci., B: Poly. Phys.*, 42: 2909-2915.

Ultracki, L. A. (2002) *Polymer Blends Handbook*, Kluwer Academic Publishers, Dordrecht, The Netherlands.

Ultracki, L. A.(1990) *Polymer Alloys and Blends: Thermodynamics and Rheology*, Oxford University Press, New York.

Wang T.T. and Nishi, T. (1977) Sperulitic Crystallization in Compatible Blends of Poly(vinylidene fluoride) and poly(methyl methacrylate), *Macromolecules,* 10(2):421-425.

Zhao, L.Y. (2002) *A thermodynamics Study of Polyolefin Blends*, Ph.D Thesis, University of Alberta.

Chapter 3

Molecular dynamics simulation

3.1 Introduction

Molecular modeling plays an important role in understanding polymer behaviors; it is an important and probably the only bridge that connects analytical theories and experiments [Kremer 2003]. For example, for synthetic polymers, polydispersity is always a critical problem when comparing experimental results with theory; however, molecular modeling usually are performed using mono-disperse models "experiments" under fully controlled conditions. Atomistic simulations can increase our understanding of the properties of polymers at the molecular level, thereby gaining insight into the molecular origins of the properties of interest [Boyd 1996], which can assist the design of new polymers and predict properties that cannot be studied in the laboratory [Kob, 1999]. Compared with the cost and time consuming trial and error laboratory experiments, molecular simulation can help to guide polymer research by illuminating trends of behavior, predicting properties of materials before polymers are made, and understating the polymer behavior on the molecular level.

Thermodynamic properties of a macroscopic system measured experimentally are an average of the properties of microstates. Although it is quantum mechanics that describes the basic physics of condensed matter, the numerical solution of Schrodinger equation is not feasible at the moment even at the fastest computers for a system containing a considerable number of atoms such as polymers. Therefore, in practice, classical mechanics has been employed for large systems. In this approach, properties of

the microstates can be determined from the positions and momenta of the N particles in the system. For property A at a certain time, it can be written as $A(\vec{r}^{\,N}(t),\vec{P}^{N}(t))$, where the $\vec{r}^{\,N}(t)$ and $\vec{P}^{N}(t)$ represent the N positions and momenta, respectively, at time t (i.e., $A(\vec{r}^{\,N}(t),\vec{P}^{N}(t))$=A($x_1$,$y_1$,$z_1$,$x_2$..., p_{1x},p_{1y},p_{1z},p_{2x},...,t), where x_1 is the position of particle 1 in the x coordinate, p_{1x} is the momentum of particle 1 in the x direction). Because of the interactions between the atoms and the available thermal energy, property A of the microstates fluctuates with time; thus, the experimentally measured property A is an average over the measurement time. As the measurement time increases to infinity, the measured values approach the "true" average value of the property, i.e.

$$\langle A\rangle = \langle A\rangle_t = \lim_{t\to\infty}\frac{1}{t}\int_0^t A(P^N(t),r^N(t))dt \qquad (3\text{-}1)$$

According to the $\langle A\rangle = \langle A\rangle_t = \lim_{t\to\infty}\frac{1}{t}\int_0^t A(P^N(t),r^N(t))dt$chanics, the time average is equal to ensemble average, in which the property is determined by integrating all the possible configurations of the system. The ergodic hypothesis requires that the time average should be independent of the initial chosen configuration. With the improvement of force field, the classical MD simulation can be used for most fluids, and it is what we employed in this study.

Molecular dynamics calculates the real dynamics of the system, from which the time average properties can be obtained. The essence of molecular dynamics simulation is to solve Newton's equations of motion $\vec{F}_i(t) = m_i\vec{a}_i(t)$ to obtain a series of positions and momenta of the constituent atoms, forces on atom *i* can be computed directly from the derivative of the potential energy *U* with respect to the coordinates $\mathbf{r}_i$,

$$-\frac{\partial U_{pot}}{\partial \vec{r}_i} = m_i \frac{\partial \vec{r}_i^{\,2}}{\partial t_i^2} = \vec{f}_i \qquad (3\text{-}2)$$

m_i is the mass of the i^{th} particle; f_i is the force acting on it. Molecular dynamics simulation is a deterministic method; the states of the system in the future time can be predicted from its current positions and velocities. The finite difference method is generally used for the integration of the equations of motion. The essential idea of this method is that the integration is broken down into many small steps; each one is separated in time by a fixed time interval Δt and the total force acting on each particle at a certain time is calculated as a vector sum of its interactions with other particles. In Cerius[2], the software that we used for the simulation, only the Verlet leapfrog integration method [Hockney 1970] is available. In such an algorithm, the following relationships are used:

$$\begin{aligned} \vec{v}(t+\frac{1}{2}\Delta t) &= \vec{v}(t-\frac{1}{2}\Delta t) + \Delta t\vec{a}(t) \\ \vec{r}(t+\Delta t) &= r(t) + \Delta t\vec{v}(t+\frac{1}{2}\Delta t) \\ \vec{a}(t+\Delta t) &= \frac{\vec{f}(t+\Delta t)}{m} \end{aligned} \qquad (3\text{-}3)$$

where $\vec{f}(t+\Delta t)$ is evaluated from $-dU_{pot}/d\vec{r}$ at $\vec{r}(t+\Delta t)$.

3.2 Force Fields

Force field provides a detailed description of intermolecular and intramolecular interactions as a function of positions of the atoms in a molecular model. It consists of a set of analytical functions and parameters. The accuracy of the simulation results depends heavily on the force field and the associated parameters used in the description of the

energy functions. The functional forms and the way of parameterization for different force fields are different. For empirical force fields, the parameters were optimized by fitting the experimental data; therefore, the quality of the force field depends on the availability of experimental data and it is usually developed for a particular molecular system. The second-class force field is derived from the combination of quantum *ab initio* calculation and empirical fitting of experimental data. It has been demonstrated that it can be used for a fairly broad range of materials and still provide accurate property predictions [Sun *et al.*1998a; Sun, 1998b]. Three force fields are commonly used for the simulation of polymers in the Cerius^2 software. They are DREIDING [Mayo *et al.* 1990], polymer consistent force field (PCFF) and condensed-phase optimized molecular potentials for atomic simulation studies (COMPASS). Here I will only discuss the recently developed COMPASS force field, which is the most elaborate force field among the three.

COMPASS is the first *ab initio* force field that enables accurate and simultaneous prediction of structure, conformation, vibrational and thermo physical properties for a wide range of molecules in isolation and condensed phases. [Accelrys website] The functional forms used in the COMPASS force field are similar to those of consistent force field (CFF) 93:

$$
\begin{aligned}
E_{total} &= E_b + E_\theta + E_\phi + E_\psi + E_{bb'} + E_{b\theta} + E_{b\phi} + E_{\theta\theta'} + E_{\theta\theta'\phi} + E_Q + E_{vdw} \\
&= \sum_b [K_2(b-b_0)^2 + K_3(b-b_0)^3 + K_4(b-b_0)^4] \\
&+ \sum_\theta [H_2(\theta-\theta_0)^2 + H_3(\theta-\theta_0)^3 + H_4(\theta-\theta_0)^4] \\
&+ \sum_\phi [V_1(1-\cos\phi) + V_2(1-\cos 2\phi) + V_3(1-\cos 3\phi)] \\
&+ \sum_\psi K_\psi(\psi-\psi_0)^2 + \sum_b \sum_{b'} F_{bb'}(b-b_0)(b'-b_0') \\
&+ \sum_b \sum_\theta F_{b\theta}(b-b_0)(\theta-\theta_0) \\
&+ \sum_b \sum_\phi (b-b_0)[F_{b,\phi}^{(1)}(1-\cos\phi) + F_{b,\phi}^{(2)}(1-\cos 2\phi) + F_{b,\phi}^{(3)}(1-\cos 3\phi)] \\
&+ \sum_\theta \sum_{\theta'} F_{\theta\theta'}(\theta-\theta_0)(\theta'-\theta_0') \\
&+ \sum_\theta \sum_{\theta'} \sum_\phi F_{\theta,\theta',\phi}(\theta-\theta_0)(\theta'-\theta_0')\cos\phi \\
&+ \sum_{i>j} \frac{q_i q_j}{\varepsilon r_{ij}} + \sum_{i>j} [\frac{A_{ij}}{r_{ij}^9} - \frac{B_{ij}}{r_{ij}^6}]
\end{aligned}
\tag{3-4}
$$

In this equation, the total energy can be divided into three categories, the first four terms are contributions from each of the internal valence coordinates. They are the short ranged intramolecular interactions which correspond to bond stretching, bond angle bending, torsion angle rotations and out-of-plane inversion potentials. The bond stretching and bond angle bending are described by quadric polynomials; the torsions are described by a three-term Fourier expansion of torsion angle defined by four consecutive atoms. The next five terms are cross-coupling terms between internal coordinates. They are bond-bond, bond-angle, bond-torsion, angle-angle and angle-angle-torsion coupling terms. Among these coupling terms, the bond-bond $E_{bb'}$, bond-angle $E_{b\theta}$, and bond-torsion

$E_{b\phi}$ are the most significant. The last two terms represent the non-bonded interactions, which are the interactions between the atoms belonging to different molecules and any pair of atoms belonging to the same molecule but are not included in the bonded terms. They are divided into electrostatic interactions and van der Waals interactions. The electrostatic interactions are represented by Columbic interactions with partial atomic charges; the van der Waals is described by Lennard-Jones(LJ) 9-6 function instead of a common LJ 12-6 function, which is believed to be too hard in the repulsion region.

The parameters of valence terms and cross-coupling terms are derived by least-square fitting of Hartree-Fock (HF)/6-31G* data calculated for a group model compounds. The *ab initio* data include the total energy and the first and second derivatives of the total energy of the model compounds; then it is scaled by a set of generic parameters to correct the system errors of *ab initio* calculation. The system errors are generally attributed to the truncation and quality of the basis set used and exclusion of the electron correlation. The parameters in VDW interactions are transferred from PCFF force field and optimized by MD simulations of condensed phase properties, such as the cohesive energy density (or heat of vaporization) and density. The modification of the VDW parameters may have an influence on the torsional energies, but would have a minimal effect on other valence terms if the initial LJ parameters were close to the optimized values [Sun, 1998b]. The partial atomic charges of the atoms can be calculated by the charge equilibration method developed by Rappe and Goddard [1991]. The partial atomic charges were kept constant during the simulation because conformations of the system of interest did not change significantly, even at elevated temperatures. Some force fields have been developed in such a way that the partial atomic charges are allowed to

change according to the molecular configuration during the simulation [Demiralp *et al.* 1999].

3.3 Ensembles of molecular dynamics simulation

Molecular dynamics is traditionally performed in the micro-canonical ensemble (NVE). However, experiments are usually done under the conditions in which temperature and/or pressure are kept constant. The two most common alternative ensembles are the constant-temperature, constant-volume ensemble (NVT) and isobaric-isothermal ensemble (NPT).

3.3.1 The NVT ensemble

There are several constant temperature MD methods that have been proposed. In the early days, the temperature was kept constant by a momentum scaling procedure, in which the velocities of the particles are scaled each time step to keep the kinetic energy constant. Obviously, the natural fluctuations of the kinetic energy of the system are suppressed in this method. The extended system method proposed by Nose in 1984 is the most widely used method for simulating NVT ensembles. In this method, an additional variable, representing the thermostat that has a fictitious mass Q, was introduced as an external system for the physical system of N particles. The Hamiltonian of the extended system in terms of virtual variables is given by [Nose 1984]:

$$H = \sum_i \frac{\overline{p}_i^2}{2m_i s^2} + \overline{\phi}(q) + \frac{p_s^2}{2Q} + gkT \ln s \qquad (3\text{-}5)$$

the parameter g is essentially the degree of freedom, P_s is the momentum of s, Q is a parameter behaves as a mass for the motion of s. The virtual variables (coordinate q_i , momentum p_i and time t) correlated to the real variables (q_i', p_i', t')by:

$$p_i' = \frac{p_i}{s}; q_i' = q_i; t' = \int_0^t \frac{dt}{s} \qquad (3\text{-}6)$$

It was proved by Nose [1984] that by using virtual variables, the Hamiltonian of the extended system remains canonical. In practice, the real time formulation was used because of the unequal time intervals in the virtual variable formulation. However, in this case, the equations are no longer canonical.

3.3.2 The NPT ensemble

The real experiments usually carried out at constant temperature and pressure, so the simulation in the isobaric-isothermal ensemble is most directly relevant to the experimental data. In the NPT ensemble, the pressure is kept constant and the volume fluctuates. The pressure is controlled by coupling with the system with a pressure "bath", i.e., changing the size of the periodic box. Usually pressure fluctuates much more than quantities such as total energy in the constant NVE MD simulation. This is because the pressure is related to the virial, which is obtained as the product of the position and the derivative of the potential energy with position, i.e. $\bar{r}\frac{d\bar{U}(\bar{r})}{d\bar{r}}$. This product changes more quickly with r than does the potential energy, therefore a greater fluctuation in the pressure. In the Anderson's method of pressure control [Anderson 1980], the volume of the cell is treated as a dynamical variable. The Lagrangian of the system is modified so that it contains an additional kinetic energy term and a potential term associated with user-defined mass M. The potential term can be interpreted as a potential derived from external pressure acting on the volume of the system.

3.3.3 Integration time step

A key parameter in the integration algorithm is the integration time step Δt. If the time step is too small the trajectory will only cover a limited portion of the phase space. To make the best use of computer time, a large time step should be used; however, too large a time step causes instability and inaccuracy in the integration process. Usually the time step is used as approximately one-tenth the highest vibration frequency of the constituent atoms of the model. In most molecular systems, the fastest motion or the motion with the highest vibrational frequency is that of C-H bond stretching, whose period is on the order of 10^{-14}s (10 fs). Therefore, the integration time step should be 0.5-1 fs. In this study, 1 fs was used for all the simulations.

3.4 Periodic boundary conditions (PBC)

Because of the limitation of computational resources, only a small number of polymer chains can be modeled, which makes most of the model molecules on the surface of the sample. However, the bulk properties are of interest in this work. The surface effects are eliminated by employing periodic boundary conditions (PBC).

When PBC are applied, the cubic box of particles is replicated in all directions and gives a periodic array. A two dimensional PBC box is shown in Figure 3.1. In this two dimensional example, the primary cell, which represents a small portion of the system, is surrounded by eight replicas. There are 26 nearest neighbors of the primary cell in three dimensions. The replica cells are called image cells and have the same number of particles in the primary cell. The velocities and the relative positions of the particles are also exactly the same as those in the primary cell. During the simulation,

when one molecule moves out the primary cell, one of its images will enter through the opposite side. Therefore the numbers of particles in the primary cell are always conserved. By using PBC, it is not necessary to store the coordinates and velocities of all the atoms in the simulation, only those in the primary cell need to be recorded and the others can be calculated through coordinate transformation.

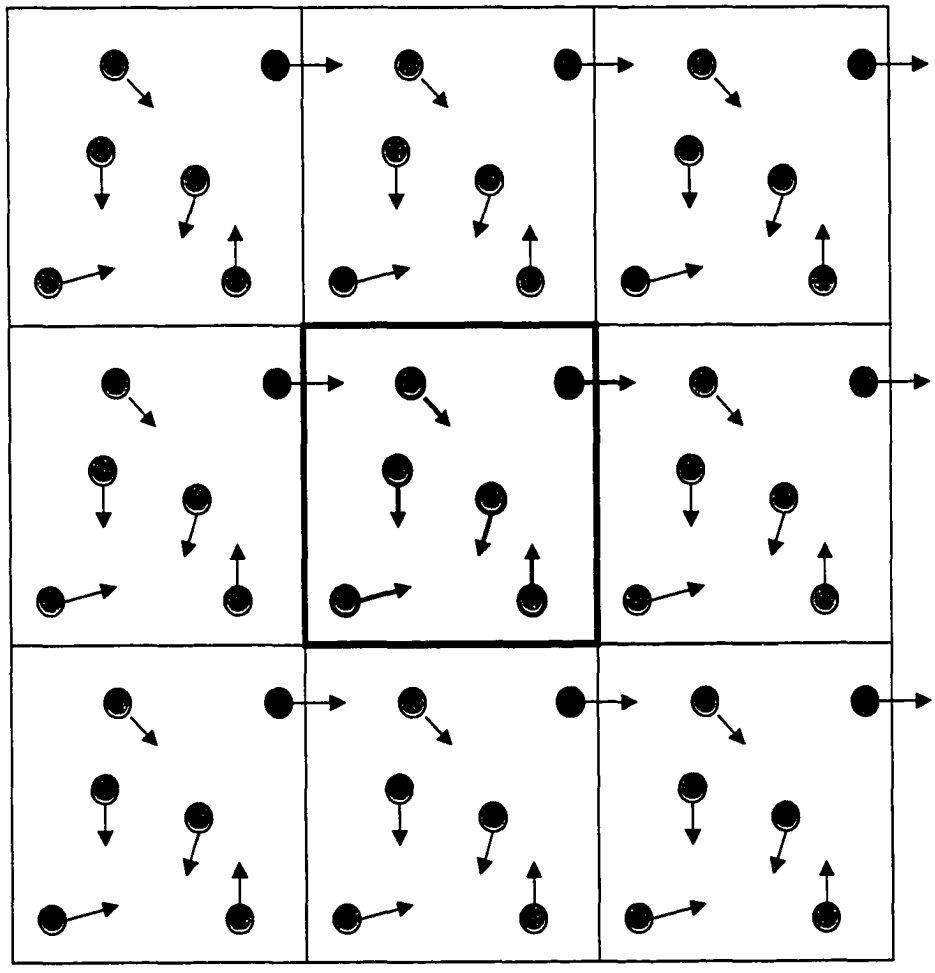

Figure 3.1: Periodic boundary conditions in two dimensions. The center box is the primary cell

3.5 Polymer models for the simulation

The initial polymer conformation was constructed based on a conventional Rotational Isomeric State (RIS) model using the Cerius^2 Amorphous Cell program. To eliminate surface effects, the PBC was employed. The size of the PBC box was determined based on the density, molecular weight of the model polymer chain and the number of chains used. According to Choi's study [Choi 1995], the simulation results of single chain and many chains model are comparable. In this study, engineering thermoplastics are of interest. Since their structures are complicated, single chain models were used for the simulation of pure polymers in this study. Many chains are included in the polymer blend models to represent the composition of the system. In the process of model building, to avoid the hard overlap of the models, usually the hard-core radius equal to 0.3 times the van der Waals radius was used. However, use of such an approach did not yield realistic models for blends. To avoid this, 0.35 to 0.4 times of the van der Waals radius were used in the construction of blend models building although it was more time consuming.

3.6 Energy minimization

After the model was built, the total potential energy of the system is likely to be high and not representative of the actual structure. The energy minimization was used to find the lowest energy conformation by changing the positions of the atoms in space. The criteria for the convergence of energy was to obtain a residual root-mean-square force in the simulated polymer system less than 0.1 kcal mol^{-1} $Å^{-1}$. When the system is far from equilibrium, the steepest-descent method should be used for the energy minimization.

However, the conjugate-gradient method is preferred when the system is close to the equilibrium [Spyrioumi and Vergelati 2001; Pavel *et al.* 1999].

3.7 Data analysis and error estimation

An enormous amount of data can be generated during the MD simulation; the data should be properly analyzed to extract the relevant properties. In this work, the MD simulation results are recorded every 1000 steps, or 1 picosecond because 1 fs (0.001 ps) picoseconds is used as the time step for the integration of Newton's equations of motion. The property of interest A is calculated by the following expression:

$$\langle A \rangle = \frac{1}{\tau_{run}} \sum_{\tau=1}^{\tau_{run}} A(\tau) \qquad (3\text{-}7)$$

where τ_{run} is the number of data points used for calculating the average. For the high degree of rigidity of the polymers we investigated in this study, it needs a shorter time for MD simulation to create equilibrated conformation compared with flexible polymers.

As with laboratory experiments, computer simulation is subject to errors. Two kinds of errors may exist: one is systematic error and the other one is statistical error. The systematic error may arise from the simulation algorithm or reliability of force field used for the simulation. The statistical errors are often reported as standard deviations. The standard deviation of the average value is calculated as follows:

$$\sigma\langle A \rangle = \frac{\sigma_A}{\sqrt{\tau_{run}}} = \frac{\sqrt{\sum_{i=1}^{\tau_{run}} (A(i) - \langle A \rangle)^2}}{\sqrt{\tau_{run}}} \qquad (3\text{-}8)$$

where $\sigma<A>$ is the standard deviation of the estimated average value <A> obtained from τ_{run} data points with a run standard deviation σ_A.

3.8 Computational hardware and software

The software we used in this study was Cerius^2, version4.6 designed by Molecular Simulations Inc. (MSI) (now is combined into Accerlys Inc.), Sandiego, CA. Silicon Graphics OCTANE workstations as well as SGI origin model supercomputers located at the University of Alberta have been used for the simulations performed in this thesis.

3.9 References

Anderson H.C. (1980) Molecular dynamics simulations at constant pressure and/or temperature, *J .Chem. Phys.*, 72(4): 2384-2393.

Boyd, R.H., (1996) Glass Transition Temperatures from Molecular Dynamics Simulations, *Trends Polym. Sci.*, 4(1): 12-17.

Choi, P. (1995) *Three-dimensional solubility and interaction parameters: inverse gas chromatography and molecular dynamics studies*, Ph.D thesis University of Waterloo.

Demiralp, E; Cagin, T and Goddard 3, W.A. (1999) Morse Stretch Potential Charge Equilibrium Force Field for Ceramics: Application to the Quartz-stishovite Phase Transition and to Silica Glas; *Phys. Rev. Lett.*; 82(8), 1708-1711.

Hockney, R.W. (1970) The Potential Calculation and Some Applications, *Methods in Comput. Phys.* 9: 136-211.

Horbach J. and Kob, W. (1999) Static and Dynamic Properties of a Viscous Silica Melt, *Phys. Rev. B* 60(5): 3169-3181.

Kremer, K. (2003) Computer Simulations for Macromolecular Science, *Macromol. Chem. Phys.*, 204: 257-264.

Mayo, S.L.; Olafson B.D. and Goddard 3 W.A. (1990) DREIDING: A Generic force field for molecular simulations, *J. Phys. Chem.*, 94, 8897-8909

Nose, S. (1984), A Unified Formulation of Constant Temperature Molecular Dynamics Methods; *J. Chem. Phys.* 81(1), 511-519.

Pavel D.; Ball J.; Bhattacharya S.; Shanks R. and Hurduc N. (1999) Molecular Simulation of Thermophysicsl Properties of Aromatic Polymers Containing Oxetane Ring in the Main Chain, *J. Polym. Sci., B: Polym. Phys.*, 37(17):2334-2352.

Rappe A.K. and Goddard3 W.A., (1991) Charge Equilibration for Molecular Dynamics Simulation, *J. Phys. Chem.* 95(8): 3358-3363.

Spyriouni, T. and Vergelati, C. (2001), A Molecular Modeling Study of Binary Blend Compatibility of Polyamide 6 and Poly(vinyl acetate) with Different Degrees of Hydrolysis: An Atomistic and Mesoscopic Approach, *Macromolecules,* 34(15):5306-5316.

Sun H.; Ren, P. and Fried, J.R. (1998a) The COMPASS Force Field: Parameterization and Validation for Phosphazens, *Comp. Theor. Polym. Sci.*, 8(1-2) 229-246.

Sun, H. (1998b) COMPASS: An Abinitio Force Field Optimization for Condensed-Phase Applications-Overview with Details on Alkane and Benzene Compounds, *J. Phys. Chem. B*, 102(38), 7338-7364.

Chapter 4

Miscibility studies of PEI/PC blends

4.1 Introduction

An industrially important amorphous-amorphous polymer blend is the blend of poly(ether imide) (PEI) and polycarbonate (PC). PEI and PC are high performance engineering thermoplastics. The chemical structures of PEI and PC are shown in chapter 1, Fig 1.1. PEI/PC blends can be used for aircraft interior components and household applications. The PEI/PC blends, Ultem LTX^{TM} series, have been available commercially since 1990 from General Electric Plastics. PEI/PC blends combine the high temperature resistance and intrinsic flame resistance of PEI with the good impact strength and ease of processing of PC. Blending PC into PEI also dilutes the cost of PEI, and reduces PEI's notch sensitivity [Ullmann 2000].

PEI has been blended with several other polymers such as liquild crystalline polymer (LCP) [Jung *et al.* 1998; Bafna *et al.* 1993], poly (ether ether ketone) (PEEK) [Morales and Bretas 1996a, 1996b], liquid crystalline polyimide (PI-LC) [Konda *et al.* 1998] and nitro-substituted polybenzimidazole (NO_2-PBI) [Cho *et al.* 2001]. The blends of PC with epoxy [Rajulu *et al.* 2001], PMMA [Kim *et al.* 1999], high performance polystyrene [Ohishi *et al.* 2001] and poly(styrene-co-methacrylic acide) [Akiyama *et al.* 2001] have been studied in recent years. There are a few papers published on PEI/PC blends. Chun *et al.* [1996] studied the thermal properties and morphology of PEI/PC blends and found that the blends exhibited two distinct glass transition temperatures.

Moreover, they found that the glass transition temperature of PEI changes at different loadings of PC, while that of PC stays constant. However, the reason for this behavior was not fully explored.

The primary objective of the study of PEI/PC blends is to use molecular dynamics simulation (MD) to delineate the molecular processes that lead to the anomalous observation. To this end, the Hildebrand solubility parameters of PEI and PC and Flory-Huggins interaction parameter of the blends at various concentrations are computed. In addition, blends at several concentrations are made and analyzed using differential scanning calorimetry (DSC) to obtain the full T_g versus concentration curves to validate previous results. To our knowledge, the morphology of PEI/PC blends in the melt state was not fully studied in the literature; therefore, another objective of this study is to investigate the morphology of PEI/PC blends at different concentrations using transmission electron microscopy (TEM).

To our knowledge, no molecular dynamics simulations have been done for PEI/PC blends, but some simulation work has been done on pure PEI and pure PC. Shih and Chen [1995] performed molecular dynamics simulation on bisphenol-A (BPA)-PC using the TRIPOS5.2 force field. They found that the carbonate group undergoes rotation more easily than that of the isopropylidene group. Fan *et al.* investigated the structure factor and some mechanical properties of BPA-PC using MD simulation with the DREIDING2 force field [Fan *et al.*1994]. Ballone *et al.* [1999] simulated PC based on a density functional force field. They calculated the structure factor of PC and compared it with the experimental results obtained from spin-polarized neutron scattering. The relationship between configuration entropy and glass transition temperature of PC with

different substitution on the isopropylidene carbon was investigated by Sundararajan [1990] using MD simulation methods. For PEI, the cohesive energy density was determined by Eichinger *et al.* [2002] using the COMPASS force field.

4. 2 Experimental

4.2.1. Materials

The polymers used in this study were obtained from commercial sources. The PEI was ULTEM 1000 provided by GE Plastics. The PC was LEXAN 101, also from GE Plastics. All materials were provided in pellet form. The physical properties of these polymers are given in Table 4.1.

Table 4.1: Properties of PEI and PC used in the current work

Polymer (Abbreviation)	Source	Molecular Weight (M_w)	Specific Heat (C_p, J/kg/K)	Density (ρ, kg/m^3)	T_g (^{0}C)
Poly(ether imide): ULTEM 1000 (PEI)	GE Plastics	30,000	1,650 (220^0C)	1,270 (25°C)	220
Polycarbonate: Lexan 101 (PC)	GE Plastics	31,600	1,580 (150^0C)	1,200 (25°C)	150

4.2.2. Experimental methods

4.2.2.1 Melt Blending of PEI/PC

PEI/PC blends were prepared in a Haake Rheocord 90 series 600 batch mixer with roller blades. The mixer was preheated to 340 ^{0}C before adding the pellets. The component weight was calculated by using the desired weight percent of each component. The combined weight of the component is required to have a total melt volume 78% of the volume of the mixing chambers. It was shown by Sundararaj *et al.* [1992] that at this loading there is optimum materials exchange between the two chambers of the mixer and there are no stagnant areas in the mixer center due to overfilling. All the experiments are performed at 50 rpm, which corresponding to a 65 s^{-1} shear rate at the minimum gap of the mixer [Lin and Sundararaj 2004]. In order to reduce degradation during melt mixing, 0.1wt% Irgafos 168 stabilizer [tris(2,4-di-tert-butylphenyl)-phosphite (Ciba Specialty Chemicals, Summit, NJ) was added to the blends.

The PEI/PC blend ratios we prepared in this study were: 90/10; 87.5/12.5; 85/15; 82.5/17.5; 80/20; 75/25; 70/30 and 60/40, 50/50, 40/60, 30/70. After the temperature of batch mixer reached the desired temperature, PEI and PC pellets were added through the chute to the mixer. The ram was then placed on the top opening of the chambers and a 5 kg weight was then placed on top of the ram. For PEI rich phase blends, the PEI pellets were added first and PC pellets were added 2 minutes later, when PEI pellets were already melted. This procedure is similar to the downstream feeding of PC in a twin screw extruder. Lin and Sundararaj [2004] found that 10 s after PC was added to the softened PEI, the PC deformed quickly and no distinct PC pellets can be observed. For PC rich phase blends, the PEI pellets and PC pellets were added together. The total

mixing time was 10 minutes. It has been shown by Sundararaj *et al.* [1992] and Macosko *et al.* [1996] that most of the size reduction occurs very rapidly during the softening of the pellets. This mixing time is sufficient to reach a fine mixing. After mixing, the motor was stopped and a sample was taken from the indents of the roller blades and quenched in liquid nitrogen.

4.2.2.2 DSC experiments of PEI/PC blends

A differential scanning calorimeter, TA Instruments DSC 2910 equipped with Thermal Analyst 2200 software was used to determine the glass transition temperatures of the samples. DSC scans were obtained from 7-12 mg samples placed in the nitrogen atmosphere at a heating rate of 20 ^{0}C/min from room temperature to 280 ^{0}C. The glass transition of the blends was taken from the heating scan of the samples. The measured glass transition temperature depends on the heating rate used, but since all the measurements were conducted at the same heating rate, the results can be compared with each other.

4.2.2.3 TEM sample preparation

As PEI and PC are in the glassy state at room temperature, the specimens used for the electron microscope were prepared by trimming a sample with a razor blade to form blocks of approximately 5×5 mm, the blocks were further trimmed to a shape of pyramid with a tip faced to an area of approximately 0.2×0.2 mm. The thin sections (about 50-100 nm thick) were obtained by microtoming using a Reichert Ultracut using diamond knife. The thickness of the thin sections was judged by a grey color of thin sections in the distilled water. The sections floating on the distilled water surface of the knife trough

were collected on 400 mesh copper grids for transmission electron microscopy. In order to enhance the contrast, the thin sections of PEI/PC blend were stained using 0.5% aqueous ruthenium teraoxide solution (Poly-Sciences) for 20-30 minutes. The morphology of PEI/PC blends at compositions of 90/10, 80/20, 70/30, 60/40, 50/50, 40/60, 70/30 and 80/20 were viewed using a Hitachi 7000 TEM at an accelerating voltage of 75 kV.

4.3 Molecular dynamics simulation details

4.3.1 DREIDING 2.21 force filed

Molecular dynamics (MD) simulations were carried out using a commercial software package, Cerius^2, version 4.6, from Molecular Simulation Inc. (now Accelrys Inc.) on a Silicon Graphics OCTANE workstation. Choosing the appropriate force field is considered to be the most important factor in obtaining valuable simulation results. There are a large number of force fields available in literature; they are parameterized for different physical systems. Three of them are usually used for the simulation of polymers. They are DREIDING 2.21 [Mayo *et al.* 1990], PCFF and COMPASS [Sun *et al.* 1998] force fields. The functional form of COMPASS force field has been descried in chapter 3.

In the DREIDING 2.21, the total energy of a system is represented by the sum of bonding and non-bonding interactions:

$$E = E_b + E_\theta + E_\phi + E_\psi + E_{VDW} + E_Q \qquad (4\text{-}1)$$

The first four terms represent bonded interactions, which correspond to the energy associated with bond stretching (E_b), bond angle bending (E_θ), tortion angle rotations

(E_ϕ), and tetrahedral center inversions (E_ψ). The last two terms represent non-bonded interactions, which consist of van der Waals (E_{vdw}) and electrostatic (E_Q) energies.

In DREIDING2.21, the bond stretching energy is described by a harmonic oscillator:

$$E_b = \frac{1}{2}k_b(l - l_0)^2 \qquad (4\text{-}2)$$

where k_b is a force constant, l is the bond length and l_o is the equilibrium bond length. Bond bending energy is described as a harmonic cosine form:

$$E_\theta = \frac{1}{2}k_\theta(\cos\theta - \cos\theta_0)^2 \qquad (4\text{-}3)$$

where θ is a bond angle between two adjacent bonds and θ_0 is the equilibrium bond angle. Torsional energy describes the interaction for two bonds connected by a common bond, it takes the form as:

$$E_\phi = \frac{1}{2}k_\phi\{1 - \cos[n(\phi - \phi_0)]\} \qquad (4\text{-}4)$$

where ϕ and ϕ_0 are torsional angle and equilibrium trosional angle respectively. n is the periodicity and is an integer, while k_ϕ is the barrier to rotation. Inversion energy in DREIDING force field takes the form:

$$E_\psi = \frac{1}{2}k_{inv}(\psi - \psi_0)^2 \qquad (4\text{-}5)$$

where ψ is the plane angle and ψ_0 is defined as zero for a plane molecule.

For non-bonded interactions, E_{vdw} is described by a Lennard-Jones 12-6 potential:

$$E_{vdw} = D_0[(\frac{R_0}{R})^{12} - 2(\frac{R_0}{R})^6] \qquad (4\text{-}6)$$

in this equation, R is the van der Waals interaction distance and R_0 is the van der Waals bond length and D_0 is the van der Waals energy well depth. The electrostatic energy is calculated based on the partial charges of the atoms in the system estimated by the charge-equilibration method [Rappe and Goddard 1991]. It takes the form:

$$E_Q = 332.0637 \frac{q_i q_j}{\varepsilon R_{ij}} \qquad (4\text{-}7)$$

q_i and q_j is the partial charges of atom i and j, respectively. R_{ij} is the distance between them and ε is the dielectric constant. In DREIDING 2.21 force field, a distance-dependent dielectric constant was used. During our simulation, the electrostatic interaction was calculated by the Ewald summation method since it calculates long-range interaction forces more accurately.

Figure 4.1: Initial conformation of a PEI/PC blend with 4 chains of PEI (red) and 1 chain of PC (black). Note unit cell (dark blue)

4.3.2 Simulation details

The bulk amorphous state of the pure polymers and their blends were built using cubic unit cells subjected to periodic boundary conditions. A typical example for the initial configuration of PEI/PC blends is shown in Fig 4.1. The number of atoms and the bulk density of the material determined the unit cell volume (the unit cell is shown in Fig 4.1). The detailed model construction procedure has been described in chapter 3. The number of chains, chain sizes and densities used for building PEI/PC blend model are summarized in Table 4.2. The density of the blend system was calculated from the density of the pure polymer and the concentration of each polymer assuming that the components' volumes are additive [Van Krevelen 1997].

After the initial construction, the blend systems were checked for a good "blending" of the different component chains. If in an initial configuration the two component chains were not well mixed, it would be discarded and a new configuration was attempted. Different initial conformations were built and subjected to energy minimization. The conformation with the lowest potential energy was selected to be used for the following MD simulation. In order to avoid the structure being trapped in a local minimum, after energy minimization, a high temperature MD simulation was employed and followed by energy minimization. This method was proposed by Li and Mattice [1992] and used by other researchers as well. [Wang *et al.* 1998; Gestoso and Brisson 2001] In this study, the amorphous cells of pure polymer and polymer blends were equilibrated at 1,000 K for 100 ps using NVT ensemble. The snapshot with lowest energy was chosen and subjected to energy minimization again until derivatives was less than 0.1 kcal mol^{-1}.

The NVT ensemble simulation was carried out for all the structures. Nose [1984] dynamics coupled with a Verlet Leapfrog numerical algorithm was used to create the canonical molecular dynamics trajectories, and a time step of 1 femto-second was used to ensure the stability of the simulation. The simulation time depends on the number of

Table 4.2: Simulation details for the PEI/PC blend system

System Label	Number of Chains per Unit Cell	Composition (Volume PEI %)	Density of the System (g/cm^3) at 340^0C	Molar Volume (cm^3/mole)	χ
1	1 PC chain	0	1.04	5625.96	N/A
2	1PEI Chain	100	1.107	4875.83	N/A
3	4PC chains 1PEI chain	19.3	1.053	5570.75	2.35
4	2PC Chains 1PEI chain	32.4	1.062	5533.27	2.46
5	1PC Chain 1PEI Chain	48.9	1.073	5488.82	2.30
6	1PC Chain 2PEI Chains	65.7	1.084	5444.96	2.30
7	1PC Chain 4PEI Chains	79.3	1.093	5409.52	0.89
8	1PC Chain 6PEI Chains	85.2	1.097	5393.80	3.96

atoms in the system and it is usually carried out until the potential energy of the system stabilizes. The last one hundred pico-seconds of the trajectory file were used for the calculation of the physical properties of interest.

4.3.3 MD simulation of polymer blends

Two polymers, with degrees of polymerization N_A and N_B, will be miscible if their Flory-Huggins interaction parameter is less than $(\chi_{AB})_{cri}$ which is given by

$$(\chi_{AB})_{cri} = \frac{1}{2}\left(\frac{1}{\sqrt{N_A}} + \frac{1}{\sqrt{N_B}}\right)^2 \qquad (4\text{-}8)$$

The most direct approach to obtain the Flory-Huggins interaction parameter for binary polymer blends is to measure the corresponding enthalpy change on mixing. Several methods have been proposed to predict the enthalpy of mixing. One experimentally available method is to measure the enthalpy of mixing using low molecular weight compounds having chemical structure closely related to those of the polymer-repeating units. However, because chain segments are bounded and the additional steric hindrances experienced by the polymers are rather different from those of low molecular weight compounds [Paul and Bucknall 2000]. MD simulation provides a direct method to determine the enthalpy of mixing, which has been attempt a few times before [Choi *et al.* 1995; Fan *et al.*1992; Lee *et al.* 1999]. Based on MD simulation, one can readily calculate the heat of mixing by comparing the enthalpies of the blends and pure polymers as shown in the following equation:

$$\Delta H_m = H_{mixture} - \sum n_i H_i \qquad (4\text{-}9)$$

where H_i is the enthalpy of component in its pure state, $H_{mixture}$ is the enthalpy of the blend system. The linear thermal expansion coefficients of PEI and PC are 5.58×10^{-5}

cm/cm/K and 6.84×10^{-5} K^{-1} respectively [Chapman & Hall, 2004]. Since they are very close to each other, we feel justified not to include the $\Delta(PV)$ effect and ΔH_m is assumed to be equal to ΔE_m. The Flory-Huggins interaction parameter can then be calculated from the following equation for ΔH_m:

$$\Delta H_m = \chi RT\phi_1\phi_2 \qquad (4\text{-}10)$$

where ϕ_1 and ϕ_2 are the volume fractions of polymers 1 and 2, respectively. In this way, we can study the concentration dependence for the Flory-Huggins interaction parameter. The primary limitation of this method is that non-combinatorial entropic contributions are not explicitly included.

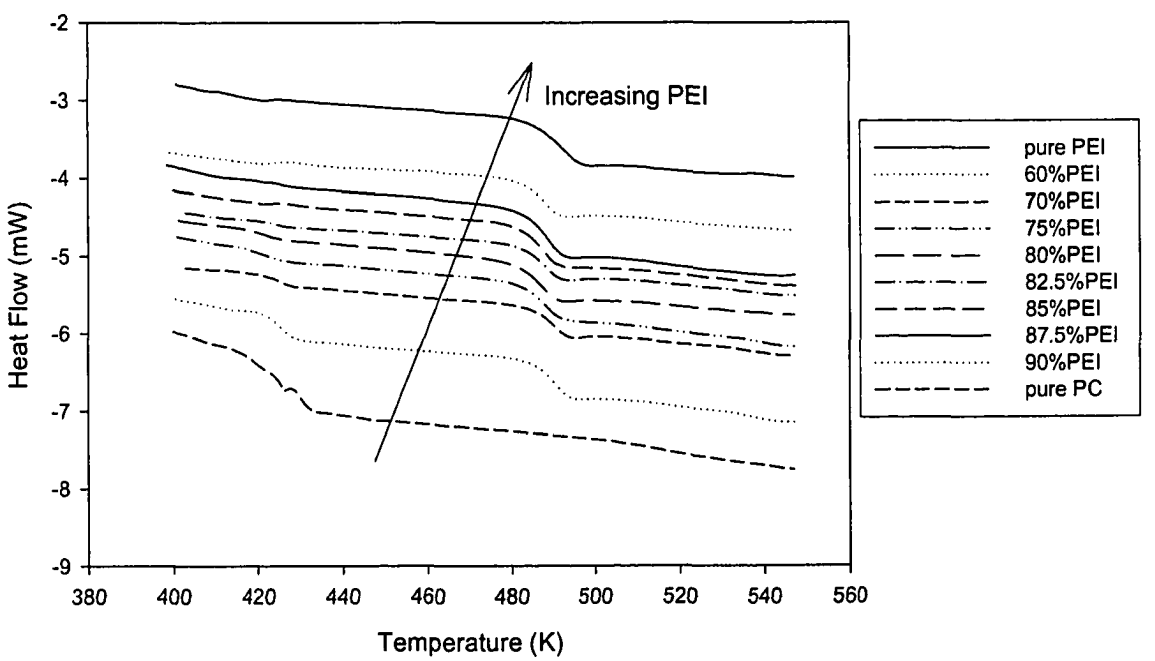

Figure 4.2: Heat flow versus temperature of PEI/PC blends. The curves are shifted vertically to avoid overlap

4. 4 Results and Discussion

4.4.1 DSC results

Similar to what Chun *et al.* [1996] observed, we also observed two distinct T_g's for the PEI/PC blends in the DSC measurements (see Figure 4.2), one corresponding to the PEI rich phase and the other to the PC rich phase. The existence of two distinct T_g's indicates that these two polymers are immiscible. The two concentration dependence of T_g is shown in Figures 4.3 and 4.4, respectively. The T_g in these figures are averaged on three parallel measurements. Fig 4.3 indicates that the T_g of PC in the blends is identical to that of pure PC. On the other hand, Fig 4.4 shows that the T_g of PEI in the blend first decreased with increasing PC content up to 20 wt%; the T_g of PEI then reached a minimum value at 20% PC; and finally the T_g of PEI increased at higher PC contents and approached the T_g of pure PEI. The maximum T_g decrease was about 6 ^{0}C, which occurred at 80% PEI. As mentioned, Chun *et al.* [1996] also reported a similar phenomenon; however, in their case, the minimum T_g of PEI occurred at 90% PEI. It should be noted that the concentration intervals they used to determine the concentration dependence of the T_g of PEI were not as fine as in this work. In addition, their blend samples were prepared by single screw extrusion and solution casting, whereas we used melt blending in an intensive batch mixer. They also found from scanning electron microscopy that the size of the minor component domains for the PEI/PC blend ratio with the lowest T_g is smaller compared with the size of the minor component for other blend ratios. They suspected that this might be due to the difference in the viscosity of the two polymers. Kinetics effect may also play a role in such observations. In the PEI rich phase, when the blend system was quenched from melt state,

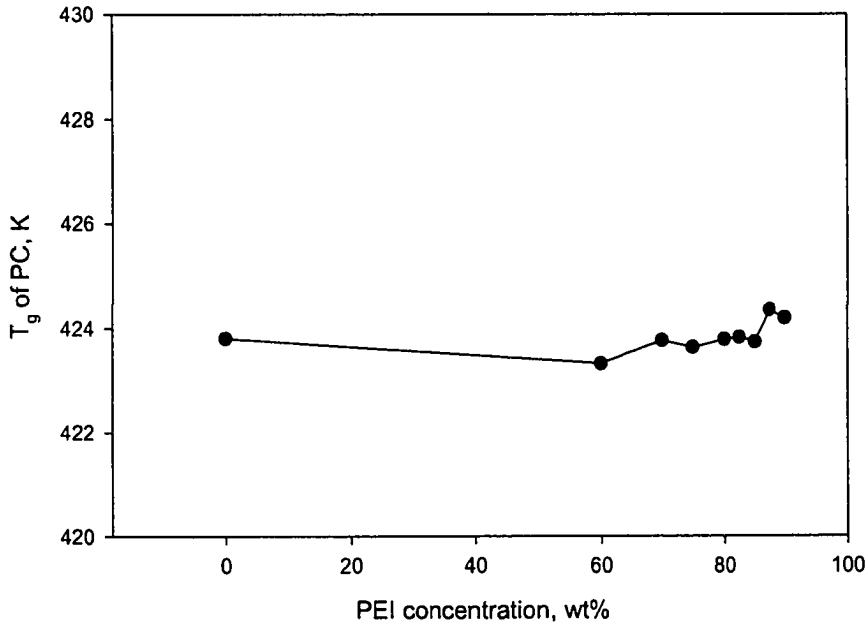

Figure 4.3: Concentration dependence of T_g of PC in PEI/PC blends

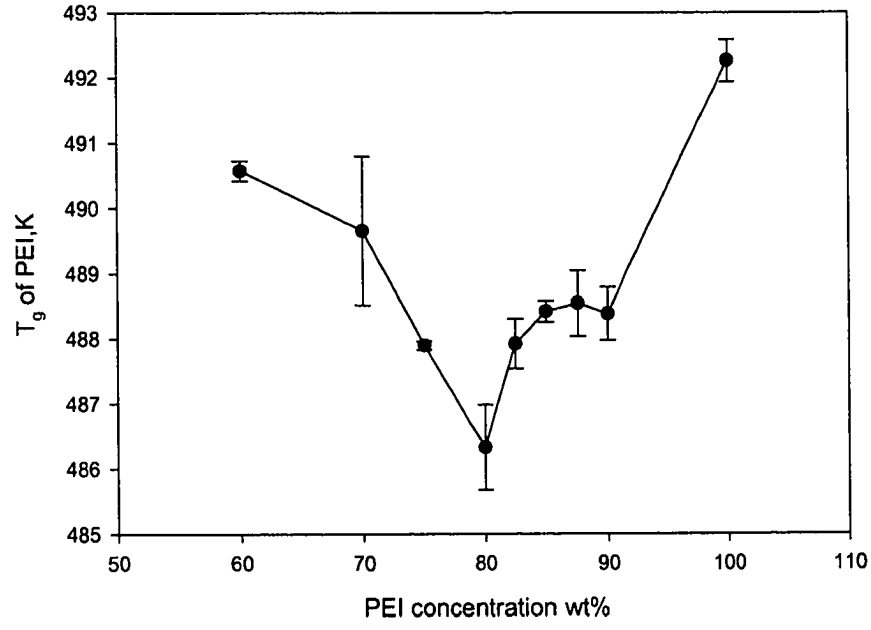

Figure 4.4: Concentration dependence of T_g of PEI in PEI/PC blends

materials exchange between the droplets will be impossible because of the low mobility in the glassy state, which prevents the coalescence between droplets. Similar phenomena has been observed for polystyrene and poly (methylphenylsiloxane) blends [Meier *et al.* 1995].

4.4.2 TEM results of PEI/PC blends

The efficiency of RuO_4 staining was first evaluated on 20:80 and 90:10 PEI/PC blends to permit unambiguous assignment of the major and minor phase. Figures 4.5(a) and (h) indicate that the PEI phase appears dark in TEM, while PC phase displays as white; therefore, compared with PC, PEI is selectively stained with RuO_4. The TEM micrographs of PEI/PC blends at different concentrations are shown in Figure 4.5 (a) to (h), which implying that PEI/PC blend systems are immiscible. Both matrix-droplet and co-continuous morphologies were observed. Below 50 wt% PEI (Figures 4.5 (a), (b) and (c)), PC is the matrix phase and PEI is dispersed in PC. The phase inversion, which is defined as a process in which matrix switches, takes place around 50wt% PEI. The PC matrix becomes the dispersed phase while the previously dispersed PEI phase becomes the matrix (Figures 4.5 (e), (f), (g), and (h)). At the intermediate blend ratio, the 50:50 PEI/PC blend showed a bicontinuous morphology as expected, the thickness of the commingling strings was about 2 μm (Figure 4.5 (d)). Below 70 wt% PEI, the size of the dispersed particle is almost the same, it is around 1 μm; however, at higher PEI concentrations, the size of the dispersed PC phase decreases dramatically, and the shape of the dispersed phase is more stretched compared with complementary blends with PC rich phase, especially at 80 wt%. The boundaries between PC and PEI in 80:20 PEI/PC

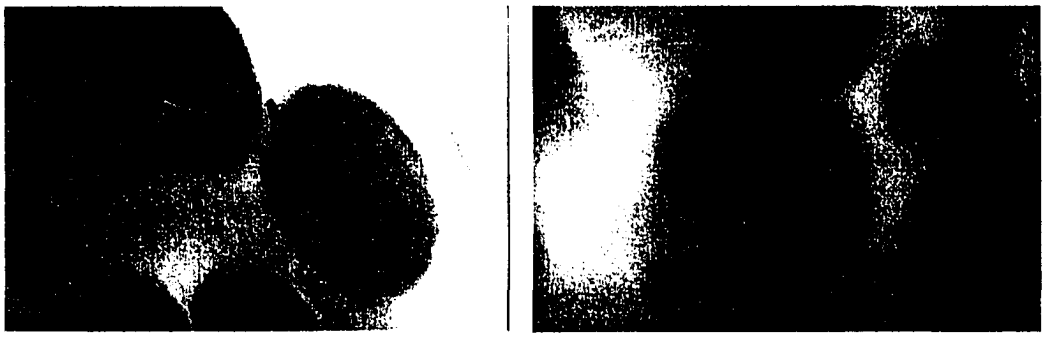

(a) PC/PEI 80:20 (b) PC/PEI 70:30

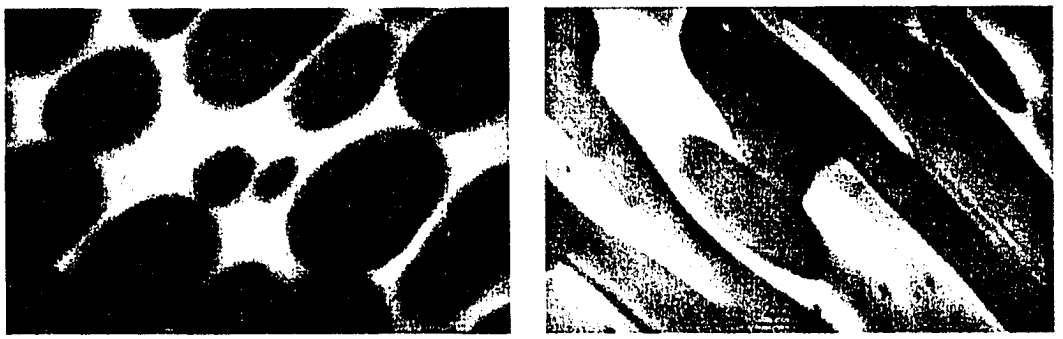

(c) PC/PEI 60:40 (d) PC/PEI 50:50

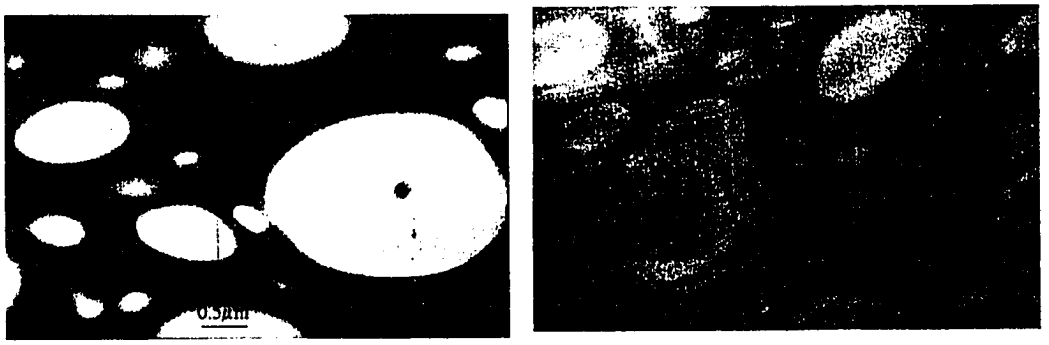

(e) PC/PEI 40:60 (f) PC/PEI 30:70

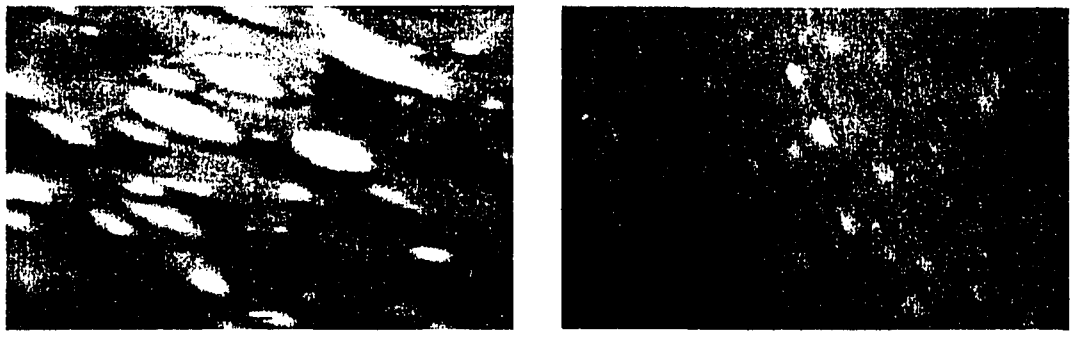

(g) PC/PEI 20:80 (h) PC/PEI 10:90

Figure 4.5 TEM micrograph of PC/PEI blends at different compositions

blend are not as sharp as in other blend ratios. Comparing 20:80 PEI/PC (Figure 4.5(a)) and 80:20 PEI/PC (Figure 4.5(g)) blends, it can be clearly seen that the dispersed phase size in PEI rich phase is much smaller than that in the PC rich phase, which is similar to the results in Chun *et al.*'s [1996] study of PC/PEI 90:10 and PC/PEI 10:90 blends. They attributed the difference to the viscosity ratio difference between PC rich phase and PEI rich phase. The viscosity values of PC and PEI are 240 Pa·s and 2850 Pa·s respectively at 340 ^{0}C with shear rate of 65 s^{-1} [Lin and Sundararaj 2004]. Therefore, the viscosity ratio of dispersed phase to matrix phase is much lower in the PEI rich phase than in the PC rich phase. The TEM results are qualitatively in agreement with our DSC measurements of the miscibility between PEI and PC; however, it should bear in mind that besides miscibility, there are other factors affecting the morphology observed in TEM, such as viscosity ratio, shear rate, elasticity of the components and processing conditions. It should be noted that although the polymer blend samples were in glassy state during microtoming, compression effect was unavoidable. The shape of the droplets may deform in the direction of cutting due to compression effect.

4.4.3 MD simulation results

4.4.3.1 Simulation of pure polymers

Cohesive energy density is one of the most important thermodynamic properties of a liquid and it is often used in the literature to validate the force field chosen for the simulation [Gestoso and Brisson 2001; Choi *et al.* 1998]. The cohesive energy density is defined in Chapter 2, equation 2.11. Compared with small molecules, Polymer molecules have a vanishing small vapor pressure and the molar energy of vaporization cannot be determined from experiment directly. MD simulation provides a direct method to calculate the cohesive energy density of polymers, and the molar energy of vaporization can be determined from $\Delta E_v \approx E_{vac} - E_{bulk}$, where E_{vac} and E_{bulk} are the potential energy of the system in vacuum state and in bulk state, respectively. They can be calculated from MD simulation. It should be pointed out that the concept of cohesive energy density of polymers is borrowed from the definition of small molecules; for polymers, because of the high internal degree of freedom, the configuration of a polymer chain in vacuum is not exactly the same as that of in the liquid state, Choi [2002] contended that the concept of cohesive energy density of polymers is ill-defined.

In the analysis of simulation results, the CED was sampled every 10 ps for the last 100 ps of the NVT simulation. The square root of CED is the solubility parameter. The solubility parameters of PC and PEI calculated based on DREIDING2.21, PCFF and COMPASS force fields are shown in Table 4.3. In this Table, the solubility parameters predicted from the group contribution and solvent swelling methods are also listed for the comparison purpose. Table 4.3 shows that the solubility parameter calculated based on PCFF force field did not match with the results obtained from the other two. It yielded a

much larger δ value than those obtained from DREIDING 2.21 and COMPASS force fields. Table 4.3 shows that the solubility parameters of PC we obtained based on COMPASS and DREIDING force fields are 19.21 and 19.93 $MPa^{1/2}$ respectively. They are fairly close to each other and also in good agreement with the experimental value and the value calculated from the group contribution method. The solubility parameters of PC from our simulation are also comparable with the values calculated by Hutnik *et al.* [1991], which are between 19.4 and 19.7 $MPa^{1/2}$. The DREIDING force field has been used By Kim and Liu [2001] to study the molecular motions of PC and Fan *et al.* [1994; 1997] for the simulation of static structure and mechanical properties as well as the local chain dynamics of PC. The DREIDING force field also has been found to give fairly accurate estimation of solubility parameter values of various systems [Choi 2000; Kavassalis *et al.* 1996; Fan *et al.* 2002] using the NVT ensemble. The solubility parameter of PEI calculated based on DREIDING 2.21 and COMPASS force fields are in the range of experimental value. However, it should be noted that there exists significant disagreement in the experimental values reported by different sources [White *et al.* 1982]. Our simulated solubility parameter of PEI is also comparable with value computed by Eichinger *et al.*[2003], which is in the range of 19.7-21.9 $MPa^{1/2}$. Compared with DREIDING 2.21 and COMPASS force fields, both of them yielded comparable results; however the COMPASS force field takes about 7 to 10 times longer CPU time than the DREIDING 2.21 force field to do the same time scale simulation. Therefore, the DREIDING 2.21 force field was chosen for subsequent simulations of PEI/PC blend. It should be noted that this force field is not suitable for NPT ensemble because it cannot reproduce the experimental density. It should also be noted that when we use the NVT

ensemble with the DREIDING 2.21 force field, the simulation often yields relatively large pressures.

Table 4.3: Solubility parameters of PEI and PC simulated by different force fields at 298K

Name	Repeating units	MWT	Solubility parameter ($MPa^{0.5}$)			
			DREIDING 2.21	PCFF	COMPASS	Experimental
PC	23	5851	19.93	22.02	19.21	19.65[a] 20.3[b]
PEI	10	5928	21.77	25.94	19.69	19.01-23.92 [c]

a: Calculated from group contribution
b: David and Misra 1999
c: White *et al.* 1982

Because of the limited computational resources, simulation cannot be performed on the actual size of polymers. However, to some extent, the size of the molecule used in the model is important in order to calculate accurate thermodynamics properties. Therefore, it is necessary to study what minimum molecular size is sufficient to represent the real polymer. To this end, the solubility parameters of PC and PEI with different molecular weights were calculated. The molecular weight dependence of the solubility parameters of PC and PEI are shown in Figures 4.6 and 4.7, respectively. Figure 4.6 shows that the solubility parameter of PC decreases sharply at first as the molecular weight increases, but levels off when the molecular weight is greater than 2,500 (ca. 10 repeating units). Similar molecular weight dependence of the solubility parameter of

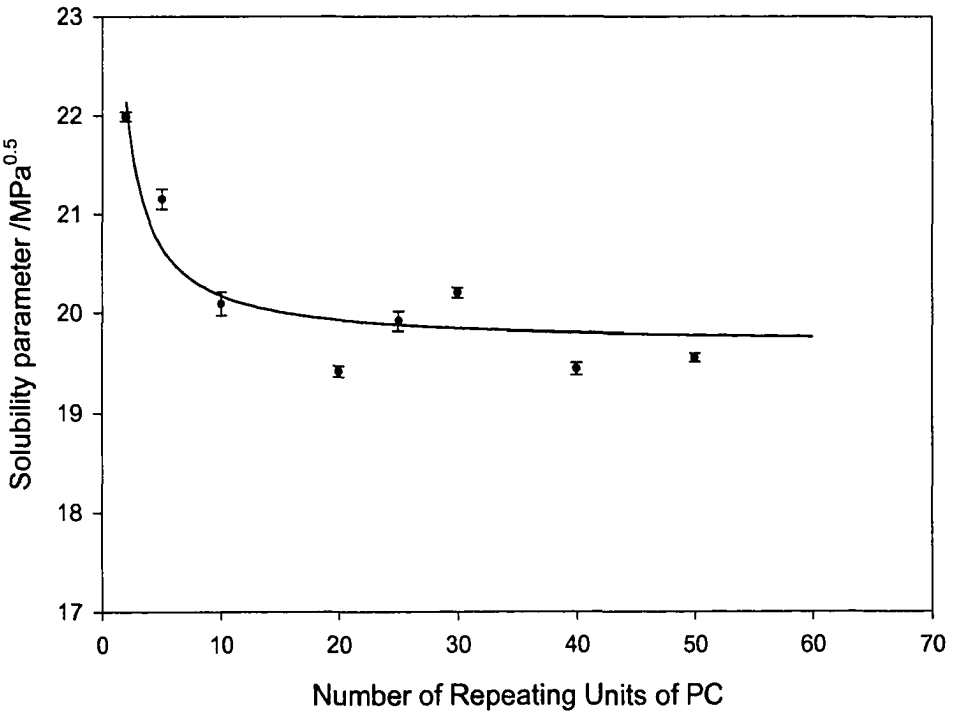

Figure 4.6: Computed solubility parameter of PC versus number of repeating units

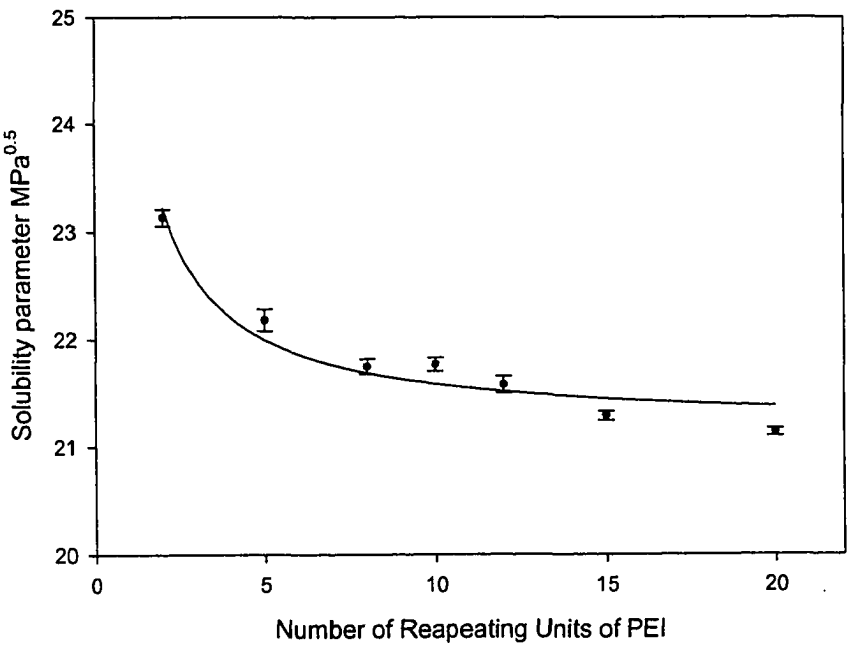

Figure 4.7: Computed solubility parameter of PEI versus number of repeating units

PMMA was observed by Patnaik and Pachter [2002]. For PEI, Figure 4.7 shows that the solubility parameter for PEI has a similar trend and δ starts to approach a constant value when the number of repeating units is greater than 8 (M_n=4,740). For the remainder of the simulations, 23 repeating units (M_n=5,851) were chosen for the PC molecule while 10 repeating units (M_n=5,928) were chosen for the PEI molecule. The PC and PEI used in the experiment had matching molecular weight ($M_{n,PC}$=31,600, $M_{n,PEI}$=30,000), and the PC and PEI molecules used in the simulation also had matching molecular weights. Previous researches have reported reasonable results when they used 21 repeating units for the simulation of PC [Fan *et al.* 1994; Fan *et al.* 1997].

4.4.3.2 MD simulation of PEI/PC blends

The NVT molecular dynamics trajectory files were created for each blend concentration. The time required for equilibrium depends on the size of the system, and the time was determined by running the simulation until a stable energy was attained for the system. The mean potential energies of the bulk and the vacuum states were then calculated by using the time average of the potential energy values over the last 100 ps of the trajectory.

Once the average total energy values were obtained for each system, ΔH_m can be calculated for the blend systems using the fact that ΔH_m is approximately equal to ΔE_m in these systems. The energy change during mixing for each type of energy was also calculated and they are summarized in Table 4.4. The system label in this table is the same as in Table 4.2. Figure 4.8 is the plot of molar enthalpy change, ΔH_m and Gibbs free energy change upon mixing, ΔG_m, versus blend concentration. The ΔG_m was

calculated from ΔH_m using the combinational entropy changes, ΔS_m^{comb} from the Flory-Huggins theory for mixing the two materials:

Table 4.4: Energy changes upon mixing (kcal/mol) for PEI/PC blend systems

System Label	ΔE_b	ΔE_θ	ΔE_ϕ	ΔE_{inv}	ΔE_{vdw}	ΔE_Q
2	28.95	11.64	-8.81	0.40	4.70	14.01
3	17.50	19.13	-12.58	-0.68	6.38	14.75
4	14.11	10.19	-0.04	-1.90	-1.43	10.62
5	15.93	7.98	-12.74	-3.25	15.87	18.79
6	27.76	12.40	-11.20	-2.28	-2.84	-4.07
7	32.04	17.63	-3.59	2.54	8.00	38.00

$$\Delta G_m = \Delta H_m - T\Delta S_m^{comb} \qquad (4\text{-}11)$$

Fig. 4.8 shows that the ΔH_m and ΔG_m curves are similar. However, polymer researchers usually use χ instead of ΔH_m. The χ values calculated using equations 4.9 and 4.10 are plotted versus concentration of PEI in Figure 4.9. The critical interaction parameter is also shown in this figure. The simulation results are in agreement with the experimental results. The calculated χ value is positive and larger than the critical χ value (from equation 4.8) calculated based upon the chain lengths of the components used, which indicated that these two polymers were immiscible. Table 4.4 shows that except the torsional energy and inversion energy change upon mixing are negative, other energy components change upon mixing are positive.

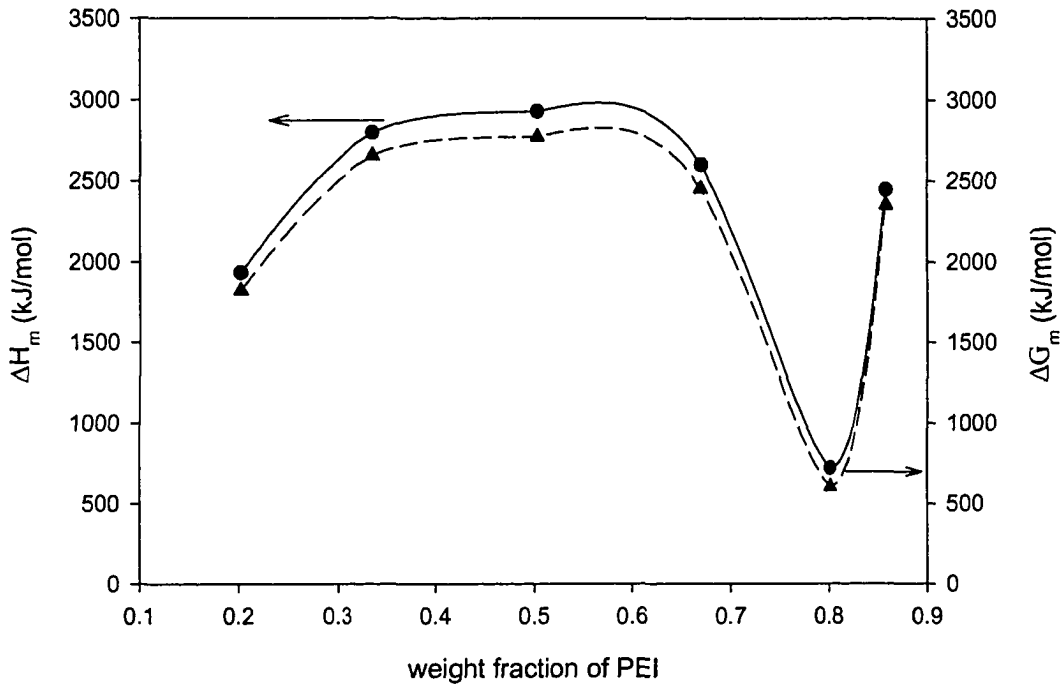

Figure 4.8: Molar enthalpy and Gibbs free energy changes upon mixing versus weight fraction of PEI

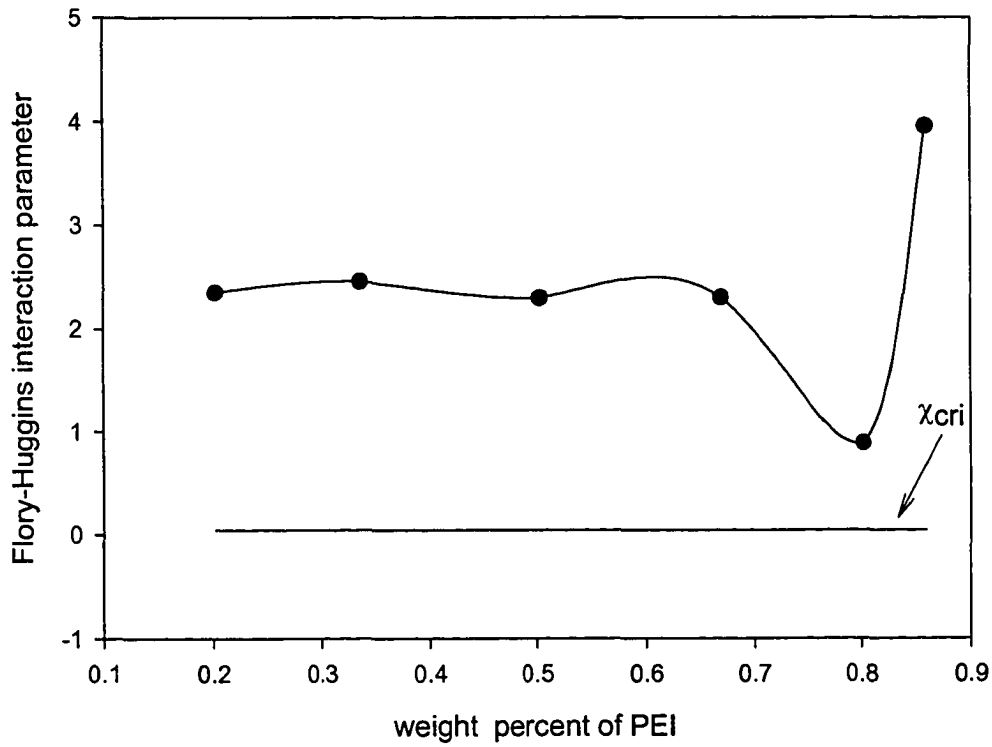

Figure 4.9: Flory-Huggins interaction parameter versus volume fraction of PEI

The present results, which are based on the use of DREIDING 2.21 force field, indicate that immiscibility of this binary polymer blend could be due to the bond stretching energy, bond angle bending energy and electrostatic energy. Heine *et al.* [2003] also observed that the intramolecular interactions could drive a blend system to phase separate in the simulation of isotactic polypropylene and polyethylene blends. The energy origin of the immiscibility of PEI/PC blends is different from that of PC/PBT blends that we will discuss in Chapter 6. Another noteworthy point is that the composition dependence of χ at approximately 80% of PEI is not smooth and monotonic; this is not consistent with what is predicted by Flory-Huggins theory. This is mainly attributed to the fact that the simulations were carried out by incorporating local concentrations of the polymers and the shapes of their repeating units. In other words, the mean field approximation, which is required in the original Flory-Huggins theory, was not appliable here.

The concentration dependence of χ calculated from simulation (Figure 4.9) has the same trend as the concentration dependence of the glass transition temperature of the PEI rich phase (Figure 4.4). The change in χ with concentration was due mainly to the van der Waals and electrostatic energy. The value of χ calculated in this paper using MD is greater than that calculated by Chun *et al.* [1995] using measured glass transition temperatures. The χ values from Chun *et al.* ranged from 0.198 to 0.271 with blend compositions whereas our values are an order of magnitude larger. The method used by Chun *et al.* to calculate the Flory-Huggins interaction parameter is delineated in Kim and Burns [1987; 1989; 1990a, 1990b]. For most concentrations, the χ calculated from MD in our work is also greater than that calculated from equation 2.12 using the δ from the MD (χ=1.053). Again, it should be kept in mind that there is no concentration dependence for

the χ value determined from equation 2.12. At 80 wt% PEI, the χ calculated directly from the energies obtained from MD is smaller than the one calculated using equation 2.12.

There are several reasons that may contribute to the quantitative disagreement between Chun *et al.*'s values and our values. First of all, the χ from experimental data was based on the apparent volume fractions of the blend system, while the χ calculated from simulation was based on the atomic level volume fraction. Secondly, for PEI/PC blends, because they are immiscible, there is no specific interaction between these two polymers, and the entropy effects may have an influence; but entropy effects are not included in the MD simulation calculation. Usually, entropy effects can be ignored. Thirdly, DREIDING 2.21 is a generic force field, and some parameters in this force field may need to be modified to make it suitable for our system. It was encouraging that the solubility parameters obtained using the DREIDING 2.21 force field in this work were comparable to literature results that were obtained by using other force fields such as COMPASS that is claimed to be more comprehensive.

4.5 Summary

The thermal analysis and TEM results showed that the PEI/PC blends are immiscible in all blend concentrations, and that there is some anomalous thermodynamic behavior in these blends. From the T_g measurements, it was found that a small amount of PC was incorporated in the PEI rich phase, but it was not the case for the PC rich phase. Based on DREIDING 2.21 and COMPASS force fields, the MD NVT simulation of PEI and PC yielded δ values that are in good agreement with experimental values in literature. Using the DREIDING 2.21 force field, the molecular dynamics simulation of

PEI/PC blends showed that these two polymers are immiscible and the concentration dependence of χ calculated from simulation has the same trend as the concentration dependence of the glass transition temperature measurements. However, the χ calculated from simulation does not quantitatively match the value obtained using experimental data. The NVT MD simulation proved to be a useful way to understand the underlying forces that are responsible the miscibility of PEI/PC blends. Since the polymer blend system studied was a very large system with complex molecules, the MD simulation consumed significant computer resources. A more efficient integration algorithm will improve our ability to do efficient MD simulation of these engineering polymer blends.

4.6 References

Akiyama, S.; Ishikawa, K.; Kawahara, S. and Akiba, I. (2001) Interaction in Blends of Bisphenol-A Polycarbonate and Poly(stryrene-co-methacrylic acid), *Polymer*, 42(15):6657-6660.

Bafna, S.S.; Sun, T. and Baird, D.G. (1993) The Role of Partial Miscibility on the Properties of Blends of a Polyetherimide and 2 Liquid-crystalline Polymers, *Polymer*, 34(4):708-715.

Ballone, P.; Montanari, B.; Jones, R.O.; Hahn, O. (1999) Polycarbonate Simulation with a Density Functional Based Force Filed, *J. Phys. Chem. A*, 103(27): 5387-5398.

Chapman & Hall (2004) *Polymers, a Property Database,* http://www.polymersdatabase.com.

Cho, J.H.; Park, M.S.; Choi, J.H.; JI, B.C.; Han, S.S. and Lyoo, W.S. (2001) Miscible Blends of nitro-Substituted Polybenzimidazole and Polyetherimide, *J. Poly. Sci.B: Poly. Phys.*, 39(15): 1778-1783.

Choi, P.; Blom, H.P.; Kavassalis, T.A. and Rudin, A. (1995) Immiscibility of Polyethylene and Polypropylene- Molecular Dynamics Study, *Macromolecules*, 28(24): 8247-8250.

Choi, P (2000) Molecular Dynamics Studies of the Thermodynamics of HDPE/Butene-Bases LLDPE Blends, *Polymer*, 41(24): 8741-8747.

Chun, Y.S.; Lee, H.S.; Kim, W.N. and Oh, T.S. (1996) Thermal Properties and Morphology of Blends of Poly(ether imide) and Polycarbonate, *Polym. Eng. Sci.*, 36(22): 2694-2702.

Chun, Y.S.; Lee, H.S. Oh, T.S. and Kim, W.N. (1995), Blends of Poly(ether imide) and Polycarbonate and the Determination of the Polyemr-polymer Interaction Parameter of the Two Polymers, *Polymer(Korea)*, 19(6): 913-920.

David, D.J. and Misra, A. (1999) . *Relating materials properties to structure: handbook and software for polymer calculations and materials properties.* Technomic, Lancaster.

Eichinger, B.E.; Rigby, D. and Stein, J. (2002) Cohesive Properties of Ultem and Related Molecules from Simulation, *Polymer*, 43(2): 599-607.

Fan, C.F.; Cagin, T; Chen, Z.M. and Smith, K.A. (1994) Molecular Modeling of Polycarbonate 1. Force Field, Static Structure, and Mechanical Properties, *Macromolecules*, 27(9): 2383-2391.

Fan C.F.; Olafson, B.D.; Blanco, M. and Hsu, S.L. (1992) Application of Molecular Simulations to Drive Phase-Diagrams of Binary-Mixtures, *Macromolecules*, 25(14):3667-3676.

Fan, Z.G.J; Williams, M.C. and Choi, P. (2002) A Molecular Dynamics Study of the Effects of Branching Characteristics of LDPE on Its Miscibility with HDPE, *Polymer*, 43(4):1497-1502.

Heine, D.; Wu, T.; Curro, J.G. and Grest, G.S. (2003) Role of Intramolecular Energy on Polyolefin Miscibility: Isotactic Polypropylene/Polyethylene Blends, *J. Chem. Phys.*, 118 (2): 914-924.

Hutnik, M.; Gentile, F.T.; Suter, U.W.; Ludovice, P.J. and Argon, A.S. (1991) An Atomic Model of the Amorphous Glassy Polycarbonate of 4,4'-Isopropylidenediphenol, *Macromolecules*, 24(22): 5962-5969.

Jung, H.C.; Lee, H.S.; Chun, Y.S.; Kim, S.B.; and Kim, W.N. (1998) Blends of a Thermotropic Liquid Crystalline Polymers and Some Flexible Chain Polymers and the Determination of the Polymer-Polymer Interaction Parameter of the Two Polymers, *Polym. Bull.*, 41(3):387-394.

Kavassalis, T.A.; Choi, P. and Rudin, A. (1996) In: Gubbins KE,Quirke N, editors. *Molecular simulation and industrial applications, methods, examples and prospects*. Amsterdam: Gordon and Breach.

Kim, M.H.; Kim, J.H.; Kim, C.K.; Kang, Y.S.; Park, H.C. and Won, J.C. (1999) Control of Phase Separation Behavior of PC/PMMA Blends and Their Application to the Gas Separation Membranes, *J. Poly.Sci. B: Poly. Phys.*, 37(21): 2950-2959.

Kim, S. and Liu, J. (2001) Molecular Modeling of Bisphenol-A Polycarbonate and Tetramethyl Bisphenol-A Polycarbonate, *Korea Polym. J.*, 9(3):129-142.

Kim, W.N. and Burns, C.M. (1990a) Phase-Behavior of Blends of Polycarbonate with Partially Miscible Polymers, *J. Appl. Poly. Sci.*, 41(7-8): 1575-1593.

Kim, W.N. and Burns, C.M. (1990b) Compatibility Studies of Blends of Polycarbonate and Poly(ethylene-terephthalate), *J. Poly. Sci. B: Poly. Phys.*, 28(9): 1409-1429.

Kim, W.N. and Burns, C.M. (1989) Thermal-Behavior, Morphology and the Determination of the Polymer-Polymer Interaction Parameter of Polycarbonate – Poly(butylenes terephthalate) Blends, *Makromol. Chem-Maromol. Chem.*, 190(3): 661-676.

Kim, W.N. and Burns, C.M. (1987) Thermal-Behavior, Morphology, and the Determination of the Flory-Huggins Interaction Parameter of Polycarbonate Polystyrene Blends, *J. Appl. Poly. Sci.*, 34(3): 945-967.

Konda, M.; Tanaka, M.; Miyamoto, M.; Kimura, Y. and Yamaguchi, A. (1998) Miscibility, Morphology and Tensile Properties of the Melt Blends of Liquid Crystalline Polyimide(PI-LC) with Two Different Thermoplastic Polyimides: Semicrystalline Polyimide (N-TPI) and Amorphous Poly(ether-imide) (PEI), *High Perform. Poly.*, 10(1):93-109.

Lee. S.; Lee, J.G.; Lee, H. and Mumby, S.J. (1999) Molecular Dynamics Simulations of the Enthalpy of Mixing of Poly(vinyl Chloride) and Aliphatic Polyester Blends, *Polymer*, 40 (18): 5137-5145.

Li, Y. and Mattice, W.L. (1992) Atom-based Modeling of Amorphous 1,4-cis-Polybutadiene, *Macromolecules*, 25(19): 4942-4947.

Lin, B. and Sundararaj, U. (2004) Visualization of Poly(ether imide) and Polycarbonate Blending in an Internal Mixer, *J. Appl. Poly. Sci.*, 92:1165-1175.

Macosko, C.W.; Guegan, P.; Khandpur, A.K.; Nakayaman, A.; Marechal, P. and Inoue, T. (1996) Compatibilizers for Melt Blending: Premade Block Copolymers, *Macromolecules*, 29(17): 5590-5598.

Mayo, S.L.; Olafson, B.D.; and Goddard, W.A. (1990) DREIDING-A General Force-Field for Molecular Simulations, *J. Phys. Chem.*, 94(26): 8897-8909.

Meier, G.; Vlassopoulos, D. and Fytas, G. (1995) Phase Separation and Glass Transition Intervention in a Polymer Blend, *Europhys. Lett.*, 30(6): 325-330.

Morales, A.R. and Bretas, R.E.S. (1996 a) Polyetherimide Poly(ether ether ketone) Liquid Crystalline Polymer Tenary Blends. 1. Calorimetric Studies and Morphology, *Euro. Poly. J.*, 32(3): 349-363.

Morales, A.R. and Bretas, R.E.S. (1996 b) Polyetherimide Poly(ether ether ketone) Liquid Crystalline Polymer Tenary Blends. 2. Approximated Interaction Parameters and Phase Diagrams, *Euro. Poly. J.*, 32(3): 365-373.

Nose, S. (1984) A United Formulation of the Constant Temperature Molecular-Dynamics Methods, *J. Chem. Phys.*, 81(1): 511-519.

Ohishi, H; Ikehara, T. and Nishi, T (2001) Phase Morphologies and Mechanical Properties of High-impact Polystyrene (HIPS) and Polycarbonate Blends Compatibilized with Polystyrene and Polyarylate Block Copolymer, *J. Appl. Poly. Sci.*, 80(12): 2347-2360.

Patnaik, S.S and Pachter, R. (2002) A molecular Simulation Study of the Miscibility in Binary Mixtures of Polymers and Low Molecular Weight Molecules, *Polymer*, 43(2): 415-424.

Paul D. R. and Bucknall C. B.(2000) *Polymer Blends*, John Wiley & Sons Inc., New York

Rajulu, A.V.; Rao, G.B. and Reddy, R.L. (2001) Miscibility of Polycarbonate/epoxy Resin in Dichloro Methane by Viscosity, Ultrasonic and Refractive Index Methods, *J. Poly. Mater.*, 18(2): 217-219.

Rappe, A.K. and Goddard, W.A. (1991) Charge Equilibrium for Molecular-Dynamics Simulations, *J. Phys. Chem.*, 95(8): 3358-3363.

Shih, J.H. and Chen, C.L. (1995) Molecular Dynamics Simulation of Bisphenol-A Polycarbonate, *Macromolecules*, 28(13): 4509-4515.

Spyriouni, T. and Vergelati, C. (2001) A molecular Modeling Study of Binary Blend Compatibility of Polyamide 6 and Poly (vinyl acetate) with Different Degrees of Hydrolysis: An Atomic and Mesoscopic Approach, *Macromolecules*, 34(15): 5306-5316.

Sun, H.; Ren, P. and Fried, J.R. (1998) The COMPASS Force Field: Parameterization and Validation fro Phosphazenes, *Comp. Theo. Poly. Sci.*, 8(1-2): 229-246.

Sundararaj, U.; Macosko, C.W.; Rolando, R.J. and Chan, H.T. (1992) Morphology Development in Polymer Blends, *Polym. Eng. Sci.*, 32(24):1814-1823.

Sundararajan, P.R. (1990) Correlation Between Conformational Features and the Glass-Transition Temperatures for a Homogeneous Series of Polycarbonates, *Macromolecules*, 23(9): 2600-2602.

Ullmann's encyclopedia of industrial Chemistry, (2000) 6th edition, Wiley, New York

Van Krevelen, D.W. (1997) *Properties of Polymers: Their Correlation with Chemical Structure; Their Numerical Estimation and Prediction from Additive Group Contributions*, 3rd edition, Elsevier, New York.

White, S.A.; Weissman, S.R. and Kambour, R.P. (1982) Resistance of a Polyetherimide to Environmental-Stress Crazing and Cracking, *J. Appl. Poly. Sci.*, 27(7): 2675-2682.

Chapter 5

Miscibility studies of PEI/PBT blends

5.1 Introduction

Blending of thermoplastic polyesters with other amorphous polymers or semi crystalline polymers has been widely studied in recent years. Poly(butylene terephthalate) (PBT), poly(ethylene terephalate) (PET), and poly(trimethylene terephthalate) (PTT), are three most important polyesters, the only difference between these polyesters are the methylene moieties per reaperting unit. Blends of PBT [Chen *et al.* 1997; Jang and Sim1998; Vallejo *et al.* 2001; Woo and Yau 1997], PET [Martinez *et al.* 1993, 1996; Chen 1995; Chen and Hsiao 1998] and PTT [Kuo *et al.* 2001; Huang and Chang 2002] with poly(ether imide) (PEI) have been extensively studied in the literature. In this chapter, the miscibility of PEI/PBT blends is investigated.

PEI is an amorphous polymer with high glass transition temperature, excellent mechanical properties and thermal stability; however, because of its amorphous nature, its solvent resistance is rather poor. And because of its high processing temperature, which is around 380 ^{0}C, the application of PEI is limited. PBT is a semi-crystalline polymer with a T_g of 40 ^{0}C and melting temperature of 227 ^{0}C. The potential disadvantage of PBT is its lower T_g. It may result in a decrease of its modulus at temperatures above T_g. Blending PEI with PBT is an alternative way to overcome the disadvantages of these two polymers. PEI/PBT blends are expected to improve the processibility of PEI and its chemical resistance. However, the PBT crystallization rate will also be reduced by blending with PEI. By blending with 10 wt% PBT, the pressure at

the exit of the extruder is reduced to 70% of the pure PEI [Vallejo *et al.* 2001]. Similar increase in the degree of ease of processibility has been observed for PEI/PET blends. By blending 25% PET with PEI can reduce the melt blend torque to half of the pure PEI [Martinez *et al.*1996].

Compared with mixing of small molecules, the combinatorial entropy of blends of two high molecular weight polymers is negligible. Unless there are some specific favorable interactions between the two types of polymers, most polymer blend pairs are immiscible. However, PEI was found to be miscible with the aforementioned polyesters and several other polymers. It has been reported in the literature that PEI/PBT, PEI/PET and PEI/PTT blends are completely miscible at all the blend compositions. Martinez *et al.* [1993;1996] showed that one single T_g is observed for the PEI/PET blends, which is generally believed to be a condition for miscibility [Olabisi 1979]; however, SEM results showed a biphasic structure for PEI/PET blends. For PEI/PBT blends, a single T_g was also observed in the DSC measurements for all the blend concentrations, the DSC results were confirmed by dynamic mechanical analysis (DMA). Only one single T_g relaxation peak was observed in the loss modulus curve, and it is believed that DMA could be used to detect phase heterogeneity on a smaller scale than DSC. SEM results also showed that the PEI/PBT blends are homogeneous [Woo and Yau 1997]. Similar results were reported for PEI/PTT blends [Kuo *et al.* 2001]. A rarely miscible quaternary blend system including PEI, PET, PTT and PBT were also reported [Woo and Lee 2003]. Besides polyesters, PEI has been found to be miscible with polymers, such as PEEK [Chen and Porter 1992; Chun *et al.*1999; Jonas *et al.*1998], PEKK [Hsiao and Sauer 1993]. This is quite unusual that PEI exhibits miscibility with quite a few structurally

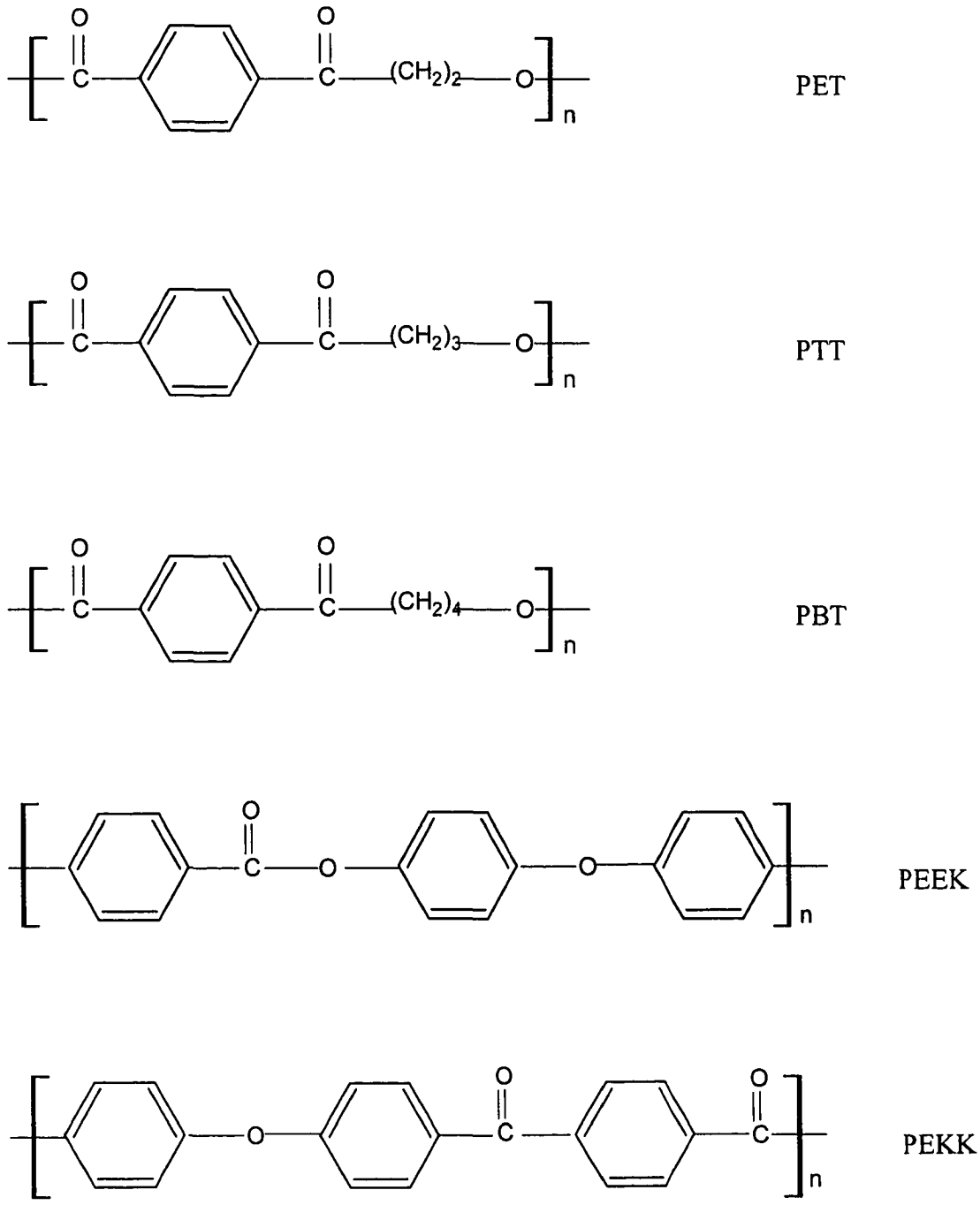

Figure 5.1: Chemical structures of polymers miscible with PEI

different polymers. The structures of some of those polymers that can form a miscible blend with PEI are shown in Figure 5.1.

The purpose of this study is two-fold. First of all, TEM of the quenched samples will be examined to confirm the miscibility of PEI/PBT blends observed in the literature due to the presence of a single T_g measured by DSC, DMA [Woo and Yau 1997] and DMTA [Jang and Sim 1998]. And because engineering thermoplastic blends are used at high temperatures sometimes, the morphology (i.e., their final properties) may change upon exposure to high temperature for a long time. Therefore, it is worth studying the morphology changes during annealing process. Secondly, it is believed that there exist strong intermolecular interactions between polyester and PEI; however, these interactions are experimentally unobservable and no clear explanation for PEI/polyester miscibility has been emerged. In this chapter, molecular dynamics (MD) simulation was used to investigate the miscibility origin of PEI/PBT blends; particular care was taken to investigate the intramolecular as well as intermolecular contributions to the potential energy of mixing.

5.2 Experiment

The polymers used in this work were Ultem 1000 (PEI) and Valox 315 (PBT), both of them were generously donated by General Electric Plastics. Their physical properties are listed in Table 5.1. PEI and PBT were dried in a vacuum oven overnight at 90 ^{0}C to remove any traces of volatile materials before their use. The PEI/PBT blends were prepared at 280 ^{0}C in a Haake Rheocord 90 series 600 batch mixer fitted with roller blades. After melt mixing, the sample was taken out from the indents of the roller blades

and quenched in liquid nitrogen. The specimens for the TEM study were prepared by microtoming using a Reichert-Jung ultracut microtome to obtain thin sections in the range of 60-100 nm. These sections were subsequently stained using RuO_4 and the stained thin sections were observed at room temperature using a Hitachi H-700 transmission electron microscope with accelerating voltage of 75 kV.

Table 5.1: Properties of PEI and PBT used in the current work

Polymer (Abbreviation)	Source	Molecular weight (M_w)	Specific heat C_p (J/kg/K)	Density ρ (kg/m^3)	T_g (^{0}C)	T_m (^{0}C)
Polyether imide: Ultem 1000 (PEI)	GE Plastics	30,000	1650 (150 ^{0}C)	1,270 (25 ^{0}C)	220	N/A
Polybutylene terephthalate, Valox 315 (PBT)	GE Plastics	110,000 M_n=33,000	1610 (25 ^{0}C)*	1,310 (25^{0}C)	39	227

*Cheng *et al.* 1988

The polymer blend film samples used for infrared transmission measurements must be sufficiently thin in order to produce infrared spectra that are recorded in the range that the Beer-Lambert law is valid. Usually the thickness of the film should be less than 10 μm [Simon, 2003]. Because of the high viscosity of the polymers we used, it is almost impossible to prepare such thin films by pressing a melt between two metal plates. Therefore, in this study, the thin films of PEI, PBT and PEI/PBT blends were prepared by solution casting. The PEI can be easily dissolved in dichloride methane. For pure PBT and PEI/PBT blends, 40/60 wt/wt of tetrachloroethylene/phenol mixture is used as the solvent to dissolve them. The solvent is removed under reduced pressure and at an

elevated temperature. In order to get rid of the phenol, the film was dipped in hot water for overnight and then placed in vacuum oven at 100 ^{0}C for 48 hours.

The spectrum was obtained on a Bio-Rad FTS 6000 FTIR spectrometer in the mid-IR region of 600–4000 cm^{-1}. The scan speed was 5 kHz at a resolution of 2 cm^{-1}. The sensitivity was set to 4. One hundred twenty-eight scans were used to obtain a spectrum.

5.3 Simulation methodology

In the last chapter, it has been shown that 10 repeating units were sufficient for the simulation of PEI, corresponding to a molecular weight of 5,927. For PBT, in order to determine the minimum molecular weight that should be used in the simulation, we performed simulation of different molecular weights of PBT at room temperature and calculated their solubility parameters. The molecular weight dependence of solubility parameter is shown in Figure 5.2. It indicates that at low molecular weight, the solubility parameters of PBT is around 22.5, while above 3,300 (about 15 repeating units), there is a sharp drop of the solubility parameter and the solubility parameters are almost constant above this molecular weight. In the simulation of PBT, 26 repeat units were used, corresponding to a molecular weight of 5,727.

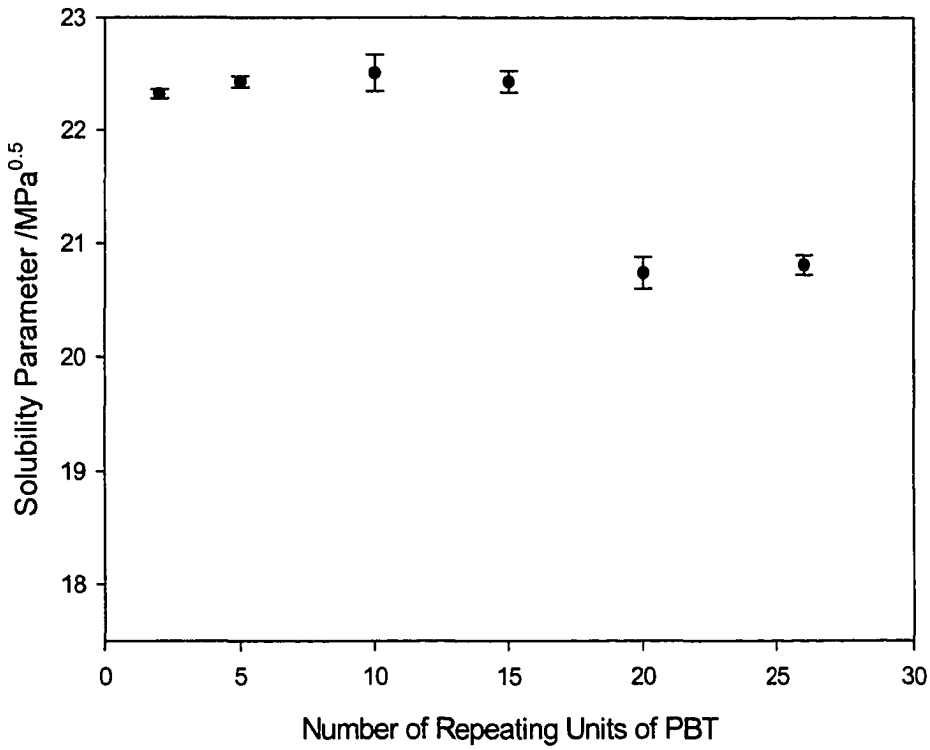

Figure 5.2: Computed solubility parameter of PBT versus number of repeating units

Different force fields were compared for the simulation of PBT with 26 repeating units. The solubility parameter of PBT at room temperature obtained from the DREIDING 2.21 force field was 22.79 $MPa^{1/2}$, and the value obtained from the PCFF force field was 18.68 $MPa^{1/2}$, they are either higher or lower than the value calculated based on the group contribution method, which is 20.2 $MPa^{1/2}$. Only the COMPASS force field yielded a comparable value with the group contribution method, i.e., 20.81 $MPa^{1/2}$. In the previous chapter, we have shown that COMPASS force field is also suitable for PEI simulation. The force field has also been used to investigate the cohesive energy density of PEI by Eichinger *et al.* [2002]. Therefore, the COMPASS force field was used for the following simulations of PEI/PBT blends. The concentration of

PEI/PBT blend was controlled by including different ratios of the number of PEI chains to that of chains PBT in the periodic boundary unit cells. The number of chains, densities and concentrations used in the simulation are summarized in Table 5.2. The density of the blend system was calculated from the density of the pure polymers at the blending temperature (280^0C) and concentration of each polymer assuming that components' volume are additive. The simulations of PEI/PBT blends were similar to what we have described in chapter 4 for the PEI/PC blend.

Table 5.2: Descriptions of model systems of PEI/PBT blends

System Label	Number of chains per unit cell	Concentration (volume PEI%)	Density (g/cm^3)	Molar volume (cm^3/mol)	χ
1	1PBT chain	0	1.0877	5,266	N/A
2	4PBT chains, 1PEI Chain	19.09	1.1078	5,207	-0.98
3	2PBT chains, 1PEI chain	32.06	1.1210	5,169	-3.90
4	1PBT chain, 1PEIchain	48.55	1.1390	5,117	-2.63
5	1PBT chain, 2PEI chains	65.36	1.1563	5,069	-4.04
6	1PBT chain, 4PEI chains	79.06	1.1709	5,028	-1.76
7	1PEI chain	100	1.193	4,969	N/A

5.4 Results and Discussion

5.4.1 TEM results

The TEM micrographs of quenched 80:20 PEI/PBT and 50:50 PEI/PBT blend are shown in Figures 5.3 (a) and 5.5 (a), respectively. Figures 5.3 (a) and 5.5 (a) demonstrated that no heterogeneous phase domains can be discerned for these two blend concentrations, which is in agreement with the SEM results of Woo and Yau's study [1997] and our simulation results which showed the Flory-Huggins interaction parameters between PEI and PBT are negative (see last column of Table 5.2). Therefore in the melt state, PEI/PBT blends are completely miscible. DSC study of this blend system also showed that only one single T_g existed for all blend concentrations [Chen *et al.* 1997].

The TEM result of a 80:20 PEI/PBT blend annealed at 200 ^{0}C for 8 hours in vacuum oven is displayed in Figure 5.3 (b). PBT crystallization was observed in the annealed PEI/PBT blend. In Figure 5.3 (b), the white layer-like lines corresponding to the PBT crystallites and the dark parts are the amorphous PEI/PBT regions, because the staining agent was rejected by crystallites and could only entered the amorphous region. The crystallization of PBT during annealing observed in TEM is also evidenced by the appearance of a melting endotherm at 216 ^{0}C in the DSC measurements (See Figure 5.4). Compared with the melting temperature of pure PBT, the depression of the apparent melting point of PBT by amorphous PEI is about 11 ^{0}C, this is also an indication of miscibility between PEI and PBT. Similar depression of the T_m was also observed in other semi-crystal/amorphous polymer blend systems [Huang and Chang 2002] and small molecule/BPA-PC blends [Khan *et al.* 2004].

A single glass transition temperature of 169 ^{0}C was observed for quenched 80:20 PEI/PBT sample (Figure 5.4), which corresponds to the value predicted from the Fox equation [Fox, 1956] for completely miscible polymer blends, the T_g of PEI is depressed by 51 ^{0}C. Although UCST [Chen *et al.* 1997] phase behavior has been observed for PEI/PBT blends, the sample was quenched rapidly from the melt state, the components in the system had been frozen and the specimen did not have sufficient time to undergo a phase transition. Therefore, a completely miscible morphology was observed from TEM and DSC measurements showed a single glass transition temperature. After annealing, a glass transition temperature of 178 ^{0}C was observed, which is 9 ^{0}C higher than the as quenched sample and corresponds to a glass transition occurred in the amorphous regions containing 85 wt% PEI calculated from Fox equation, the recovery of the T_g during annealing was also observed by Khan *et al.* [2004] in the study of TPD/BPA-PC blends. The increase of the glass transition temperature for the annealed sample can be attributed to the crystallization of PBT, after crystallization, some PBT was consumed, which results in an increase of PEI concentration in the amorphous phase, and hence an increase of T_g. Another reason is that a strong segregation of PEI have been occurred during the PBT crystallization. The PEI segregation was not only due to the crystallization, [Chen *et al.*1997] but also the liquid-liquid phase separation that took place simultaneously with the crystallization of PBT, just as what happened in PEI/PET blends [Chen 1995]. The UCST of the PEI/PBT blend was determined to be 215 ^{0}C [Chen *et al.*1997]; therefore, 200 ^{0}C is out of miscibility window of PEI/PBT blend and both phase separation and PBT crystallization occurred during the annealing.

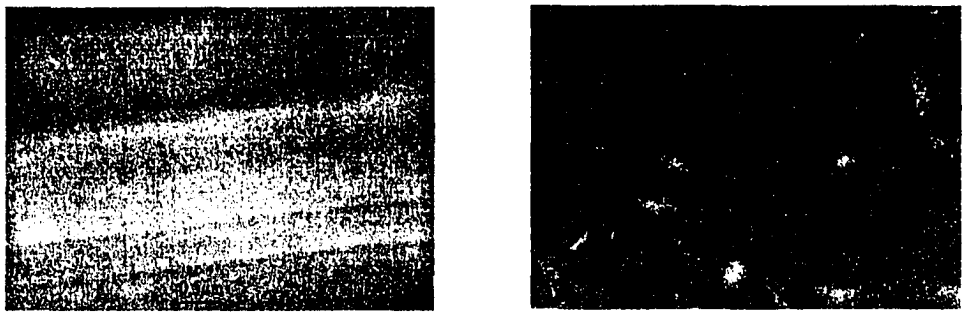

(a) (b)

Figure 5.3: TEM micrograph of 80:20 PEI/PBT blend (a) As quenched sample (b) annealing at 200 ^{0}C for 8 hrs

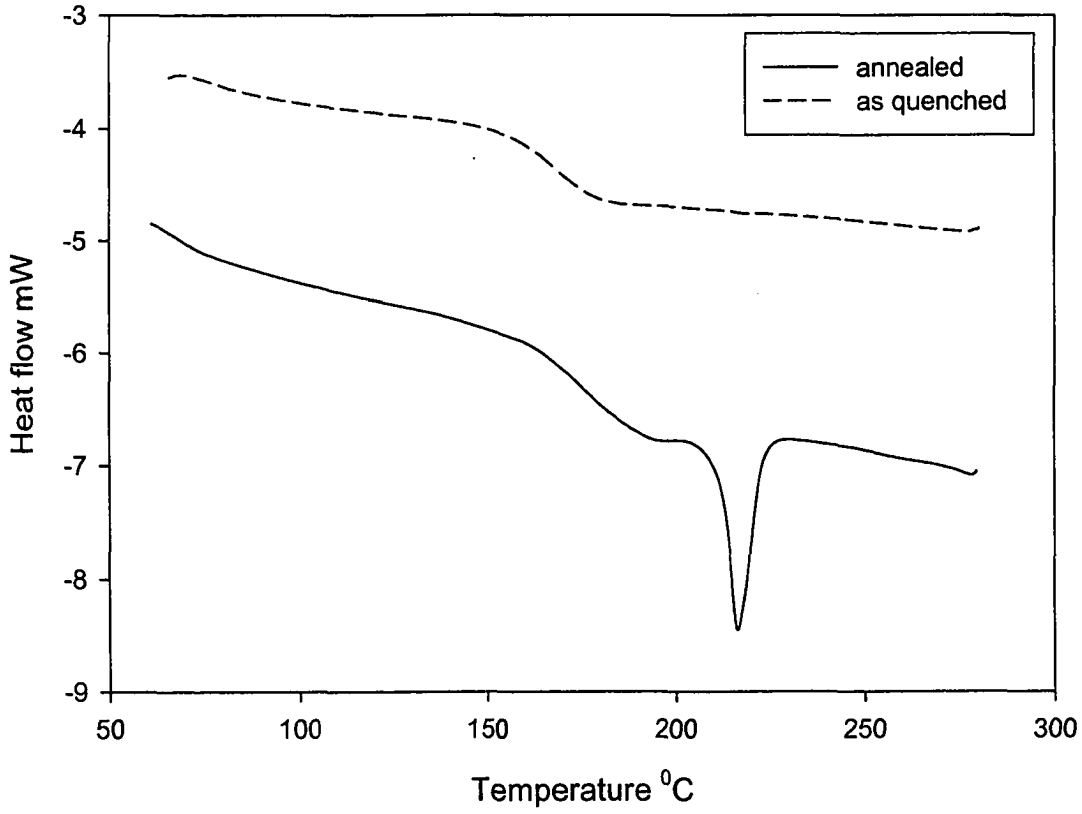

Figure 5.4: DSC of 80:20 PEI/PBT blend

Compared with as quenched morphology, the annealed 50:50 PEI/PBT blends also showed some structures corresponding to the PBT crystallization (Figure 5.5 (b)). We dissolved the PEI part in the blends by exposing the TEM grid to CH_2Cl_2 vapor for 3 days, the TEM micrograph of the etched sample is shown in Figure 5.5 (c). It indicated that during annealing, besides the PBT crystallization, the 50:50 PEI/PBT blend also undergoes spinodal decomposition. The two phase structure with unique periodicity and phase connectivity is one of the hallmarks of spinodal decomposition, the similar TEM results of PBT/PC-copolymer and PBT/PC blends were observed by Okamoto and Inoue [1994] and Hobbs *et al.* [1988], respectively. Optical micrographs of PEI/PET blends also showed similar results [Lee *et al.* 2002]. DMTA results of Jang and Kim [1998] also showed that there are two T_g's after annealing of PEI/PBT blends. The phase separation is of important consequence, especially when the materials are used at elevated temperatures.

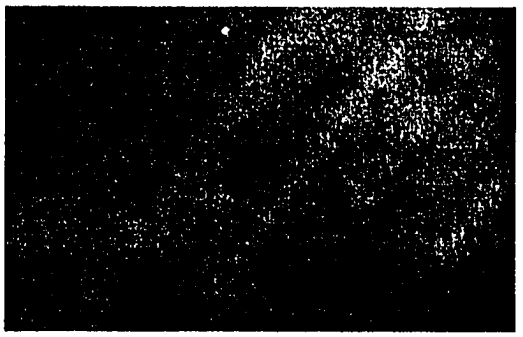

(a)

(b)

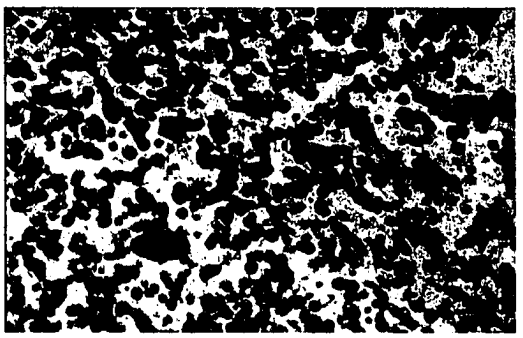

(c)

Figure 5.5: TEM micrograph of 50:50 PEI/PBT blend (a) As quenched sample (b) Annealing at 200 ^{0}C for 8hrs (c) dissolved PEI

5.4.2 FTIR results

The FTIR spectra of PEI and PBT are shown in Figures 5.6 and 5.7, respectively. For the spectrum of PBT, C=O stretching and (C=O)-O stretching vibration corresponded to peaks at 1,711 and 1,268 cm^{-1}, respectively [Jang and Sim 1998]. In the spectrum of PEI, the C=O symmetric stretching and asymmetric stretching appeared at 1,780 and 1,724 cm^{-1} respectively, and C=N stretching vibration appeared at 1,724cm^{-1} and 1,356

cm^{-1} respectively [Huang and Woo 2000]. The peaks at 1,275cm^{-1} and 1,237 cm^{-1} were due to the asymmetric C-O-C stretching vibration of PEI.

In the literature, carbonyl peak is one of the widely used peaks in the analysis of FTIR spectra because it shows an important shift owing to the electron density change resulting from the environmental elements. Figure 5.8 shows the FTIR spectra of 80:20 PEI/PBT and 50:50 PEI/PBT blends and the spectra of pure polymers in the wave number range of 1,700 to 1,800 cm^{-1}. No significant shift was observed for C=O absorption at 1,780 cm^{-1} for the blends in Figure 5.8. It also indicated that for 80:20 PEI/PBT blend, a broad absorbance peak around 1,723 cm^{-1} was displayed, while for 50:50 PEI/PBT blends, the C=O peaks of the pure polymers at 1,724 and 1,711 cm^{-1} disappeared, and a new peak at 1,720 cm^{-1} was emerged. This is qualitatively in agreement with our simulation results that the Flory-Huggins interaction parameter at 50% is smaller than that in 80% PEI. It should be noted that the overlap of the C=O absorptions at 1,711 and 1,724 cm^{-1} makes it difficult to calculate the wave number shift due to molecular interactions. Similar FTIR spectra were observed for PEI/PBN (poly(butylenes naphthalate)) blends [Lin and Wang 2001]. These FTIR results suggested that there exist some specific interactions. MD simulation can give us a molecular detail of these interactions.

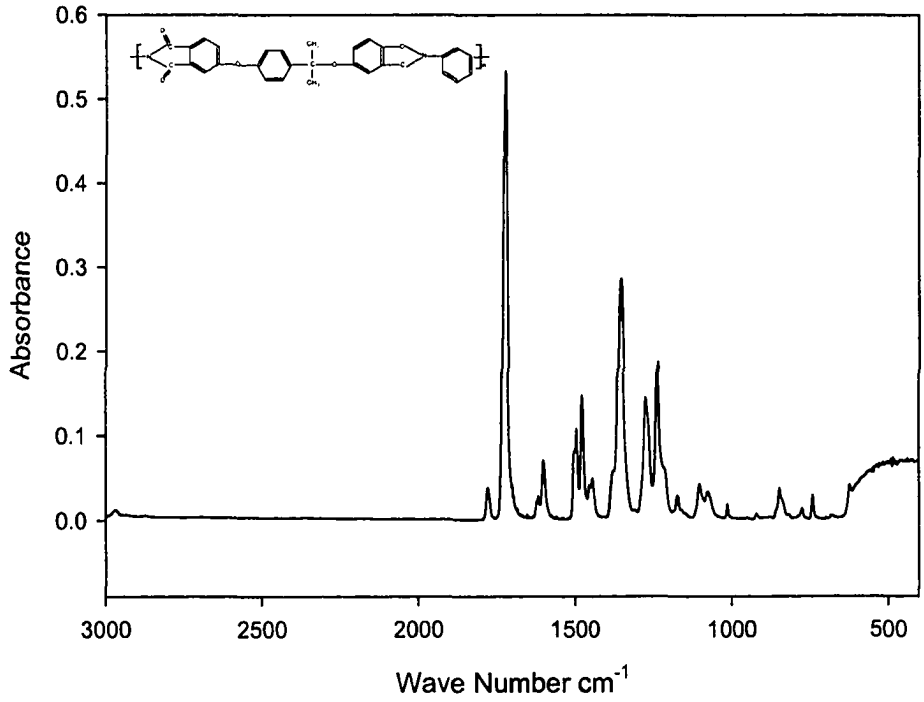

Figure 5.6: FTIR spectrum of PEI

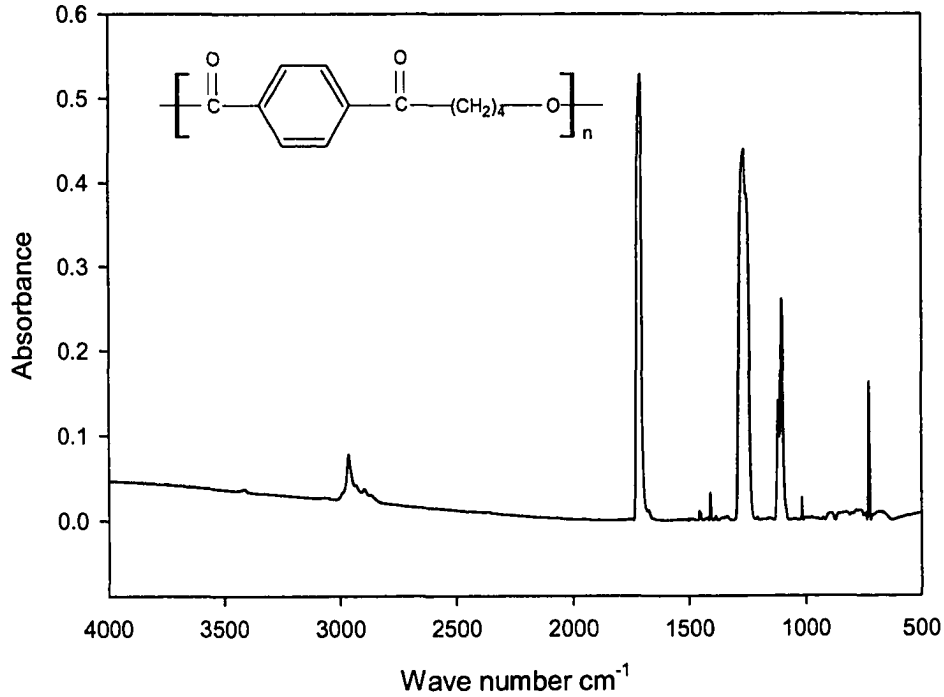

Figure5.7: FTIR spectrum of PBT

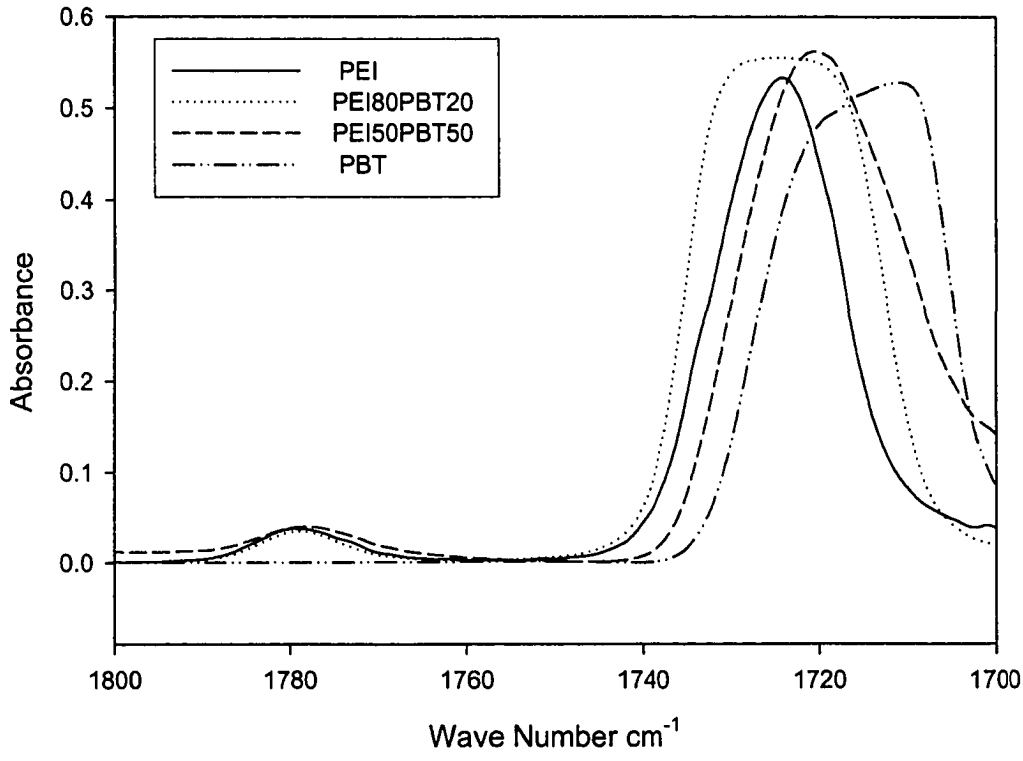

Figure 5.8: FTIR spectra of PEI/PBT blends

5.4.3 Simulation Results

The critical Flory-Huggins interaction parameter calculated based on equation 2.6 is 0.079; here, N_{PEI}=24 and N_{PBT}=26 were used. The specific volume of a PBT repeating unit was taken as a reference volume. The χ values calculated from MD simulation using equations 4-9 and 4-10 at different concentrations are shown in the last column of Table 5.2. Flory-Huggins interaction parameters between PEI and PBT are negative at all simulated concentrations. Being negative, they are obviously smaller than the critical interaction parameter, which means that they are completely miscible in the melt state. This is in agreement with previous experimental results. The simulation results also

confirmed that the miscibility between PEI and PBT are miscible even without transesterification between PEI and PBT [Chen 1995].

Table 5.3: Values of solubility parameters of PEI and PBT from simulation and PVT data fitting

Polymer	MD simulation		Polynomial fitting	FOV EOS fiiting	Experiment
	280 ^{0}C	25 ^{0}C	280 ^{0}C	280 ^{0}C	25 ^{0}C
PEI	19.08	21.06	19.28	20.62	19.01-23.92[a]
PBT	17.05	20.81	N/A	N/A	20.2 [b]

a: White *et al.* 1982
b: Van Krevelen, 1997.

Compared with the simulated solubility parameters of PEI and PBT (see Table 5.3), there is only 1.2% difference at room temperature; however, the difference at 280 ^{0}C is as large as 2 MPa$^{1/2}$. It should be noted here that our simulated solubility parameter of PBT at 280 ^{0}C is much lower than the values extracted from surface tension by Sauer and Dee [2002]. The solubility parameter of PBT at 260 ^{0}C is 20.49 [Sauer and Dee 2002], which is close to our simulated value at room temperature (20.81 MPa$^{1/2}$). We believe that the solubility parameters listed in Sauer and Dee's paper may not be accurate. The solubility parameters of PET and PTT extracted from surface tension are also higher than the value determined from group contribution methods [Van Krevelen, 1997]. For PET, the experimental value at room temperature is in the range of 19.90 to 21.89 MPa$^{1/2}$ [Van Krevelen 1997], while the solubility parameter of PET at 300 ^{0}C inferred from surface

tension is 21.77 $MPa^{1/2}$ [Sauer, 2002]. For PTT, the solubility parameter obtained from molecular dynamics simulation is 20.8 $MPa^{1/2}$ [Jang and Sim 1999] at room temperature compared with 20 $MPa^{1/2}$ at 260 ^0C derived from surface tension. Although the solubility parameters of PET, PBT and PTT in melt state are quite different [Sauer and Dee 2002], all of them are found to be completely miscible with PEI. Therefore, caution must be excised when using the solubility parameter method (equation 2-12) to estimate the miscibility of polymer blends.

The calculated Flory-Huggins interaction parameter in the melt from MD simulation is qualitatively consistent with the melting point depression method results; both methods result in negative interaction parameters; however, the absolute values of χ calculated from experiment and simulation are different. The χ value calculated based on melting point depression method is about –0.62 [Woo and Yau 1997], which is close to the value of interaction parameter for PEI/PET blends, -0.66 [Martinez *et al.* 1993]. It is different from the simulated values, which are in the range of -0.98 to -4.04. Several factors may contribute to the quantitative disagreement. First of all, it is due to the choice of the reference volume. The interaction parameter χ, which is defined in terms of energy per lattice site, is proportional to the reference volume used for the calculation. However, the choice of reference volume is somewhat arbitrary. In the original Flory-Huggins polymer solution theory, the solvent volume is taken as the reference volume; for polymer blends, generally the smaller repeating unit's molar volume between the two polymers is taken as the reference volume. In this work χ was calculated using the molar volume of a PBT repeat unit at 280 ^0C as the reference volume, which is 202.54 cm^3/g. In the melting temperature depression method, the χ value depends on the molar volume

ratio of repeat units of crystalline and amorphous polymers [see Chapter 2, Equation 2-8]. Secondly, in our simulation, the χ values calculated from simulation reflects the interactions between PEI and PBT in the melt state; however, experimentally, the PBT crystallizes during the quenching process, even though the amount of crystallite was small. Therefore, during quenching, PEI would be rejected from the crystalline portion of PBT. Similar phenomenon has been observed for PEI/PEEK blends [Jonas *et al.*1998] and PEI/PET blends [Chen 1995]. The χ value obtained from experiments only reflects the interaction of the amorphous parts of polymer blends. This may be another reason that our simulated χ value is much lower than the experimental one. Thirdly, the melting temperature depression method may not be reliable owing to small melting temperature depression. It may result in quite large errors. The reliability of deriving interaction parameters based on this method is critically examined in the literature [Runt and Gallagher 1991; Rim and Runt 1984] and it was not recommended for the calculation of interaction parameter. The quantitative disagreements between simulated and experimental interaction parameters are also observed by Akten *et al.* in the simulation of polyethylene and polypropylene. They attributed the difference to differences in molecular weight and the force field used for the simulation [Akten and Mattice 2001].

Table 5.4 presents the average potential energy per chain along with its decomposition into two components arising from the short-ranged intramolecular interactions, i.e., valence terms and cross terms and long range intermolecular interactions represented by van der Waals interactions and electrostatic interactions. The valence energies of PEI and PBT in their pure state are approximately the same as in the blend environment. The information in Table 5.4 is used to calculate the enthalpy

Table 5.4: Average energy (kcal/mol) per chain and the contributions to the average from the valence and intermolecular interactions (VDW and electrostatic energies) and cross terms

System Label	Total Potential Energy	Valence Energy (PBT)	Valence Energy (PEI)	Cross Terms	VDW	Electrostatic
1: Pure PBT	1,527	1,041		-101	-154	742
2: PBT4PEI1	1,304	1,040	1,441	-120	-159	463
3: PBT2PEI1	1,148	1,033	1,440	-133	-165	278
4: PBT1PEI1	973	1,047	1,443	-150	-166	44
5: PBT1PEI2	783	1,032	1,446	-166	-173	-186
6:PBT1PEI4	644	1,052	1,450	-180	-175	-371
7: Pure PEI	433		1,446	-201	-161	-651

changes upon mixing of PEI and PBT. The energy changes during mixing for all types of energy were calculated and are summarized in Table 5.5. It shows that van der Waals interaction is the main contribution to the miscibility of PEI/PBT blends, which is in contrast to the fact that the van der Waals interaction is responsible for the immiscibility of PC/PBT blends as will be discussed in chapter 6. According to Utracki [Utracki 1990], there are three main contributions to the Flory-Huggins interaction parameter: dispersion forces, free volume and specific interactions. In our simulated systems, since free volume change of mixing was not modeled, and intra-molecular interaction energy did not change much upon mixing except for system 2 (19% PEI). It means that miscibility of PEI and PBT blends results from the favorable van der Waals interaction between PEI

and PBT. It is in agreement with the miscible polymer blend systems comprising PEI, in which the miscibility are suspected to be attributed to closely matched dispersive forces, i.e., van der Waals forces rather than stronger specific interactions [Huang and Woo 2000; Woo and Tseng 2000].

Table 5.5: Energy changes upon mixing (kcal/mol) for PEI/PBT blend systems

System Label	ΔE_{Poten}	$\Delta E_{valence}$	ΔE_{cross}	$\Delta E_{valence}+\Delta E_{cross}$	ΔE_{vdw}	ΔE_Q	$\Delta E_{vdw}+\Delta E_Q$
2: PBT4PEI1	-4.30	-1.80	1.00	-0.80	-3.60	-0.40	-4.00
3: PBT2PEI1	-14.32	-7.30	1.33	-5.97	-8.67	0.33	-8.34
4:PBT1PEI1	-7.31	1.50	1.00	2.50	-8.50	-1.50	-10.00
5:PBT1PEI2	-15.11	-3.00	1.67	-1.33	-14.33	0.67	-13.66
6:PBT1PEI4	-7.95	5.40	1.00	6.40	-15.40	1.40	-14.00

Experimentally, it was observed that the composition dependence of glass transition temperature of PEI/PBT blends is asymmetric [Woo and Yau 1997], such behavior was also reported for PEI/PET blends [Chen 1995] and PEI/PTT blends [Kuo *et al.* 2001]. At low volume fractions of PEI, the effect of the PEI component on the glass transition is small; however, at higher concentrations of PEI, the contribution of PEI to raise the T_g is significant [Woo and Yau 1997]. They attributed this kind of behavior to the uneven contributions to the free volumes of the mixture of the pure polymers. Vallejo

et al. [2001] ascribed this to the decrease in crystallinity of PBT in the PEI/PBT blends with increasing PEI concentration. In our simulation, we found that the cohesive energy density of the blends showed similar trend with concentration as that of the experimental determined glass transitions [Woo and Yau 1997].

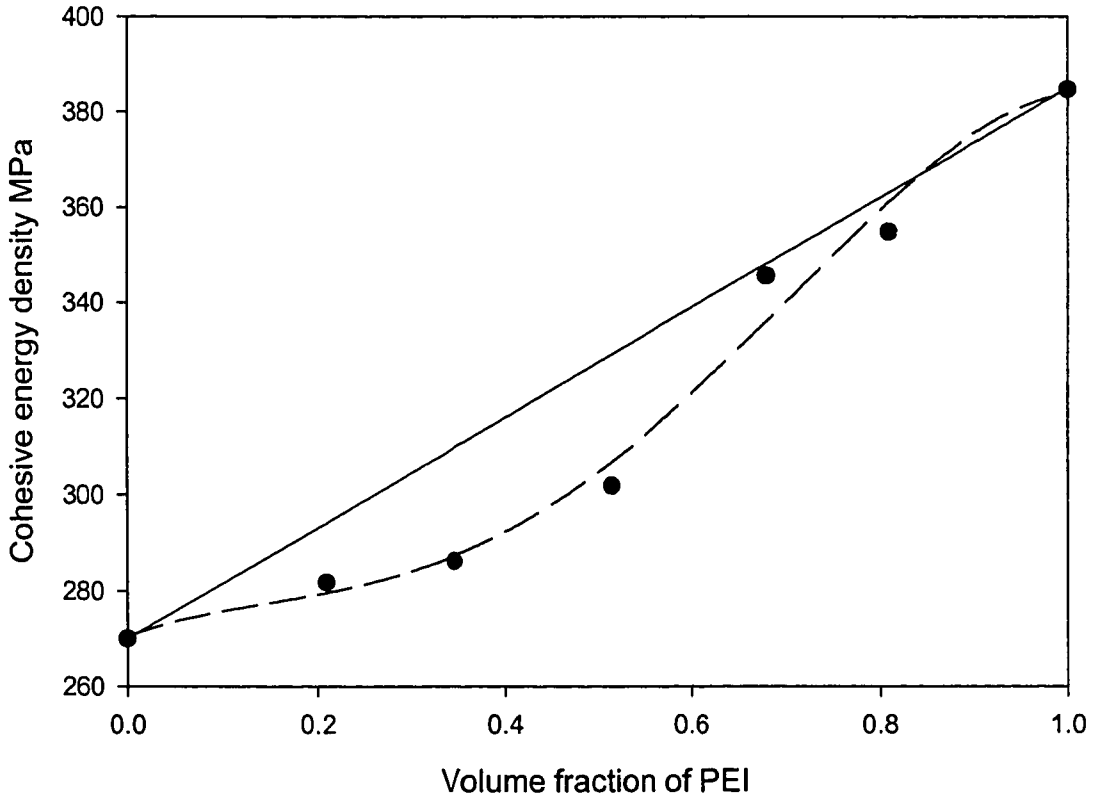

Figure 5.9: Concentration dependence of cohesive energy density of PEI/PBT blends

Figure 5.9 shows that the cohesive energy density increase with increasing PEI component. However, at low PEI concentration, say below 50%, the cohesive energy density of the blends increase slowly with PEI component. Beyond 60% PEI, the cohesive energy density of the blends is close to the additive cohesive energy density of

the pure polymers. Obviously, the phenomena here are not due to the free volume change because in our simulation, the volume change upon blending was neglected. Whether the experimentally observed glass transition change with concentration can be explained by the cohesive energy change is still under investigation.

5.5 Summary

Based on the COMPASS force field, the molecular dynamics simulation was used to study miscibility between PEI and PBT. The Flory-Huggins interaction parameters calculated from the simulation are negative at all concentrations studied, confirming the experimental results that PEI/PBT blends are completely miscible at all the blend concentrations. The homogeneous phase morphology of quenched PEI/PBT blends was also observed using TEM, which again confirms the miscibility. The energy analysis of the simulation results also showed that the miscibility in the melt state is driven by favorable van der Waals interactions between the PEI and PBT, with negligible contributions from short-ranged intramolecular interactions. Annealing of PEI/PBT blends introduces crystallization of PBT and PEI/PBT undergoes phase separation during this process.

5.6 References

Akten, E.D.; Mattice, W.L. (2001) Monte Carlo Simulations of Head-to-Head, Tail-to-Tail Polypropylene and its mixing with Polyethylene in the Melt, *Macromolecules*, 34(10), 3389-3395.

Chen, H.L. and Porter, R.S. (1992) Phase and Crystallization Behavior of Solution-Blended Poly(ether ether ketone) and Poly(ether imide), *Polym. Eng. Sci.*, 32(24): 1870-1875.

Chen, H.L. (1995), Miscibility and Crystallization Behavior of Poly(ethylene terephthalate)/Poly(ether imide) Blends, *Macromolecules*, 28(8):2845-2851.

Chen, H.L.; Hwang, J.C.; Chen, C.C.; Wang, R.C.; Fang, D.M. and Tsai, M.J. (1997) Phase behavior of Amorphous and semicrystalline Blends of Poly(butylenes terephthalate) and poly(ether imide), *Polymer*, 38(11): 2747-2752.

Chen, H.L. and Hsiao, M.S. (1998): Morphological Structure Induced by Combined Crystallization and Liquid-liquid Demixing in Poly(ethylene terephthalate)/Poly(ether imide) Blends, *Macromolecules*, 31(19): 6597-6584.

Cheng, S.Z.D.; Pan, R.; Wunderlich, B. (1988) Thermal Analysis of Pol(butylenes tereohthalate) for Heat-capacity, Rigid-Amorphous Content and Transition Behavior, *Makromol. Chem. Macromol. Chem Phys.*, 189(10):2443-2458.

Chun, Y.S.; Lee, H.S.; Jung, H.C. and Kim, W.N. (1999) Thermal Properties of Melt-Blended poly(ether ether ketone) and Poly(ether imide), *J. Appl. Poly. Sci.*, 72:733-739.

Eichinger, B.E.; Rigby, D. and Stein, J. (2002) Cohesive Properties of Ultem and Related Molecules from Simulation, *Polymer*, 43(2): 599-607.

Hobbs, S.Y.; Dekkers, M.E.J. and Watkins, V.H. (1988) Toughened Blends of Poly(butylenes terephthalate) and BPA Polycarbonate. 1. Morphology, *J. Mater. Sci.*, 23(4): 1219-1224.

Hsiao, B.S. and Sauer, B.B. (1993) Glass Transition, Crystallization and Morphology Relationships in Miscible Poly(aryl ether ketones) and Poly(ether imide) Blends, *J Poly. Sci. B:Poly. Phys.*, 31: 901-915.

Huang, J.M. and Chang, F.C. (2002) Miscibility, melting and Crystallization of Poly(trimethylene terephthalate)/Poly(ether imide) Blends, *J. Appl. Poly. Sci.*, 84: 850-856.

Huang, B.S and Woo, E.M. (2000) Blends of a Novel High-temperature Poly(oxy-1,4'-diphenyleneoxy-1,4-phenylenecarbonyl-1,4-phenylene) with Poly(ether imide): Structure, Interaction , and Miscibility, *Colloid Polym. Sci.*, 278: 392-398.

Jang, J. and Sim, K. (1998) Crystallization Behavior in Poly(etherimide) Poly(butyleneterephthalate) Blends Using a Spectroscopic Method, *Polym. Test.*, 17(7): 507-521.

Jang, S.S. and Jo, W.H. (1999) Analysis of the Mechanical Behavior of Poly(trimethylene terethphalate) in an amorphous State Under Uniaxial Extension – Compression Condition Through Atomistic Modeling, *J. Chem. Phy.*, 110(15):7524-7532.

Jonas, A.M.; Ivanov, D.A. and Yoon, D.Y. (1998) The semicrystalline Morphology of Poly(ethr-ether-ketone) Blends with Poly(ether imide), *Macromolecules*, 31(16): 5352-5362.

Kamath, S.Y.; Colby, R.H. and Kumar, S.K. (2003) Evidence for Dynamic Heterogeneities in Computer Simulations of Miscible Polymer Blends, Phys. Rev. E, 67, 010801.

Khan, F.; Hor, A.M. and Sundararajan, P.R. (2004) Influence of Polycarbonate Flexibility on the Annealing-Induced Phase Separation of the Hole Transport Molecule TPD in a Model Change Transport Composites, *J. Phys. Chem. B*, 108(1):117-126.

Kuo, Y.H.; Woo, E.M. and Kuo, T.Y. (2001) Completely Miscible Blend of Poly(trimethylene terephthalate) with Poly(ether imide), *Polymer J.* 33(12): 920-926.

Lee, J.K.; Choi, W.S.; Kwon, Y.K. and Lee, K.H. (2002) Liquid-liquid Phase Separation and Crystallization Behavior of Poly(ethylene terephthalate)/Polyether Imide Blend, *Polymer*, 43(9): 2827-2833.

Lin, C.H. and Wang, C.S. (2001) Miscibility of Poly(ether imide) and Poly(butylenes naphthalate) Blends, *Polym. Bull.*, 46:191-196.

Martinez, J.M.; Eguiazabal, J.I. and Nazabal, J. (1996) Miscibility Level and Properties of Poly(ether imide)/Poly(ethylene terephthalate) Blends, *J. Appl. Poly. Sci.*, 62(2): 385-391.

Martinez, J.M.; Eguiazabal, J.I. and Nazabal, J.(1993) Miscibility of Poly(ether imide) and poly(ethylene-terephthalate), *J. Appl. Poly. Sci.*, 48(5): 935-937.

Okamoto, M. and Inoue, T. (1994) Phase Separation Mechanism and Structure Development in Poly(butylenes terephthalate) /Polycarbonate Blends, *Polymer*, 35(2): 257-261.

Olabisi, O.; Robeson, L.M. and Shaw M.T. (1979) *Polymer-Polymer Miscibility*, Academic Press, New York.

Rim, P.B. and Runt, J.P. (1984) Melting-point Depression in Crystalline Compatible Polymer Blends, *Macromolecules*, 17(8): 1520-1526.

Runt, J.P. and Gallagher, K.P. (1991) Polymer-Polymer Interaction Parameters via Melting-point Depression- A critical Analysis, *Poly. Comm.* 32(6): 180-182.

Sauer, B.B. and Dee, G.T. (2002) Surface Tension and Melt Cohesive Energy Density of Polymer Melts Including High Melting and High Glass Transition Polymers, *Macromolecules*, 35(18): 7024-7030.

Simon, G.P. (2003) *Polymer Characterization Techniques and Their Application to Blends*, Oxford University Press, New York.

Utracki, L.A. (1990) *Polymer Alloys and Blends: Thermodynamics and Rheology*, Oxford University Press, New York.

Van Krevelen, D.W. (1997) Properties of Polymers: Their Correlation with Chemical Structure; Their Numerical Estimation and Prediction from Additive Group Contributions, 3rd edition, Elsevier, New York.

Vallejo, F.J.; Eguiazabal, J.I. and Nazabal, J. (2001) Solid State Features and Mechanics Properties of PEI/PBT blends, *J. Appl. Poly. Sci.*, 80(6): 885-892.

White, S.A.; Weissman, S.R. and Kambour, R.P. (1982) Resistance of a Polyetherimide to Environmental-Stress Crazing and Cracking, J. Appl. Poly. Sci. 27: 2675-2682.

Woo, E.M. and Lee, L.T. (2003) A Noval Quaternary Blend System of Poly(ethylene terephthalate), Poly(trimethylene terephthalate), Poly(butylenes terephthalate), and Poly(ether imide), *Polym. Bull.*, 50: 33-38.

Woo, E.M. and Tseng, Y.C. (2000) Analysis and Charaterization of Unusual Ternary Polymer Miscibility in Poly(ether diphenyl ether ketone), Poly(ether ethr ketone), and Poly(ethr imide), *Macromol. Chem. Phys.* 201(14): 1877-1886.

Woo, E.M. and Yau, S.N. (1997) Peculiar Glass Transition Behavior and Miscibility in a Binary Mixture Compring Amorphous Poly(ether imide) with Semicrystalline Poly(butylenes terephthalate), *Macromolecules*, 30(12): 3626-3631.

Zoller, P.; Walsh, D. (1995) *Standard Pressure-Volume-Temperature data for Polymers*, Tech. Pub.Co., Lancaster.

Chapter 6

Miscibility studies of PC/PBT blends

6.1 Introduction

Biphenol-A polycarbonate (PC) is one of the most important engineering thermoplastic polymers because of its technologically favorable properties. PC has some exceptional properties such as high impact strength even at low temperatures (down to -100 ^{0}C), ductility, extreme toughness and transparency, resistance to burning, and a high glass transition temperature (150 ^{0}C). However, it is susceptible to solvent because of its amorphous nature. High melt viscosity also makes it difficult for melt processing. Polybutylene terephthalate (PBT) is semi-crystalline polyester with a melting point of 227 ^{0}C; it exhibits some excellent properties such as tensile strength, abrasion resistance, chemical resistance and electrical insulation. However, its T_g is low (ca. 40 ^{0}C), which results in a decrease of the mechanical properties of PBT at temperatures above 30 ^{0}C. PC/PBT blends have attracted both academic and industrial interest because both polymers are widely used high performance plastics and their properties can compensate each other. The solvent resistance as well as the processibility of PC can be improved by blending it with PBT. It has been reported by Singh *et al.* that a small amount of PBT can cause large decrease of the melt flow index of PC [Singh, 1984]. The low impact strength of PBT, especially at low temperatures, can be improved by the high impact

strength of PC. The PC/PBT blends have been commercialized under the trade name of Xenoy (GE Plastics) and Makroblend (Bayer).

The PC/PBT blends have been extensively studied in the literature. However, conflicting conclusions have been reached regarding the miscibility of this blend. Solution casting PC/PBT blend has been considered to be completely immiscible because the glass transition temperatures of PC and PBT as well as the melting temperature of PBT do not change with composition [Wings and Trafara 1994]. For PC/PBT melt blends, miscibility ranging from complete immiscible to various degrees of miscibility has been reported. Kim and Burns [1990] concluded that PC/PBT and PC/PET blends are partially compatible even without the addition of transesterification inhibitors. No transesterification was detected between PC and PBT blends in their study. Van Bennekom *et al.*'s study [1997] showed that PC/PBT blends are partially miscible with the transesterification being inhibited by TPPi(triphenyl phosphite). Sanchez *et al.* [1993] also found that the un-reacted PC/PBT blends are partially miscible and the overall mechanical properties of PC/PBT blends are improved. A single T_g between the T_g's of PC and PBT is observed for melt blending PC/PBT by Wings and Trafara [1994] and they considered PC/PBT blends prepared by melt blending as completely miscible.

The controversy of miscibility arises from complex melting behavior of PC/PBT blends, which is caused by transesterification reaction occurring between PC and PBT. The commercial PBT is produced by transesterification of dimethyl terephalate with a surplus of 1,4- butandiol. Metal-organic compounds such as titanium isopropoxide are used as catalyst. There is a residual amount of catalyst in the commercial PBT, which makes transesterification occur during the melt blending of PC/PBT [Karavia *et al.*

2002]. There are three possible mechanisms of the exchange reaction between PC and PBT: the first one is alcoholysis, it is the reaction of the –OH end groups of PBT with PC; the second mechanism is the reaction of PBT –COOH end groups with PC by acidolysis; the third one is direct transesterification, and it was proven that the direct transesterification is the most possible reaction mechanism between PC and PBT in the present of catalyst residue in PBT [Devaux *et al.* 1992; Montaudo *et al.* 1998; Marchese *et al.* 2002]. The transesterification reaction between PC and PBT leads to the formation of random copolymers or block copolymers largely depending on the reaction time and processing temperature. With increasing mixing time and processing temperature, the transesterification is enhanced and the resultant copolymer tends to change from di-block copolymer to random copolymer [Marchese *et al.* 2002].

In terms of miscibility of PC/PBT blends, the drawbacks of the current experimental approaches are: for solution casting blends of PC/PBT, the solvent has an effect on the miscibility of the blends. For melt blending, although the transesterification inhibitor can prevent the reaction between PC and PBT from occurring; however, it was reported that the inhibitor added can serve as a compatibilizer [Pompe and Haussler 1997]. So it could alter the measured glass transition temperature and therefore the miscibility. Another drawback of the experimental studies is that melt miscibility is inferred using solid-state samples. Obviously, crystallinity of PBT may have an effect on the blend miscibility.

In the previous chapters, MD simulation has been successfully used to investigate the miscibility of the PEI/PC blend and PEI/PBT blend, and the simulation results are consistent with the experimental results. Since the inherent miscibility of PC/PBT blends

are of fundamental and practical relevance, in this chapter, we extends the predictive capacities of MD simulation to PC/PBT blend to clarify the controversy of experimentally observed miscibility at the molecular level. This is the first attempt to study miscibility of PC/PBT blends using MD simulation. The simulation results are compared to those reported from experiments in the literature.

6.2 Molecular dynamics simulation details

Construction of pure PC and PBT models has been described in previous chapters. For the PC model, 23 repeating units were used; while 26 repeating units were used for PBT. It has been shown in our previous studies that the molecular weights used are sufficient to model the polymers' bulk properties. Three PC/PBT blends with different compositions were constructed. The concentration of PC/PBT blend was controlled by including different ratios of the number of PC chains to that of PBT in the periodic boundary unit cells. One system contained two chains of PC and one chain of PBT, corresponding to volume concentration of 32.22% of PBT. The second system composed of one chain of PC and one chain of PBT, which has a volume concentration of 48.74% of PBT. The third system included one chain of PC and two chains of PBT, corresponding to 65.54% volume concentration of PBT.

The densities of pure PC and PBT at 260 ^{0}C were obtained experimentally from pressure-volume-temperature measurements [Zoller and Walsh, 1995]. Densities of PC/PBT blends were calculated using a weight average over the densities of the pure components. The characteristics are listed in Table 6.1. After the initial model construction, each model was subject to energy minimization; in order to avoid the

system to be trapped in a local minimum, the structure was relaxed at 1,000 K for 100 ps, followed by a minimization of the snapshot having the lowest potential energy. The energy minimized structures were subject to NVT MD simulation at 260 ^{0}C, which is the melting temperature used in experiments.

Table 6.1: Description of model systems of PC/PBT blends

System number	Number of chains per unit cell	Number of Atoms	Box length (Å)	Concentration (volume PBT%)	Density (g/cm^3)*	Molar volume (cm^3/mol)	χ
1	1PC chain	761	20.89	0	1.066	5491	N/A
2	2PC chains, 1PBT Chain	2252	29.96	32.22	1.076	5401	1.11
3	1PC chains, 1PBT chain	1491	26.10	48.74	1.081	5356	1.53
4	1PC chain, 2PBTchain	2221	29.79	65.54	1.086	5311	1.51
5	1PBT chain	730	20.54	100	1.097	5221	N/A

* Density at 533K, the density of pure PC and PBT were obtained from Zoller, 1995

6.3 Results and Discussion

In order to demonstrate the evolutions of conformations of the molecules used in the PC/PBT blend during the simulation, four snapshots of one PC chain and two PBT chains blend at 0, 50, 100, and 150 ps are shown in Figure 6.1. The red chains represent PBT while the white chain for PC. It can be seen that the overall conformations of the

polymers do not change significantly within the simulation time although the local conformations change due to the molecular motions caused by thermal energy at 260 ^{0}C.

The energy profiles of simulation in Figure 6.1 are shown in Figure 6.2. The potential energy (Figure 6.2 (a)) gradually decreases in the first 100 ps and stays around 2,378 kcal/mol for the last 100 ps. The kinetic energy (Figure 6.2 (b)) fluctuates around 3,500 kcal/mol through the simulation, which indicates that the temperature is constant as desired. The van der Waals energy (Figure 6.2(c)) and electrostatic energy (Figure 6.2 (d)) levels off very quickly. It should be noted that the relaxation at 1,000 K before the simulation at 260 ^{0}C is of great help for the system to reach equilibrium quickly, especially for a system with many atoms.

Table 6.2: Solubility parameters of PC and PBT simulated using COMPASS force fields

Name	Repeating units	MWT	Solubility parameter ($MPa^{0.5}$)	
			@260 ^{0}C	@25 ^{0}C
PC	23	5851	17.01	19.21
PBT	26	5727	17.81	20.81

As discussed in Chapter 5, the COMPASS force field is the only suitable force field for the simulation of PBT, and it also gives fairly accurate simulation results of PC. Therefore, it was used for the simulations of PC/PBT blends. The simulated solubility parameter values of PC and PBT at 260 ^{0}C and room temperature are shown in Table 6.2, which shows that solubility parameters of PC and PBT at 260 ^{0}C are lower than the value

at room temperature, as expected. Since we are concerned on the miscibility of PC/PBT blends in the melt state, the solubility parameters of PC and PBT at 260 ^{0}C are of interest. The difference between PC and PBT is 0.8 $MPa^{0.5}$, which is larger than the critical value of solubility parameter difference being around 0.3-0.5 $MPa^{0.5}$ [Brandrup *et al.* 1999]. The difference of solubility parameters obtained from simulation is in agreement with the experientially observed immiscibility without transesterification. However, as we stated before, the solubility parameter cannot be relied upon to predict the miscibility. The methodology by which enthalpy change upon mixing is calculated is a more reliable.

Based on equations 4-9 and 4-10, the calculated Flory-Huggins interaction parameters of PC/PBT blends at different blend concentrations are listed in the last column of Table 6.1. They range from 1.11 to 1.53. The molar volume of 201 cm^3/mol for a PBT repeating unit at 260 ^{0}C, was taken as the reference volume for the calculation of the Flory-Huggins interaction parameters. The critical Flory-Huggins interaction parameter calculated based on equation 2-6 is 0.075, where N_{PBT} = 26 and N_{PC} = 27 were used and they are based on the same reference volume. The Flory-Huggins interaction parameters calculated based on MD simulation are much larger than the critical interaction parameter; therefore, our simulation results showed that at lease qualitatively, PC and PBT in the melt state are immiscible without transesterification reaction between them.

(a) 1ps

(b) 50 ps

(c) 100 ps

(d) 150 ps

Figure 6.1: Snapshots of PC2PBT1 simulation at different times

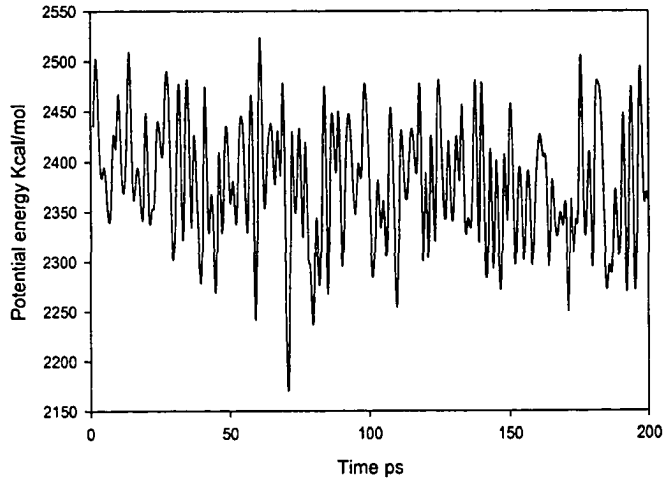

(a)

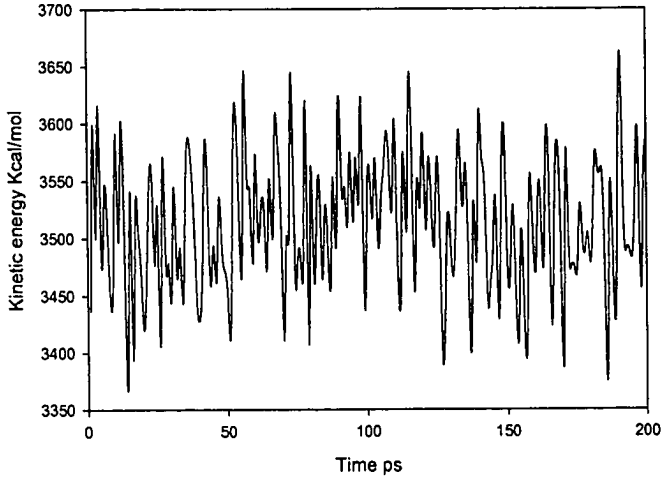

(b)

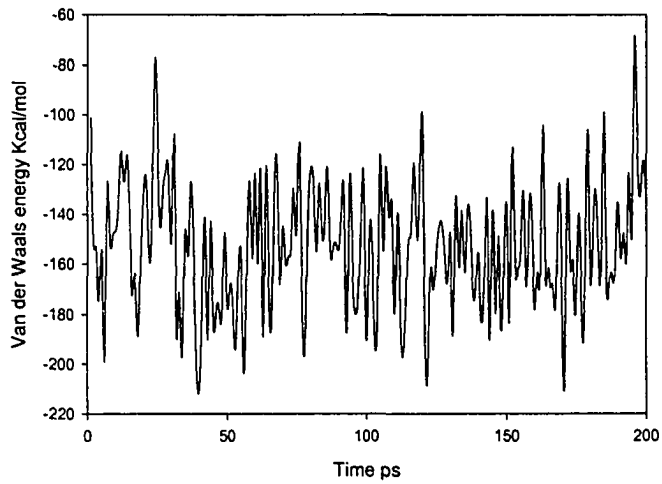

(c)

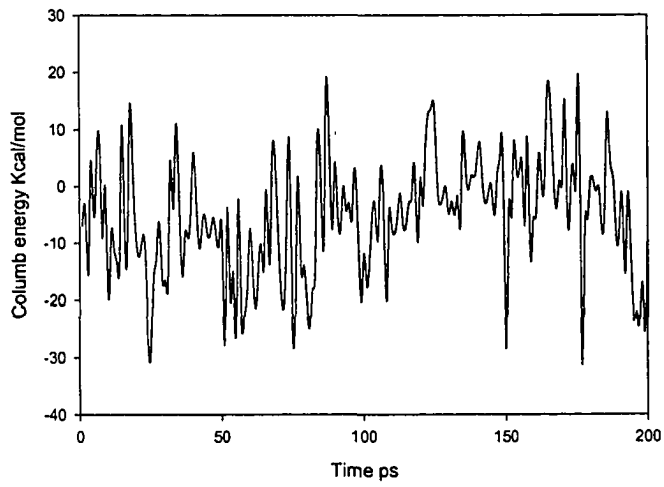

(d)

Figure 6.2: Profiles of (a) potential energy, (b) kinetic energy, (c) van der Waals energy and (d) electrostatic energy for the simulation shown in Figure 6.1

Table 6.3: Average energy (kcal/mol) per chain and the contributions to the Average from the valence and intermolecular interactions (VDW and electrostatic energies) as well as cross terms

System Number	Total potential energy	Valence Energy (PC)	Valence Energy (PBT)	Cross terms	VDW	Electrostatic energy
1: Pure PC	442.85	994		-178.48	-0.591	-372.8
2: PC2PBT1	790.93	993	1,000	-152.02	-51.51	-0.88
3: PC1PBT1	965.36	1,003	1,001	-146.44	-76.94	186.74
4: PC1PBT2	1,134.70	999	1,001	-132.13	-104.46	370.94
5 Pure PBT	1,466.28		988	-95.61	-164.58	738.47

Table 6.3 presents the average potential energy per chain along with its decomposition into the two components arising from the short-ranged intramolecular interactions (i.e., valence terms) and long range intermolecular interactions represented by van der Waals interactions and electrostatic interactions. Compared the valence energy of PC in its pure state with that in the blend environment, Table 6.3 shows that they are virtually identical to each other, and so does the PBT. The energy changes upon mixing for all types of energy were calculated and are summarized in Table 6.4. The potential energy change per chain is positive which is an indication of immiscibility of PC/PBT blends in the melt state without transesterification. The simulation results are in good agreement with the experimental results of Hopfe *et al.* [1997], in which they showed that PC/PBT are inherently immiscible provided that the copolyester content is zero, and Hanrahan *et al.*'s results of PC/PBT blends prepared by solution casting [1985]. Energy decomposition into intramolecular (include valence terms and cross terms) and

intermolecular interactions showed that the enthalpy change is dominated by the contribution from intermolecular interactions, especially van der Waals interactions. The intramolecular interactions including cross terms contribute about 11% to 28% of the total potential energy change, and the rest was due to the intermolecular interaction change during mixing. In the intermolecular interactions, the van der Waals energy change is roughly twice of the electrostatic energy change. This energetic origin of immiscibility is similar to the origin of immiscibility of polypropylene and polyethylene [Akten and Mattice 2001]; however, the results on the PC/PBT blend are different from our simulation results of PEI/PC blends, in which the electrostatic energy change is much greater than the van der waals energy contribution.

Table 6.4: Energy changes upon mixing (kcal/mol) for PC/PBT blend systems

System Number	ΔE_{Poten}	$\Delta E_{valence}$	ΔE_{cross}	$\Delta E_{valence} + \Delta E_{cross}$	ΔE_{vdw}	ΔE_{Q}	$\Delta E_{vdw} + \Delta E_{Q}$
2:PC2PBT1	6.93	-1.35	3.35	1.99	3.80	1.13	4.93
3:PC1PBT1	10.79	-0.62	1.83	1.21	6.54	3.04	9.58
4:PC1PBT2	9.56	2.43	-0.63	1.80	5.58	2.18	7.76

6.4 Summary

In summary, the inherent miscibility of PC and PBT blend in the melt state has been investigated by MD simulation using the COMPASS force field. The enthalpy changes upon mixing and the Flory-Huggins interaction parameters have been calculated

by simulating the pure PC and PBT and their blends at different concentrations. It was found that the enthalpy changes on mixing are positive and the corresponding Flory-Huggins interaction parameters are higher than the corresponding critical interaction parameter. Therefore, PC and PBT are inherently immiscible in the melt state without transesterification. The simulation results suggested that partially miscible and miscible PC/PBT blends observed in the experiments are mainly due to different levels of transesterification that occurred during the melt blending process, instead of the inherent miscibility of the polymers. Energy analysis showed that the immiscibility of PC/PBT blend is driven by intermolecular interactions, especially the van der Waals interactions, and the contribution from the valence interactions is negligible.

6. 5 References

Akten, E.D. and Mattice, W.L. (2001) Monto Carlo Simulations of Head-to-head Tail-to-tail Polypropylene and Polyethylene in the Melt, *Macromolecules*, 34(10): 3389-3395.

Brandrup, J; Immergut, E. H. and Grulke, E.A. (1999) Polymer Handbook, 4th edition, Wiley, New York.

Devaux, J.; Godard, P. and Mercier, J.P. (1982) The Transesterification of Bisphenol-A Polycarbonate (PC) and Polybutylene Terephthalate (PBTP): A New Route to Block Copolycondensates, *Poly. Eng. Sci.*, 22(4):229-233.

Gestoso, P. and Brisson, J. (2001) Effect of Hydrogen Bonds on the Amorphous Phase of a Polymer as Determined by Atomic Molecular Modeling, *Comp. Theo. Poly. Sci.*, 11: 263-271.

Hopfe, I.; Pompe, G. and Eichhorn, K.J. (1997) Ordered Structures and Progressive Transesterification in PC/PBT Melt Blends Studied by FTIR Spectroscopy Combined with DSC and NMR, *Polymer*, 38(10): 2321-2327.

Karavia, V.K.; Koulouri, E.G. and Kallitsis, J.K. (2002) Characterization of Melt-mixed Poly(ethylene-2,6-naphthalate) (PEN)/Polycarbonate (PC) Blends, *J. Macromol. Sci.: Pure & Apply Chem.*, 39(6): 527-544.

Kim, W.N.; Burns, C.M. (1990) Phase behavior of Blends of Polycarbonate with Partially Miscible Polymers, *J. Appl. Polym. Sci.*, 41(7-8): 1575-1593.

Marchese, P.; Celli, A. and Fiorini, M. (2002) Influence of the Activity of Transesterification Catalysts on the Phase Behavior of PC-PET Blends, *Macromol. Chem. Phys.*, 203(4): 695-704.

Montaudo, G.; Puglisi, C. and Samperi, F. (1998) Mechanism of Exchange in PBT/PC and PET/PC Blends: Composition of the Copolymer Formed in the Melt Mixing Process, *Macromolecules*, 31(3): 650-661.

Patnaik, S.S and Pachter, R. (2002) A molecular Simulation Study of the Miscibility in Binary Mixtures of Polymers and Low Molecular Weight Molecules, *Polymer*, 43(2): 415-424.

Paul D. R. and Bucknall C. B.(2000) *Polymer Blends*, John Wiley & Sons Inc., New York

Pompe, G. and Haussler, L. (1997) Investigating of Transesterification in PC/PBT Melt Blends and the Proof of Immiscibility of PC and PBT at Completely Suppressed Transesterification, *J. Poly. Sci., B: Poly. Phys.*, 35(13): 2161-2168.

Hanrahan, B.D.; Angeli, S.R. and Runt, J. (1985) Miscibility and Melting in Poly(butylenes Terephthalate) Poly(bisphenol A-carbonate) Blends, *Polym. Bull.*, 14(5):399-406.

Sanchez, P.; Remiro, P.M. and Nazabal, J. (1993) Physical Properties and Structure of Unreacted PC/PBT Blends, *J. Appl. Polym. Sci.*, 50(6): 995-1005.

Van Bennekom, A.C.M.; van den Berg, D.; Bussink, J. and Gaymans, R.J. (1997) Blends of Amide Modeified Polybutylene terephthalate and Polycarbonate: Phase Separation and Morphology, *Polymer*, 38(20) 1997: 5041-5049.

Van Krevelen, D.W. (1997) Properties of Polymers: Their Correlation with Chemical Structure; Their Numerical Estimation and Prediction from Additive Group Contributions, 3rd edition, Elsevier, New York.

Wings, N. and Trafara, G. (1994) Transesterification in Blends of Poly(butylenes Terephthalate) and Bisphenol-A-Polycarbonate, *Angew. Makromol. Chem.*, 217: 91-105.

Zoller, P.; Walsh, D. (1995) *Standard Pressure-Volume-Temperature data for Polymers*, Tech. Pub.Co., Lancaster.

Chapter 7

Glass transition temperature simulation

7.1 Introduction

The glass transition temperature (T_g) is probably one of the most important but least understood property of both amorphous and semi-crystalline polymers. In general, at the glass transition temperature, a polymer exhibits abrupt changes in many of its physical properties, most notably its viscosity (η). This explains why some researchers define T_g as the temperature at which $\eta = 10^{13}$ Poise [Jackle 1986]. The relaxation time of the molecules could increase by up to as much as 15 decades over the glass transition temperature. Below this temperature, the relaxation time exceeds the time scale of experiments and the system falls out of equilibrium. Since T_g, to a certain extent, determines the temperature ranges at which a polymer can be processed and used, study of the glass transition phenomenon is of great practical and theoretical significance. Among the features associated with the glass transition phenomenon, the two most puzzling ones are its rate dependence and an abrupt increase in viscosity over a short range of temperatures. Over the past few decades, theories have been developed for explaining such observations. However, there has not been a single theory that is capable of explaining all the observed features of the glass transition phenomenon. There are essentially three major types of theories proposed in the polymer literature: the free volume theory [Fox and Flory 1950], the thermodynamics theory [Gibbs and DiMarzio

1958] and the recently developed mode coupling theory [Lobe and Baschnagel 1994; Bentzelius 1986; Leutheusser 1984].

In the free volume theory, it is proposed that the total volume of a polymer consists of the van der Waals volume of the molecules and free volume. The free volume is defined as the unoccupied volume consisting of holes of molecular size, or resulting from the imperfections of packing of the molecules that arise from random arrangement. The unoccupied volume is the space available for molecular rearrangement. The glass transition corresponds to the temperature below that the free volume reaches a critical value and there is no sufficient room for molecular rearrangement to occur. It is worth noting that the volume that is not occupied by the molecules may not necessarily be accessible to them. Therefore, it is questionable whether such a volume is really "free". The fractional free volume at the glass transition temperature in this theory, f_g, which is equal to V_f/V_g, has a constant value of 0.025 for all polymers [Haward 1973]. The free volume theory is particularly successful in predicting the experimentally observed molecular weight dependence of T_g [Haward 1973; Pezzin *et al.* 1970]. This is because low molecular weight polymers tend to have higher concentrations of chain ends resulting in more free volume than high molecular weight polymers. Consequently, they require lower temperatures to squeeze out the extra free volume. The theory could also be used to explain the observed rate dependence of T_g. However, since the theory starts with a phenomenological postulate rather than any microscopic theoretical description of liquids, its validity has always been criticized. In fact, as mentioned earlier, free volume is a somewhat ill-defined concept [Binder *et al.* 2003]. As a result, one could obtain different free volumes for the same system using different experimental techniques, such

as positron annihilation spectroscopy and photoisomerization of probe molecules [Robertson 1992]. Nonetheless, a recent molecular dynamics study of Yang *et al.* [1999] showed that free volume below T_g is not a constant, and it even increases with decreasing temperature under isochoric cooling. Observations such as this suggest that free volume is probably not the only material characteristics that determine the glass transition temperature. However, the presence of free volume is a necessary (but not a sufficient) condition for large scale molecular movements. Colucii *et al.* [1997] made similar conclusions based on their study of polycarbonate under isochoric and isobaric conditions.

Gibbs and DiMarzio [1958] proposed the thermodynamic approach to explain the Kauzmann's entropy paradox. In this theory, they considered glass transition as a second order thermodynamic transition. In particular, the authors introduced a temperature, T_2, at which the configurational entropy of the system becomes zero. It can only be reached by using an infinitely slow cooling rate. The T_g, which is about 50 °C ~ 60 °C higher than T_2, is simply a kinetic reflection of T_2 [Angell 1997]. Experimental studies showed that the Gibbs-DiMarzio theory is successful in the following aspects: it predicts the molecular weight dependence of the glass transition, and the effects of copolymerization, plasticization and cross-linking [Hawárd 1973; DiMarzio, 1997]. The arguments in this theory are based on crude and hardly justifiable assumptions and approximations. It is not accepted by other researches. Monte Carlo simulations of bond fluctuation models showed that the configurational entropy does not go to zero at T_2. Although, when T_2 is approached, there is a noticeable decrease in configurational entropy [Binder *et al.* 2002; Wolfgardt *et al.* 1996]. Monte Carlo simulations of lattice model performed by Santen

and Krauth [2000] also showed that there is no clear evidence that the glass transition phenomenon is a real thermodynamic phase transition. The simulation of Bennemann *et al.* showed that there seems to be a divergence in a dynamical length scale at the glass transition temperature, *i.e.*, the distance over which monomer displacement on the polymer chains are correlated [Bennemann, 1999a].

The mode coupling theory (MCT) of the glass transition proposes that there is a dynamic phase transition from ergodic to nonergodic behavior rather than a real thermodynamic transition. The MCT was developed based upon the density-density correlation function and utilizes such a function and the memory kernel on a microscopic basis to predict T_g [Gotze and Sjogren 1992]. The physical idea behind the MCT theory is the "cage effect", in which movements of a particle were confined by a cage formed by its neighbors. The cage effect has been observed in the time dependent mean square displacement (MSD). At low temperatures, in the intermediate times, the MSD showed a plateau [Lyulin and Michels 2002a]. It is because the particle was trapped in a cage formed by its neighbors, which result in a slow down motions of the particles. The ideal MCT predicts that the dynamic transition will occur at a critical temperature T_c, below which the system will get "stuck"; it was demonstrated that the dynamics of various glass forming liquids follow the MCT predictions qualitatively at high temperatures ($T>T_c$) [Bennemann 1999b]. However, the T_c appears to be much higher than T_g. To address this discrepancy, the extended MCT theory includes the hopping process at low temperatures, *i.e.*, the thermally activated process can make the atoms escape from their cages. Whether the extended MCT theory can describe the dynamics of supercooled liquids in the regime between T_g and T_c is still unclear [Binder *et al.* 2003].

Molecular dynamics simulation is probably the best approach to examine the validity of some of the ideas proposed in the theories noted above and elucidates the molecular mechanisms of glass transition. Since one of the most widely used experimental technique to determine T_g is dilatometry, *i.e.*, a specific volume-temperature curve, much effort has been made to generate similar curves for a variety of polymers using molecular dynamics (MD) simulation. Recently, Boyd [1996] has reviewed the advantages and disadvantages of such an approach. The MD simulation of cis-poly(1,3-butadiene), polyisobutylene, atactic polypropylene, polystyrene, polyethylene and poly(ethylene terephthalate) were reported by Han *et al.* [1994], Deazle *et al.* [1996] performed simulation of polysulfone and determined its T_g using the DREIDING 2.21 force field. The same force field was used by Fan *et al.* [1997] to study the local chain dynamics of polycarbonate near its glass transition temperature. In recent years, more sophisticated force fields, so-called Class 2 force fields, such as CFF95, PCFF and COMPASS have been employed in the hope of predicting T_g more accurately. Yu *et al.* [2001] used the CFF95 force field to study the glass transitions of polyethylene, polypropylene, polyisobutylene poly(oxymethylene) and poly(dimethylsiloxane). With the use of the PCFF force field, Soldera was able to predict the difference in T_g between isotactic and syndiotactic poly(methyl methacrylate) [1998]. An *ab inito*-based molecular mechanics force field COMPASS has been used by Fried *et al.* to study the glass transitions of polyphosphazenes and di-substituted polysilanes [Fried and Ren 1999; Fried and Li 2001]. Their work showed that the simulated T_g's agree satisfactorily with the experimental values. More recently, molecular dynamics simulation was used to

study the segmental dynamics of atactic polystyrene in the glassy state [Lyulin *et al.* 2002c].

In this chapter, we report the application of a modified MD strategy proposed by Fried and Ren [1999] along with the use of the COMPASS force field to determine T_g's of two most commonly used polymers, *i.e.*, atactic polystyrene (PS) and atactic polypropylene (aPP) and two engineering amorphous thermoplastics polycarbonate (PC) and poly(ether imide) (PEI). The purpose of this simulation is several-fold. First, we investigate whether the MD simulated specific volume-temperature can reproduce the glass transition temperature of these polymers using a fairly accurate force field, despite the time scales of MD simulation is much shorter than the experiment. Secondly, we investigate that whether the predictions can be improved by using the local specific volume characterized by the radial distribution function obtained from the same MD simulations. Thirdly, the energy components will be examined to determine which one is responsible for the glass transition.

7.2 Models and Simulation

The full atomistic models of PC and PEI in the condensed state used in the study of glass transition have been described in previous chapters. The PC model used consisted of 23 repeating units (M_n = 5,850 g/mol) while the PEI model consisted of 10 repeating units (M_n = 5,930 g/mol). The PS model used consisted of 30 repeating units, which corresponds to a molecular weight of 3,127 g/mol. The atactic PP model consisted of 50 repeating units which correspond to a molecular weight of 2,106 g/mol. Although previous chapters showed that the PEI and PC chain lengths are adequate for the purposes

of calculating their solubility parameters [Zhang *et al.* 2003], use of such low molecular weight models may not yield T_g of the polymers at their typical molecular weights. Therefore, caution must be exercised when the data are analyzed.

According to a recent study of Fried and Li [2001], in addition to the force field used, the method that is used to equilibrate an amorphous cell to obtain specific volume from MD simulation could also have a significant effect on the subsequent T_g determination. In particular, they compared two commonly used amorphous cell equilibration approaches. As shown in Figure 7-1(a), the first method uses the final conformation generated at a higher temperature as the starting conformation for the MD annealing at a lower temperature and such a procedure is applied for a series of simulation temperatures. Usually integration time step of 1 fs is used in the MD simulation; therefore, even very long runs can hardly exceed 10-100 ns. At all temperatures, only short MD runs were performed. The procedure essentially corresponds to a fairly high cooling rate experiment. The cooling rate dependence of T_g has been observed both experimentally and in the simulation [Buchholz *et al.* 2002], the higher the cooling rate, the higher is the determined T_g. The cooling rate that corresponds to the MD approach described is about 10^9 times higher than the rate commonly used in actual experiments. Thus, such a MD approach would yield glass transition temperature that could be much higher than the corresponding experimental values. Vollmayr *et al.* [1996] attributed discrepancy between simulated T_g and experimentally determined T_g of amorphous silica to the difference of the cooling rate accessible in the simulations and those used in experiment. Nonetheless, the method is widely used in the literature and the predictions are often close since such an overestimation is offset by the

underestimation of T_g due to the fact that the molecular models used are of low molecular weight [Yu *et al.* 2001; Soldera, 1998; Pozeuelo and Baselga 2002; Roe, 1994; Yoshioka *et al.* 2003].

Another approach for the simulation of T_g (see Figure 7-1(b)), which avoids the cooling rate problem, is to build a series of different amorphous cells at different temperatures and carry out isobaric-isothermal (NPT) simulations separately at different temperatures using longer equilibration times. In terms of the degree of equilibration that could be achieved, it was found that the second approach is more effective than the first one [Fried and Ren 1999]. In the present work, we more or less followed the latter method; however, we used only one instead of many initial amorphous structures for the MD simulations at each of the different temperatures. This is because the complexity of the polymers of interest precluded us from generating a long list of structures for all the simulation temperatures.

The initial conformations of PC, PEI, PS and aPP were created using the built-in Amorphous Module of Cerius^2 from Acceryls Inc. The experimental density at room temperature was used. Periodic boundary conditions were used to model the condensed state of the materials. The parameters used for the construction of initial conformation at room temperature are summarized in Table 7.1. The periodic cells of these polymers were subjected to energy minimization to reach a gradient in the potential energy of 0.01 kcal/mol Å or less. Since energy minimization is likely to trap the system in a meta-stable local minimum, an isochoric-isothermal (NVT) MD simulation at 1000 K over a period of 100 ps was carried out to ensure the molecules would be able to explore more of the phase space. The snapshot with the lowest potential energy was chosen from the

resulting trajectory file and was subjected to energy minimization again. The energy-minimized structure was then used as the initial conformation for all subsequent NPT MD simulations at the chosen temperatures. The standard Verlet algorithm was used to integrate Newton's equations of motion, and an integration time step of 1 femtosecond (fs) was used for all simulations in order to capture the fastest modes accurately. The Anderson [1980] and Nose [1984] extended ensemble was used to control the pressure and temperature of the cells, respectively. The external pressure was set to 0 atm, which was believed to yield results comparable to simulations performed using 1 atm pressure [Yu *et al.* 2001]. This is because polymer melts tend to have relatively high internal pressures. Each MD simulation was started by assigning initial velocity for the atoms according to Maxwell-Boltzman distribution at twice the target temperature. The velocities of the atoms were quickly downscaled so that the final temperature of the atoms reached the target temperature. During the NPT MD simulation, the trajectories were recorded every 1 ps for subsequent analysis. The COMPASS force field was used for all the simulations.

Table7.1: Parameters used for the construction of initial conformation of polymers at room temperature

Polymer	Number of repeating units	Molecular Weight (g/mol)	Density (g/cm^3) 25 ^0C	Cell Length (Å)
PC	23	5,851	1.20	20.08
PEI	10	5,928	1.27	19.79
PS	30	3,127	1.05	17.04
aPP	50	2,106	0.85	16.02

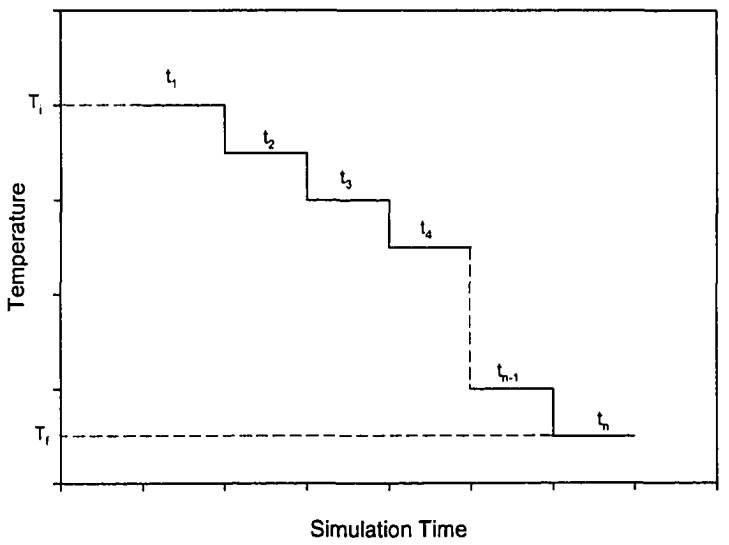

(a)

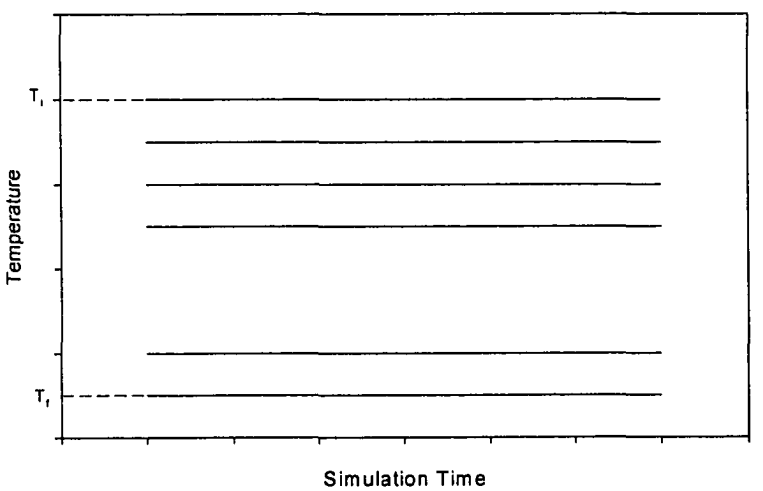

(b)

Figure 7.1: Ensemble equilibration methodologies. (a) The final conformation of the model at a higher temperature is used as the initial conformation at a lower temperature. Therefore, the cooling rate is $(T_i-T_f)/(t_1+ t_2 + \cdots t_n)$. (b) Different initial conformations are used for different equilibration temperatures. No cooling is involved and a longer equilibration time is used.

7.3 Results and Discussion

7.3.1 Specific volume versus temperature

Specific volumes of PC, PEI, PS and aPP obtained from NPT MD simulations at different temperatures and the PVT measured specific volumes, are shown in Figures 7.2 to 7.5. As expected, an abrupt change in temperature dependence of specific volume was observed in the regions of the experimental glass transition temperatures. To determine the glass transition temperature, a linear regression lines in the form of $v = a + bT$ were used to fit to the specific volume-temperature data well above and below the glass transition region. The intersection of the two fitted lines is taken as the T_g. The temperature range for the linear fitting for each polymer and the fitting coefficients are presented in Table 7.2. In this table the subscript "*r*" indicates the polymer in a rubbery state while "*g*" indicates the polymer in glassy state. The parameters obtained from PVT experimental data fitting are listed in the parentheses for comparison.

Table 7.2: Parameters obtained from fitting of the specific volume vs. temperature

Polymer	T<T_g			T>T_g		
	Fitting range (K)	a_g	b_g*10^4	Fitting temperature (K)	a_r	b_r*10^4
PC	50-300	0.82(0.78)	1.22(2.05)	500-750	0.63(0.61)	5.71(6.17)
PEI	50-350	0.80(0.75)	0.56(1.19)	600-800	0.58(0.58)	4.71(4.62)
PS	50-350	0.89(0.88)	2.86(2.39)	400-650	0.76(0.75)	6.30(5.89)
aPP	50-250	1.08(1.049)	3.69(3.50)	300-500	0.89(0.87)	10.06(9.9)

For polycarbonate, a value of 419 K was obtained for the glass transition temperature from the simulated specific volume-temperature plot. As shown in Figure 7.2, the glass transition temperature is slightly higher than the experimental value of 413 K determined from the pressure-volume-temperature (PVT) data by Zoller and Walsh [1995]. T_g of PC obtained from DSC measurement at a heating rate of 20 K/min has been reported to be 423 K [Zhang *et al.* 2003]. Here, we prefer to compare our computed T_g with the value from PVT rather than DSC simply because the cooling rate in the PVT experiments is fairly low, and therefore, data from PVT measurements are more comparable to those obtained from MD simulations based on the approach of Fried and Ren [1999]. As can be seen in Figure 7.2 as well as Table 7.2, the simulated specific volumes agree very well with the PVT data above the glass transition region, indicating that the force field and the equilibration time (i.e., 200 ps) we used for the MD simulations were adequate in this region. However, at temperatures below the glass transition region, MD simulation tends to overestimate the specific volume of the polymer. For example, at room temperature, the computed specific volume of PC is about 1.3% higher than the experimental value. This suggested that the conformation of our PC model is less dense than the real material. This statement is made based on the fact that, in the glassy state, equilibrium specific volumes of PC are always lower than the non-equilibrium ones measured by PVT experiments which must be carried out at a finite cooling rate. The discrepancies in the computed and measured specific volumes imply that PC may contain a certain amount of local order in its glassy state [Siegmann and Geil 1970]. In fact, using Monte Carlo simulation, Lobe and Baschnagel [1994] demonstrated in a very recent article that some local order exists in the glassy state of

polymers. The local ordering of other polymers below the glass transition temperature was also observed using neutron scattering [Frick and Richter 1995].

Our inability to obtain the correct specific volumes at temperatures in the glassy state is attributed to the fact that the simulation time used (200 ps) was very short compared with the relaxation time of the molecule even though the total energy of the systems had leveled off within the first 100ps of the simulations. At elevated temperatures, when the relaxation time of PC is much shorter, COMPASS was able to reproduce the experimental specific volumes, as demonstrated in Figure 7.2. Since computational resources are always limited in every laboratory, being able to build proper initial conformations in the glassy state would definitely facilitate the prediction of T_g. This would require detailed knowledge of the conformation of the polymer of interest in its glassy state, which is still a topic under intensive investigation. The overestimations observed for the simulated specific volumes in the glass transition region are very likely due to the fact that the correlation length of the system is much longer than the length scale of the periodic boundary cells we used in the simulations. The cell length of the simulated polymers at room temperature is listed in the last column of Table 7.1. It was found that the correlation length of polybutadiene increased to 34 Å below the T_g by neutron scattering experiments [Frick and Richter 1995]. Although we do not understand the exact nature of the transition and the correlation length of the simulated polymers, we suspect that the correlation length of such a transition may be fairly long. Note that the correlation length of a first order phase transition such as melting or vaporization is infinite. Nevertheless, since the predicted T_g depends to a large extent on the data above and below the glass transition region, overestimations in the specific

volumes in the glass transition region would have minimal effect on the T_g value determined.

Figure 7.3 shows the temperature dependence of the specific volume of PEI obtained in the present work as well as the PVT results of Zoller and Walsh [1995]. The trends are fairly similar to those that have been seen for PC. Once again, the computed specific volumes at high temperatures agree very well with the experimental values, while the data around and below the glass transition region exhibit significant deviations. The glass transition temperature of PEI obtained from the simulation data is approximately 537 K while that from the PVT data 480 K. The experimental value from DSC is 493K [Zhang *et al.* 2003]. The simulated specific volume at room temperature is about 4% higher than the corresponding value from PVT measurements. It seems that the rigidity of the PEI backbone makes the T_g predictions from MD V-T curves worse than that seen of PC. Note that the backbone of PEI contains more ring structures than PC. Therefore, we suspect that, similar to liquid crystal polymers, the backbone of PEI may form liquid crystal type of order below T_g. As a result, the estimation of PEI's T_g using MD V-T curves is not nearly as good as that for the PC case.

The temperature dependence of specific volume of PS was shown in Figure 7.4. A value of 396 K was obtained for the T_g of PS, which is 6.2% higher than the experimental glass transition value of 371 K [Zoller and Walsh 1995]. Using united atom models, Lyulin *et al.* [2002a, 2003] determined the T_g of PS with a molecular weight of 8,300from simulated specific volume-temperature plot to be around 370 K. From simulation results, they also found that the molecular weight dependence of glass transition temperature is weak. The T_g increased 5 K when the molecular weight

increased from 4,000 to 33,000. For aPP, the simulated T_g is 285K (Figure 7.5), which is 30K higher than that of the PVT experimental value [Kaufman and Falcetta 1977]. Both overestimation [Han *et al.* 1994] and underestimation [Yu *et al.* 2001] of the T_g of aPP was reported in the literature. For both PS and aPP, the simulated specific volume above the glass transition temperature is close to that of the experimental value; while below the glass transition temperature, the simulated specific volume are higher than the corresponding experimental values, similar to what we observed for PEI and PC.

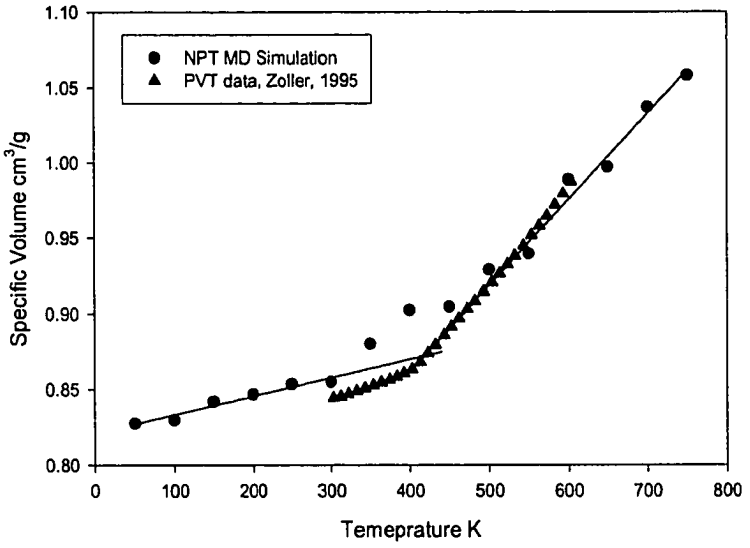

Figure 7.2: Specific volumes of PC computed from NPT MD simulations and PVT measurements

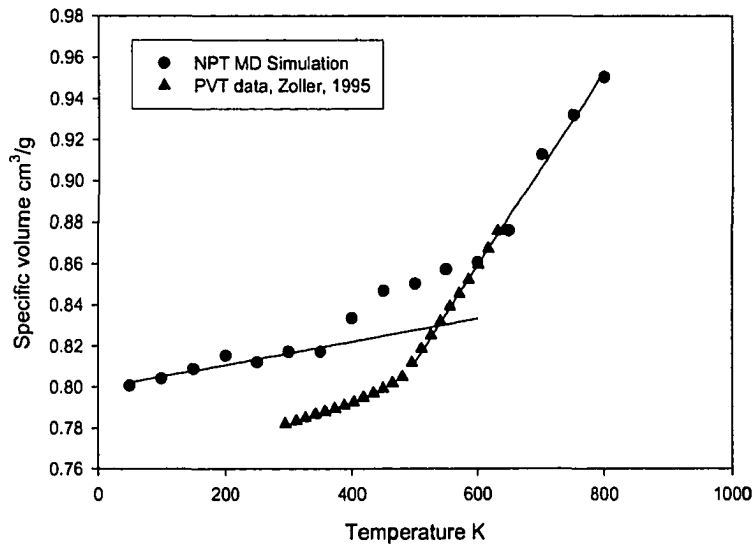

Figure 7.3: Specific volumes of PEI computed from NPT MD simulations and PVT measurements

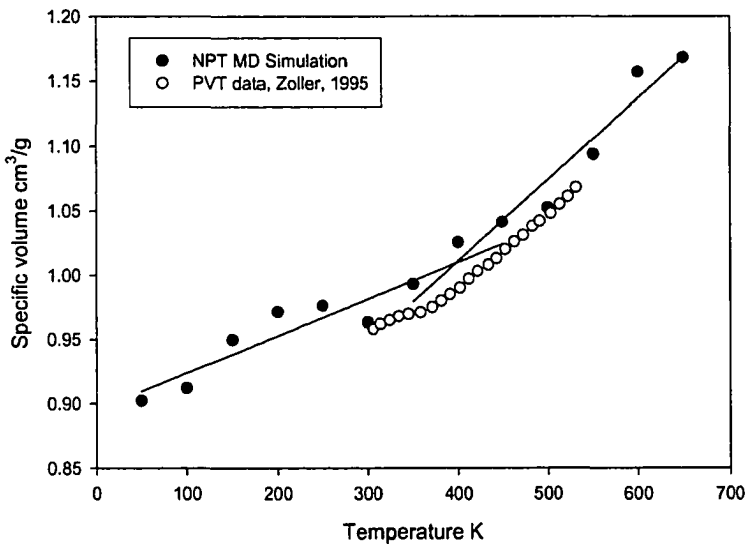

Figure 7.4: Specific volumes of PS computed from NPT MD simulations and PVT measurements

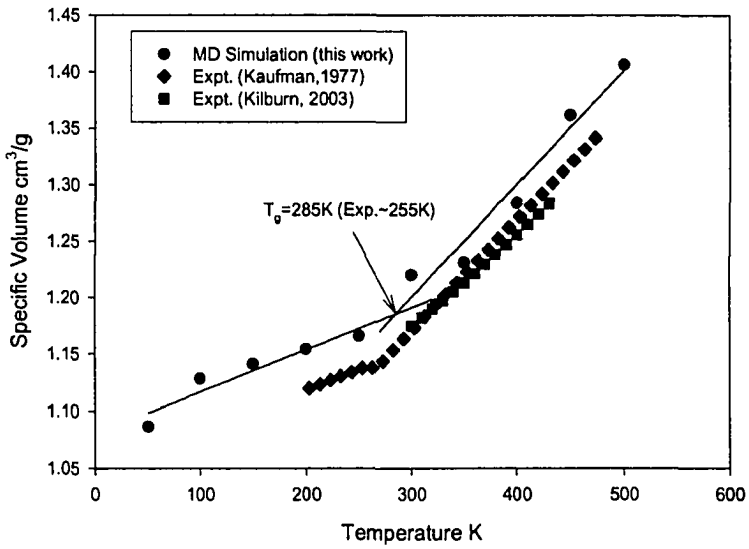

Figure 7.5: Specific volumes of aPP computed from NPT MD simulations and PVT measurements

For the four polymers we investigated, an overestimation of the T_g's was observed; this led us to wonder whether the size of the models we used would contribute to the overestimations. In general, use of small molecular models would lead to a computed T_g lower than the corresponding experimental value. Obviously, this is not the case here. However, since we overestimated the specific volumes of the systems, especially at low temperatures, it is very likely that the simulated free volumes of these polymers in the glassy state are higher than those of the real materials since the van der Waals volumes of the molecules could be calculated accurately. This implies that the extra free volume obtained from the MD simulations is a result of the use of improper conformations rather than having high concentrations of chain ends due to the size of the models. It is noteworthy that the prediction would be even worse if one plotted free volume rather than

specific volume in Figures 7.6 and 7.7. This is because free volume usually constitutes such a small fraction of the total volume of a polymer. As a result, errors in the estimation of free volume are overshadowed by the relatively large value of the van der Waals volume of the system in T_g predictions. This is shown by the plots of the free volumes of PC and PEI (Figure 7.6) as well as those of PS and aPP (Figure 7.7) at the simulation temperatures. Free volume was calculated by probing the polymer cell with a probe sphere using the built-in free volume calculator in Cerius^2. A van der Waals scale factor of 1 at the corresponding simulation temperature and high grid spacing was used. The radius of the probe is set to 1.4 Å and volume occupied by the test probe is 11.49 Å^3. Both Figures 7.6 and 7.7 indicate that below the glass transition temperature, the free volume is not a constant as predicted from the free volume theory [Fox and Flory 1950], it increases with increasing temperature. The resultant T_g's of PC and PEI were determined to be 433 K and 530 K, respectively; while the T_g'*s* of aPP and PS determined from the free volume-temperature plots to be 280 K and 390 K, respectively. It should be pointed out that the conformation of the polymer molecule and free volume interact with each other; improper conformations lead to incorrect free volume values.

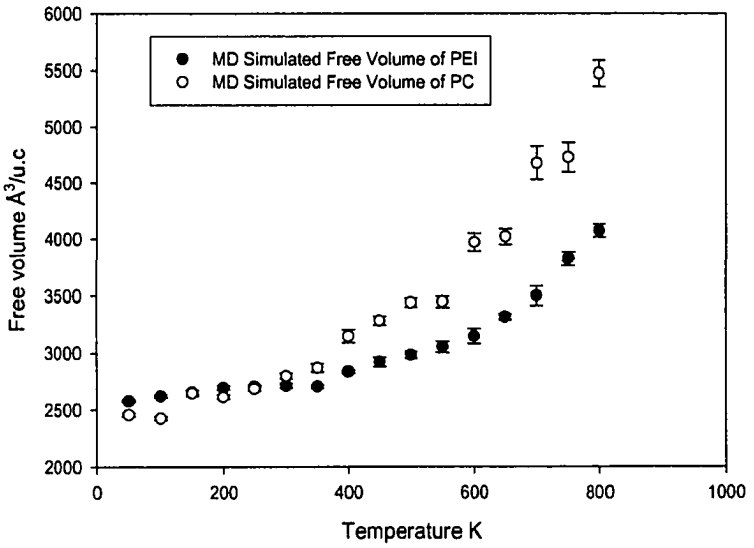

Figure 7.6: MD simulated free volumes of PC and PEI versus temperature

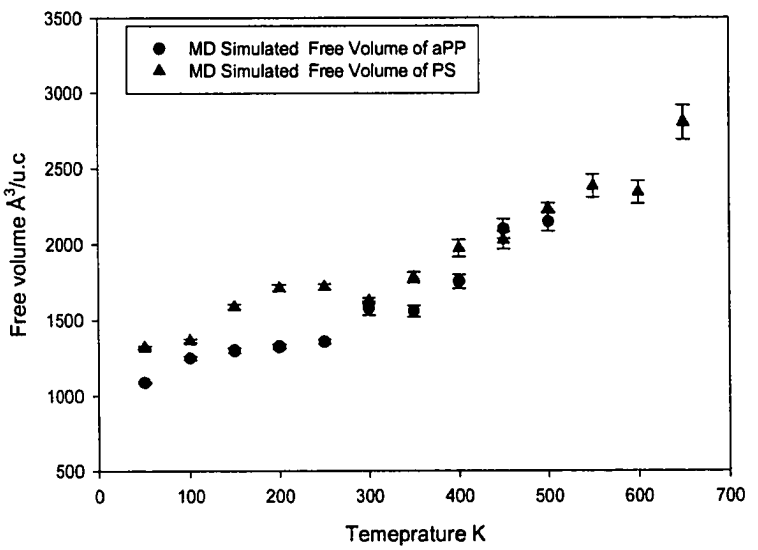

Figure 7.7: MD simulated free volumes of PS and aPP versus temperature

7.3.2 Energy analysis

The roles played by different types of atomic interactions, such as bond energy, angle energy, torsional energy and non-bonded energy, were also examined to help the understanding of glass transition. In the literature, there is some controversy about the roles of different energy components played in the glass transition. In the simulation of PMMA, Soldera found that there are small changes in potential energy, intramolecular energy and intermolecular energy versus temperature [Soldera, 1998]. An abrupt change was found in the plot of the internal energy versus temperature by Fried *et al.* in the simulation of poly[bis(n-butoxy)-phosphazene) (PnBuP) [Fried and Ren 1999] and Rigby and Roe [1987] in the simulation of polyethylene. Buchholz *et al.* [2002] also found there is a kink in the plot of Lennard-Jones part of potential energy around the T_g. Some energy components of the simulated polymers are plotted in Figures 7.8 to 7.11. For the four polymers we studied, the bond stretching energy, angle bending energy increase linearly with increasing temperature; they are insensitive to the glass transition. It is believed these degrees of freedom can reach equilibrium both below and above the T_g. For PC (Figure 7.8 (c)) and aPP (Figure 7.11 (c)), the torsional energy showed an abrupt change around the glass transition temperature; however, the freezing of torsional energy do not happen for all the polymers. The torsional energy of simulated PEI and PS increase linearly with increasing temperature. The non-bonded energy for these four polymers also showed a kink in the glass transition region. (Figure 7.8 (d) to 7.11(d)) Yang *et al.* [1999] concluded that the glass transition is controlled primarily by the non-bonded and torsional interactions, similar conclusion was reported by Yu *et al.* in the simulation of polyoxymethylene (POM) [2001].

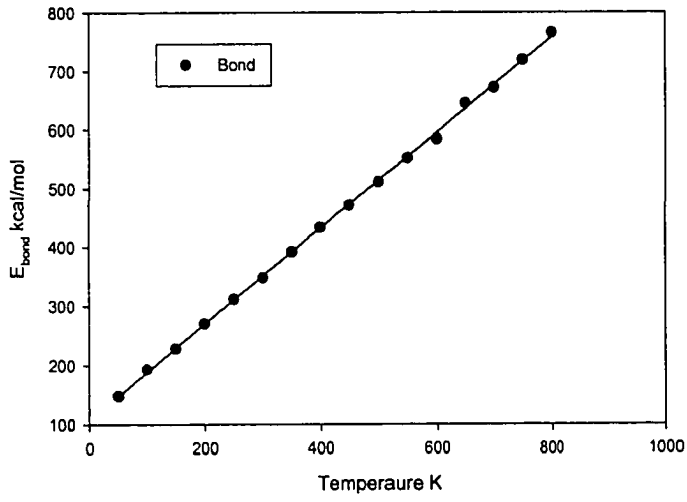

(a)

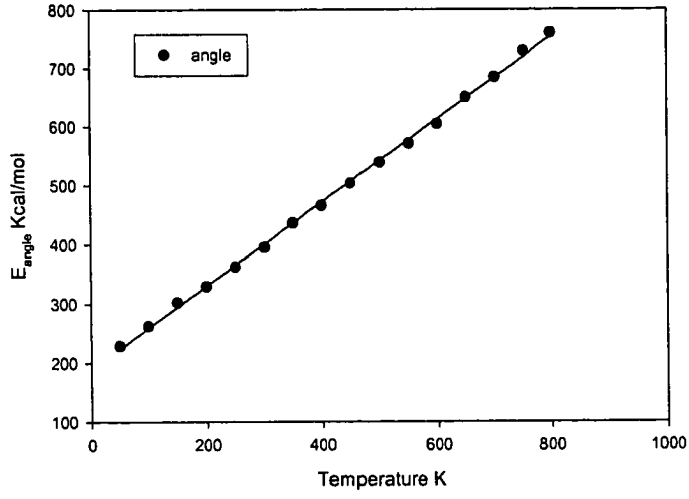

(b)

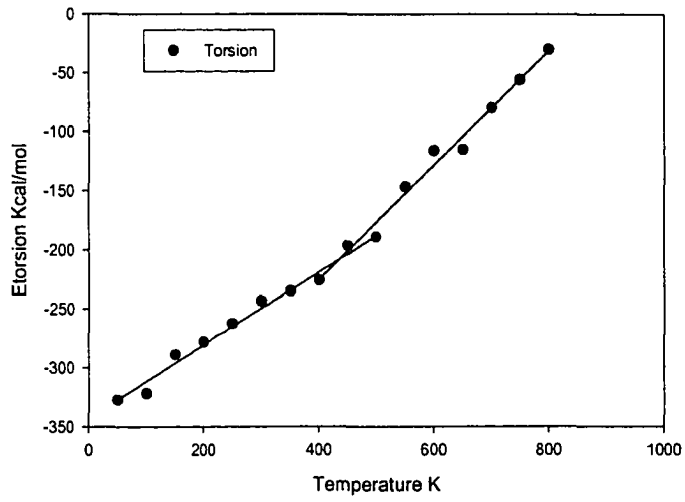

(c)

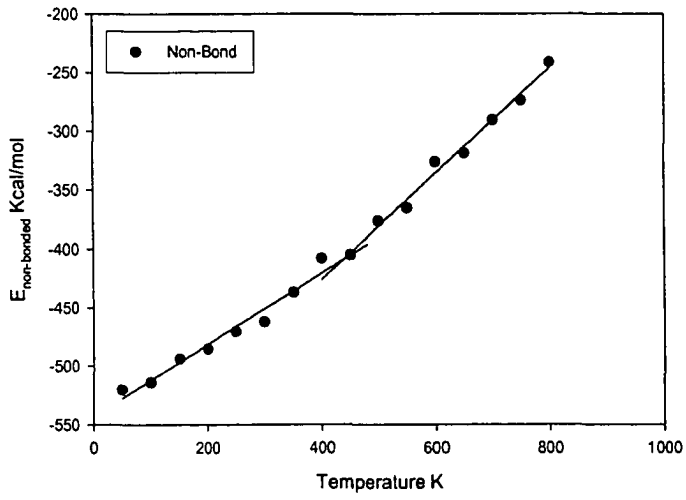

(d)

Figure 7.8: Plots of some energy components versus temperature for PC (a) bond stretching energy (b) angle bending energy (c) torsion energy (d) non-bonded energy

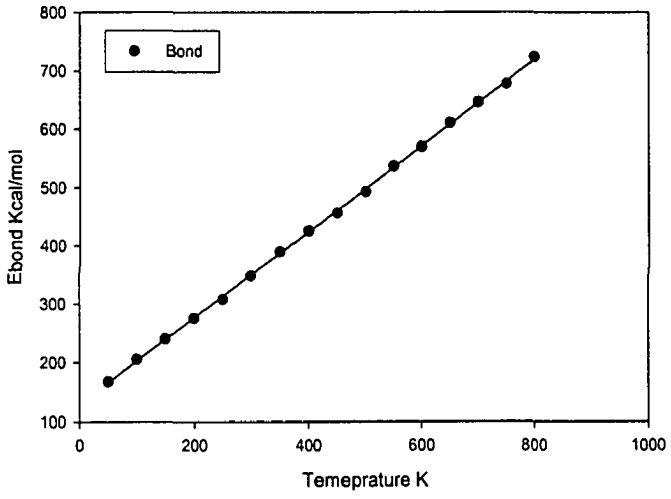

(a)

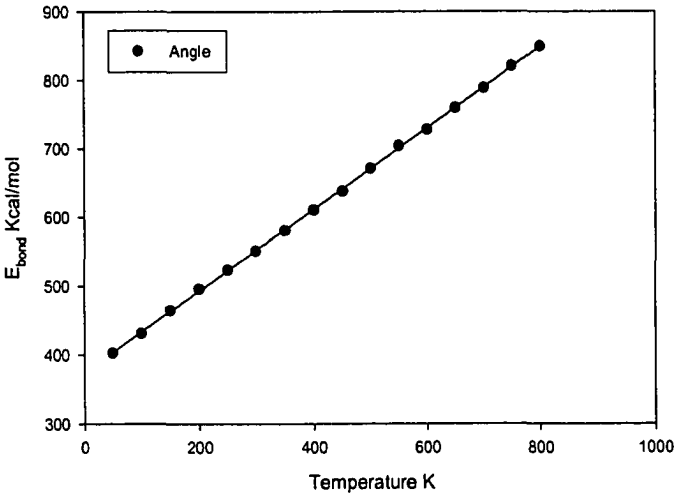

(b)

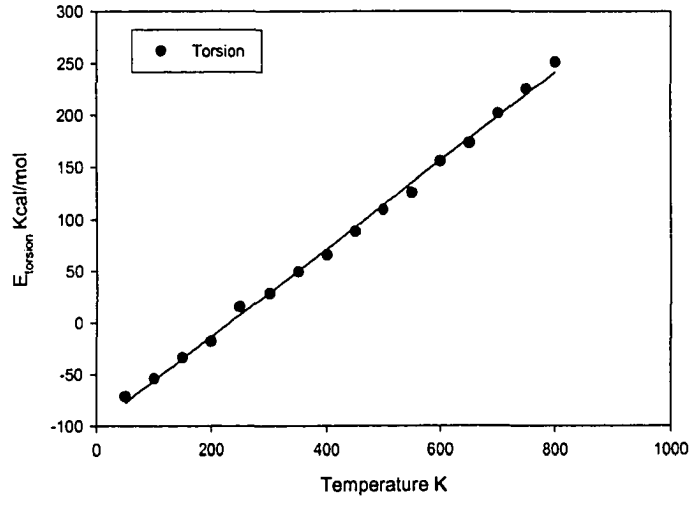

(c)

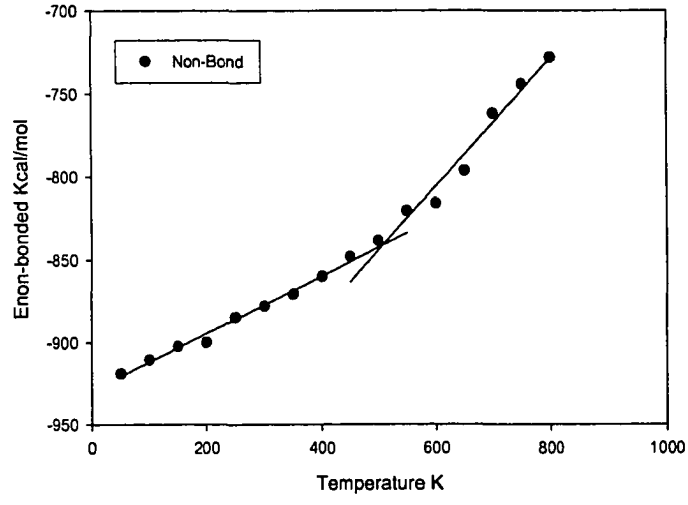

(d)

Figure 7.9: Plots of some energy components versus temperature for PEI (a) bond stretching energy (b) angle bending energy (c) torsion energy (d) non-bonded energy

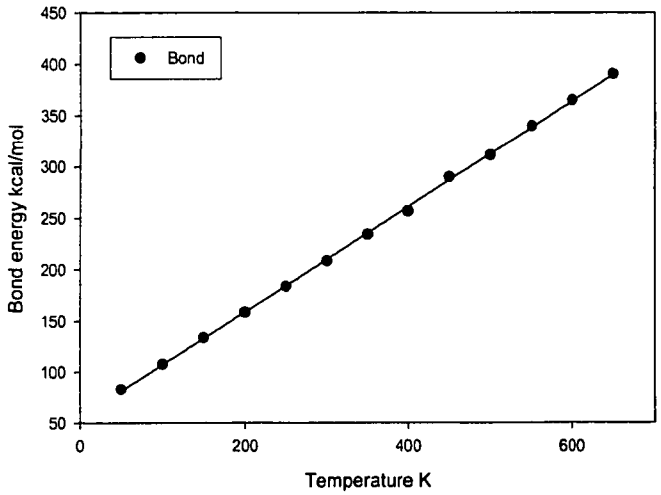

(a)

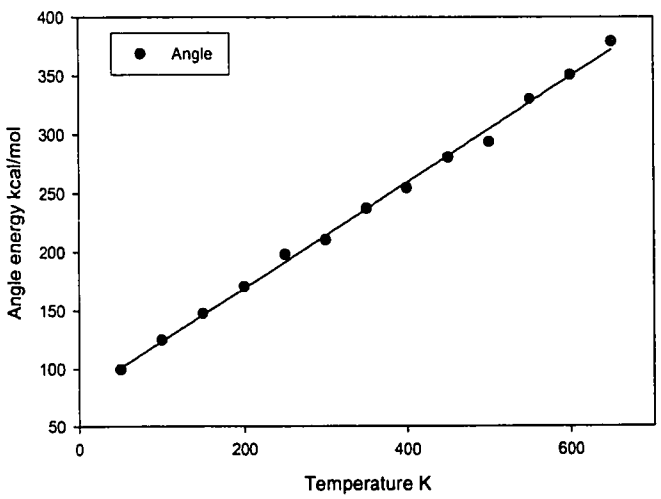

(b)

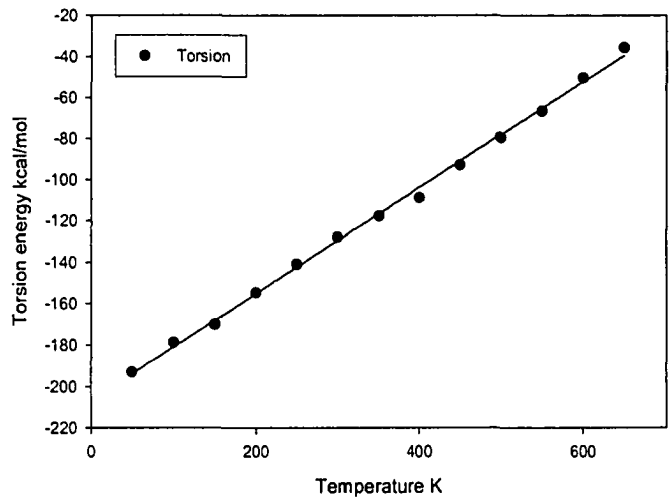

(c)

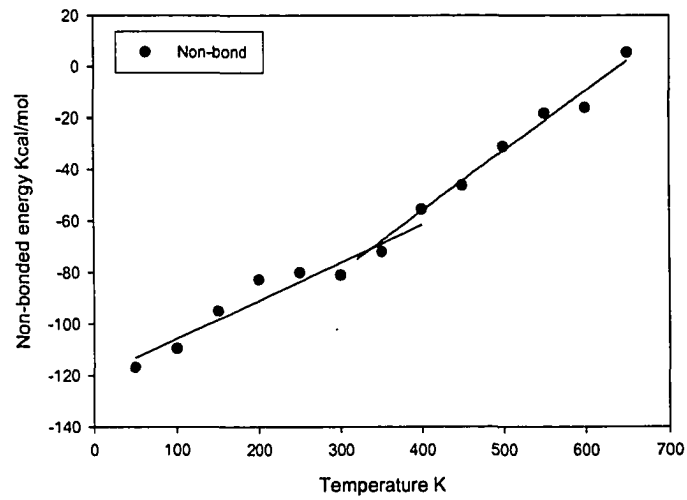

(d)

Figure 7.10: Plots of some energy components versus temperature for PS (a) bond stretching energy (b) angle bending energy (c) torsion energy (d) non-bonded energy

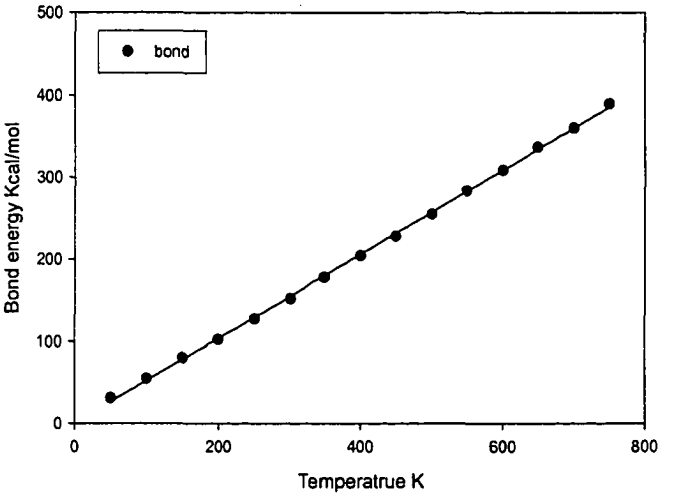

(a)

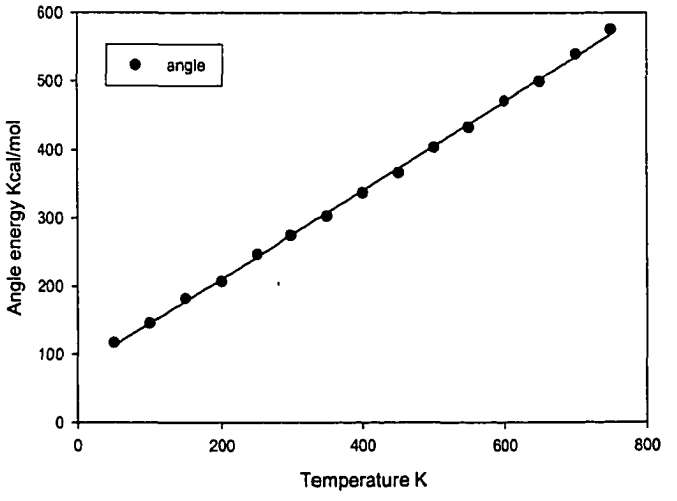

(b)

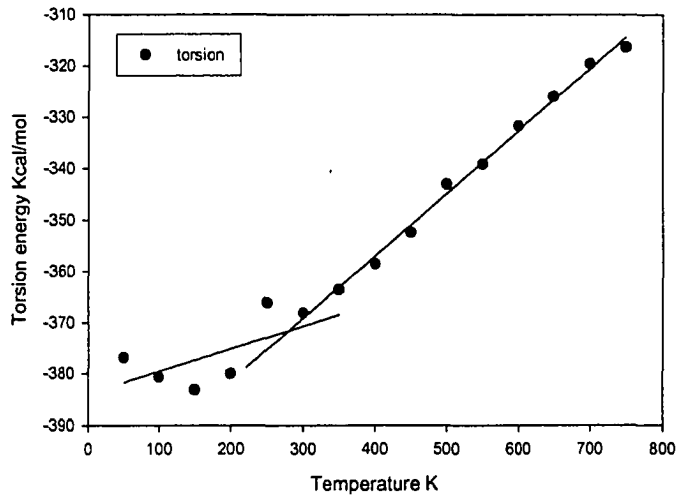

(c)

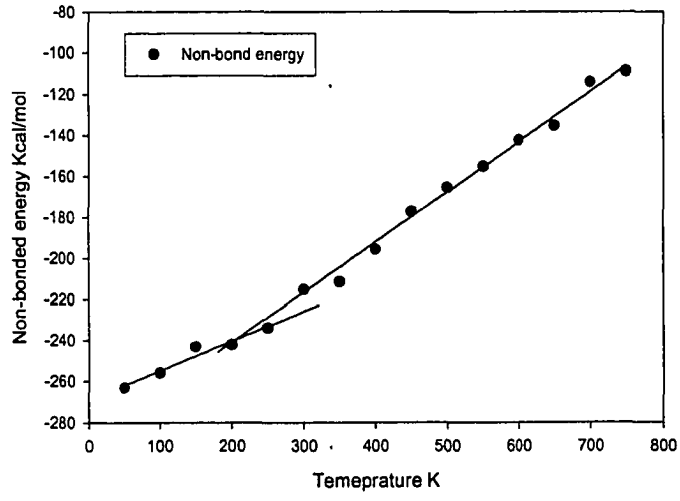

(d)

Figure 7.11: Plots of some energy components versus temperature for aPP (a) bond stretching energy (b) angle bending energy (c) torsion energy (d) non-bonded energy

They attributed the glass transition to the freezing of the torsional degrees of freedom as well as the degrees of freedom of the non-bonded LJ interactions. The glass transition

obtained from the linear fit of non-bonded energy and torsional energy and specific volume is only roughly in agreement with each other (Figure 7.24). Buchholz *et al.* attribute the difference to the difference between the relaxation times of volume fluctuations and energy fluctuations, therefore the process of falling out of equilibrium is felt somewhat differently in these quantities [2002]. Why PC and aPP showed a kink for torsional energy PEI and PS not is still under investigation. We suspect that it is because PEI and PS are more rigid than PC and aPP, it is more easier for the torsional degree of freedom of PEI and PS to reach equilibrium.

7.3.3 Mean square displacement of simulated polymers

Mean square displacement is often used for the determination of the T_g [Yoshioka *et al.* 2003]. The mean-square displacements of all the atoms in the system at different temperatures for our simulated systems are shown in Figures 7.12 to Figure 7.15. In order to remove the trivial temperature dependence, all the curves in Figures 7.12 to 7.15 are normalized to the ratio of T_0/T, where T_0 is some reference temperature [Lyulin, 2002a]. Curves are plotted in a log-log scale in order to display the flat behavior of MSD in the intermediate time region. Since we recorded the trajectory file every 1 ps, the ballistic region that occurred below 1 ps [Sciortino *et al.* 1996; Lyulin *et al.* 2002a] cannot be observed in Figure 7.12 to 7.15. At low temperatures, an intermediate region developed and the MSD remains flat and the plateau continues until the maximum simulation time. It confirms the mode coupling theory that below the T_c, the atoms were trapped in a cage formed by their neighbors before starting to diffuse. In this region, no significant diffusion was observed. The plateau is related to the Debye-Waller factor

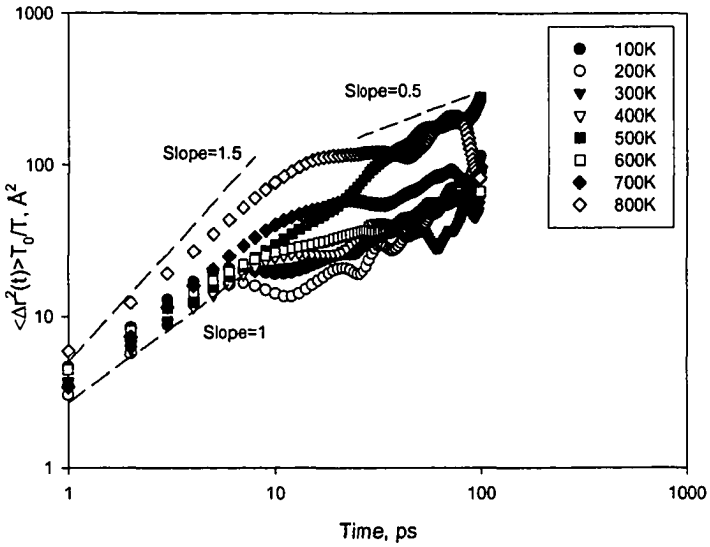

Figure 7.12: Mean square displacements of PC at different temperatures vs. simulation time

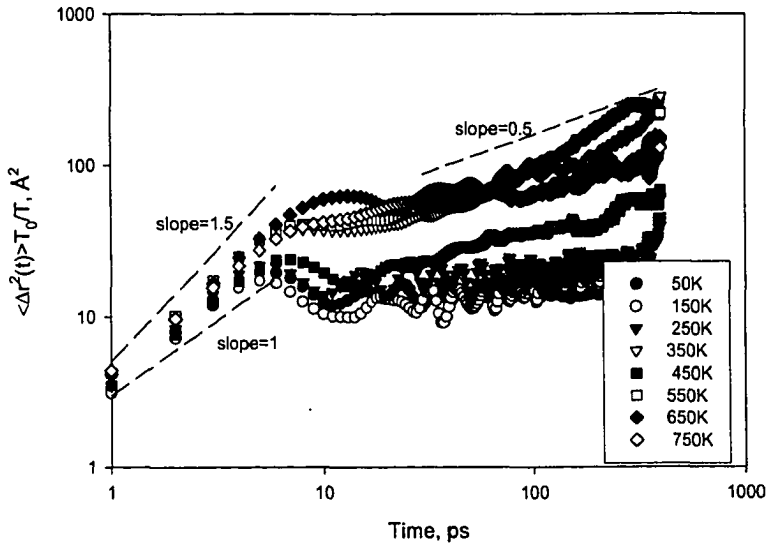

Figure 7.13: Mean square displacements of PEI at different temperatures vs. simulation time

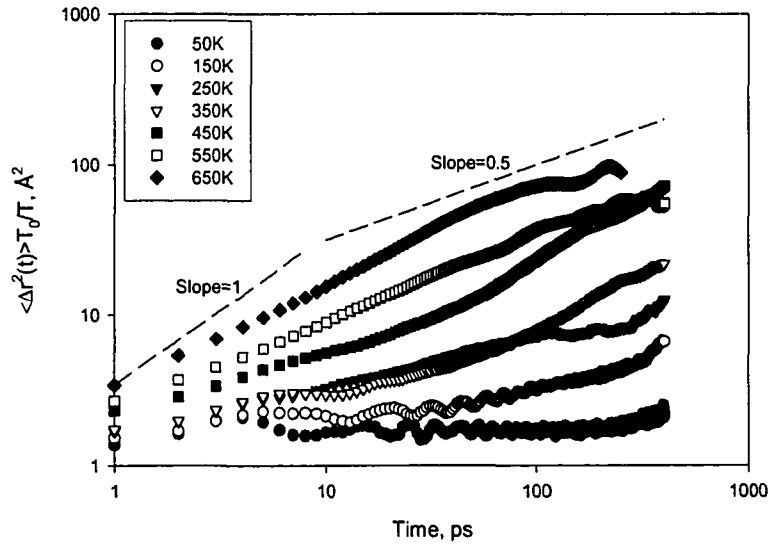

Figure 7.14: Mean square displacements of PS at different temperatures vs. simulation time

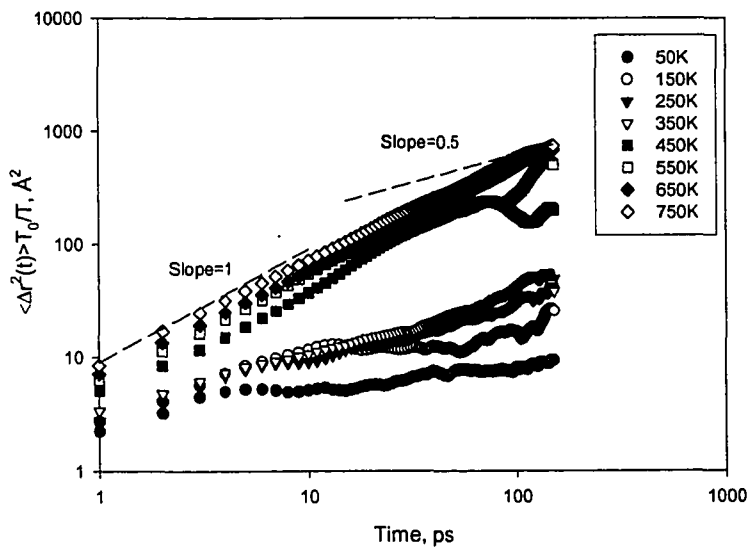

Figure 7.15: Mean square displacements of aPP at different temperatures vs. simulation time

in X-ray and Neutron Scattering. With increasing temperature, the length of plateau decreases. At temperatures above the glass transition, no plateau was observed, the slopes of the MSD with time close to 0.6, which is higher than the value 0.5 predicted from Rouse model [Rubinsten and Colby 2003], the difference can be attributed to the short length used in the simulation [Lyulin *et al.* 2002a].

7.3.4 Radial distribution function (RDF)

Although the simulation time we used was not sufficient for the model molecules to move towards conformations that would yield correct specific volume values, it should be sufficient for various local segments of the molecules (e.g., in the length scale of 5 Å or less) to equilibrate. In addition, since the conformation of local segments is largely controlled by the short-range intra- and inter-molecular interactions rather than local free volume, use of local specific volume may yield a more precise estimation of T_g. The local specific volume can be obtained by multiplying the bulk specific volume by the inverse of the radial distribution function *g(r)* [McQuarrie, 1976]. It is well known that *g(r)* can be multiplied by the bulk density ρ, to obtain the local density ρ(r). Therefore, the local specific volume (i.e., 1/ ρ(r)) is equal to 1/(ρ*g(r)*). However, since the bulk specific volumes in the glassy state computed from the MD simulations are incorrect, use of 1/ρ would reduce the accuracy of such an approach. Therefore, we propose to plot 1/*g(r)*, rather than 1/(ρ*g(r)*), versus temperature to obtain glass transition temperatures.

Radial distribution function is defined as the probability of finding a pair of all kinds of atoms in the system at a distance r apart, relative to the probability expected from completely randomly distribution at the same density. The radial distribution functions of PC, PEI, PS and aPP at various simulation temperatures obtained from the

same NPT MD simulations used to obtain the specific volumes depicted in Figures 7.2 to 7.5 are shown in Figures 7.16 to 7.19. These figures show that the locations of the peaks are insensitive to temperature which simply means that local segmental structures of the molecules are more or less governed by short-ranged interactions. However, the intensity of the peaks increases and their width becomes narrower with decreasing temperature, as expected [Yoshioka *et al.* 2003]. This illustrates that the nearest- and the next-nearest neighbors become more and more well defined as decreasing temperature. The first peak at about 1.11 Å corresponds to the C-H bonds, and the second peak at about 1.39 Å is associated with the C-C bonds of the phenyl rings, and so on. Beyond 4.5 Å, the intensity of $g(r)$ approaches unity indicating that no long-range order exists in the condensed state of the polymers, which confirms the amorphous nature of these simulated polymers. As described previously, we plot $1/g(r)$ against temperature to determine the T_g of the polymers. Here, we only do so for the first two peaks. The temperature dependence of the heights of the short-range peaks of $g(r)$ is essentially equivalent to the Debye-Waller factor phenomenon observed in elastic neutron scattering experiments. It is well documented in the literature that the amplitude of the vibration of hydrogen atoms in a polymer (i.e., the amplitude of the first peak of $g(r)$) reflects the local environment, especially the local free volume of the hydrogen atoms [Ngai 1993; Adachi 1990; Bahar *et al.* 1990]. Since the distribution of the vibrational amplitudes (i.e., the distribution of the local free volumes) can be described by the Van Hove function and the use of such a function is consistent with the use of the Debye-Waller factor for the determination of T_g

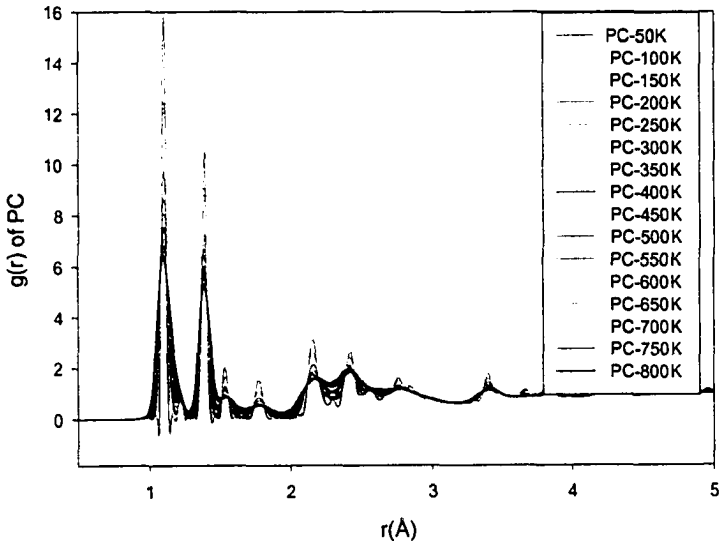

Figure 7.16: Radial distribution functions of PC at various simulation temperatures

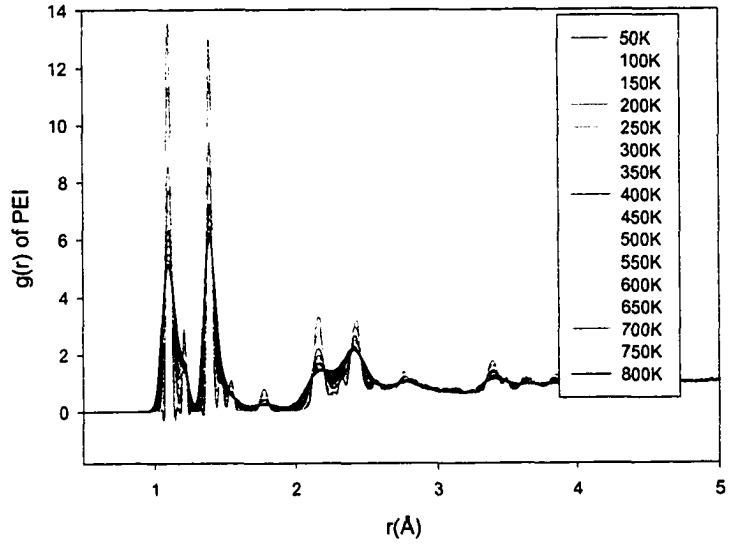

Figure 7.17: Radial distribution functions of PEI at various simulation temperatures

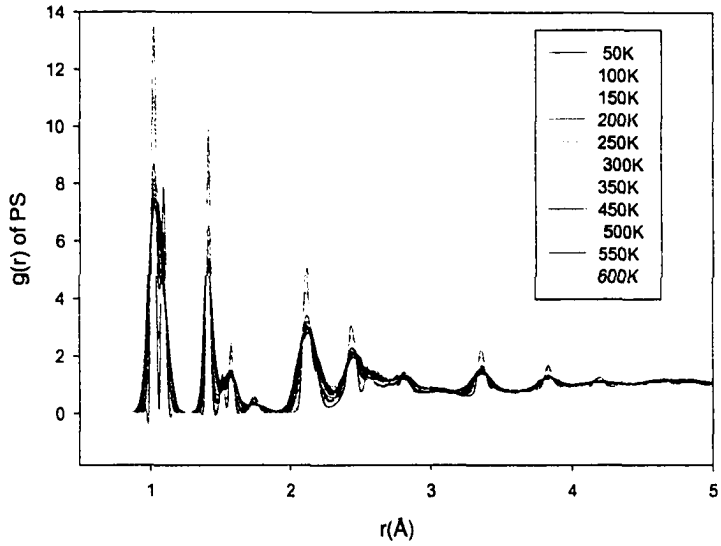

Figure 7.18: Radial distribution functions of PS at various simulation temperatures

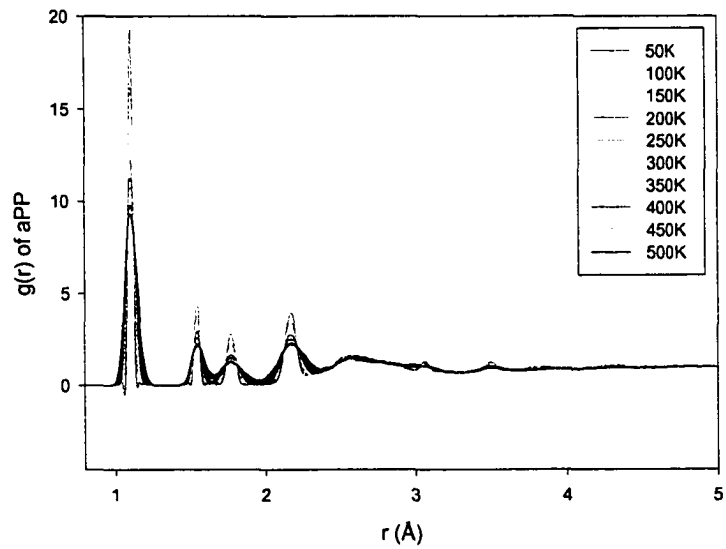

Figure 7.19: Radial distribution functions of aPP at various simulation temperatures

from elastic neutron scattering experiments [Frick and Richter 1995], we feel justified in using heights of the short-ranged peaks of *g(r)* to obtain T_g.

The reason why such an approach works is attributed to the fact that high frequency motions, even at low temperatures, possess short relaxation times. As a result, the computed local free volumes (i.e., amplitudes of the short-ranged *g(r)* peaks) are more accurate than the specific volume of the whole system. The curves were fitted by two straight lines using the least squares fitting procedure. Data well above and below the experimentally determined glass transition temperature were used to produce high and low temperature fits. For polycarbonate (Figure 7.20), the glass transition temperatures obtained from the first peak and second peak are 428 and 425 K, respectively (experimental T_g from PVT measurements is 413 K). When we average results from the first two peaks, the glass transition temperature predicted is 426K. The results are similar to the original V-T method. It should be noted that for PC, the overestimation in the T_g is small for both new method and the more common V-T method. However, in the case of PEI (Figure 7.21), the improvement in the T_g prediction is significant. Compared with the T_g value of 537 K found using the MD V-T method, the newly proposed method yielded a T_g value of 502K (averaged over first 2 peaks) that is much closer to the experimental value of 480 K. The glass transition temperatures predicted from the first and second peaks of radial distribution function are 373 K and 368 K, respectively of PS, as shown in Figure 7.22. The prediction is greatly improved compared with specific volume-temperature methods, which predict the T_g of PS to be 396 K. Since the second peak in radial distribution function of aPP is relatively small compared with the first peak, only first peaks at different temperatures were used to obtain the glass transition

temperature of aPP. The results are shown in Figure 7.23. The glass transition predicted from this method was 258 K, compared with experimentally determined value of 255K. The glass transition temperatures predicted

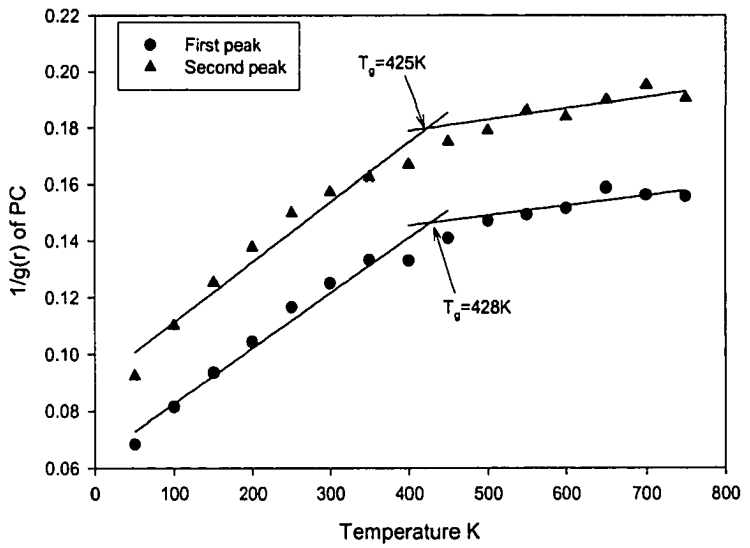

Figure 7.20: Temperature dependence of the inverse of radial distribution function, *g(r)*, of PC

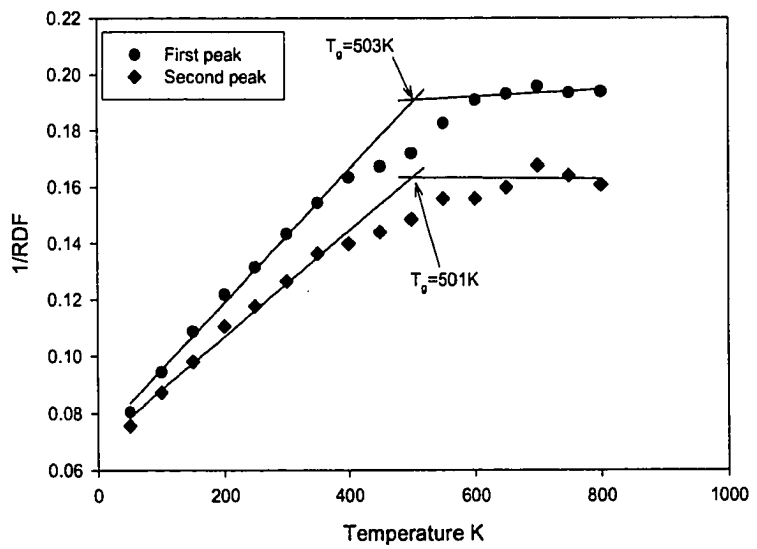

Figure 7.21: Temperature dependence of the inverse of radial distribution function, *g(r)*, of PEI

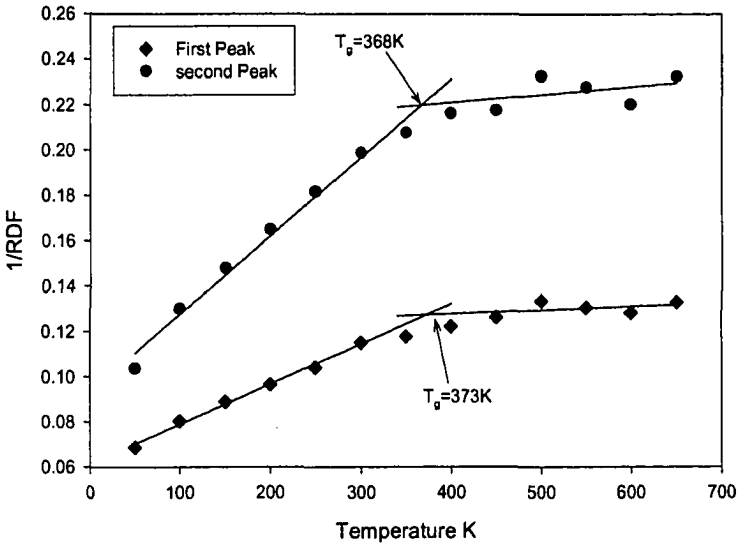

Figure 7.22: Temperature dependence of the inverse of radial distribution function, *g(r)*, of PS

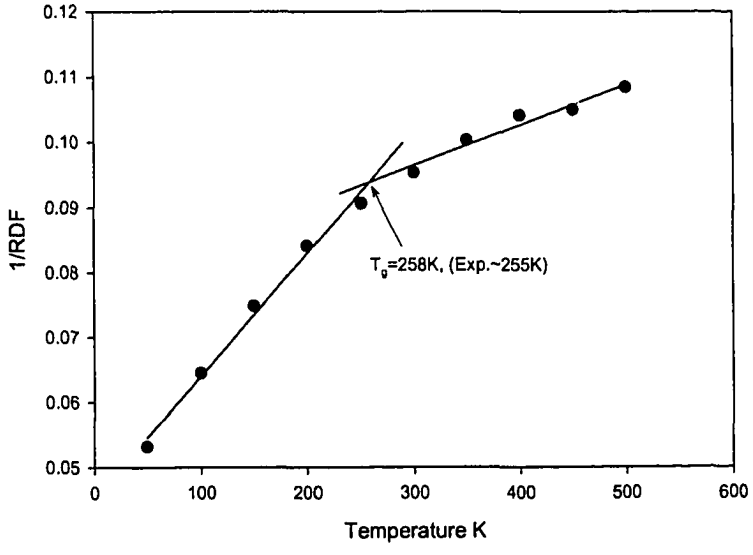

Figure 7.23: Temperature dependence of the inverse of radial distribution function, *g(r)*, of aPP

from specific volume-temperature method, radial distribution method, torsional energy versus temperature and non-bonded energy versus temperature are compared in Figure 7.24, which shows that the radial distribution method gives the best prediction than the other methods. It should be pointed out that the radial distribution function of polymers is not sensitive the molecular weight of the simulated polymers, the simulation of short chains appear to be able to capture the total radial distribution functions of polymers with high molecular weights [Pant *et al.* 1993].

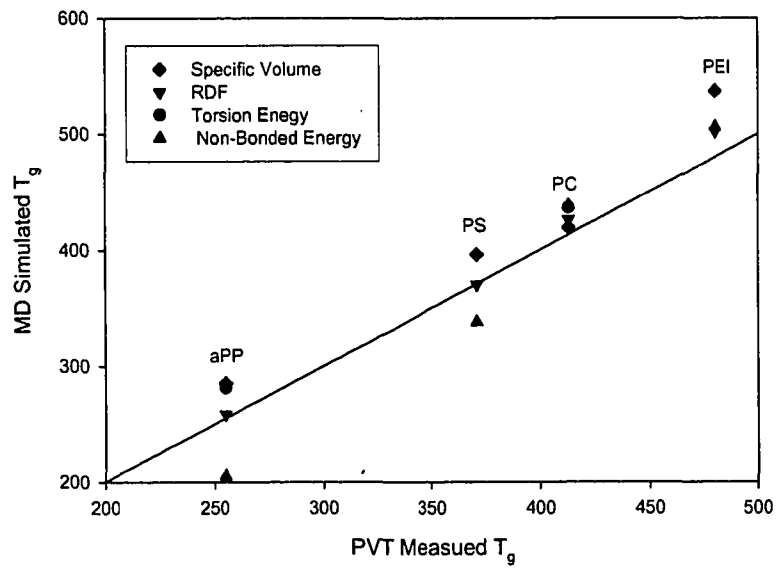

Figure 7.24: T_g comparison obtained from different methods

7.3.5 Reduced RDF of polymers

The glass transition of polymers is a fairly universal phenomenon and polymers with rather disparate chemical structures show qualitatively very similar behavior, which led us to plot the reduced peak intensity of the first peak of the radial distribution function against the temperature normalized by their experimentally determined glass transition temperature. Because the intensity of the first peak of the radial distribution function approaches a constant value at higher temperatures, the reduced intensity of radial distribution function is defined as the intensity at different temperatures divided by the intensity at the reference temperature. In Figure 7.25, we show the reduced intensity of the first peak of radial distribution function as a function of the normalized temperature. The scaled data for these polymers shows a remarkable collapse to a single reduced curve. This curve can be described by the following function:

$$\tilde{g}(T) = 0.9824 + 1.6696e^{(-2.5138\frac{T}{T_g})} \qquad (7.1)$$

where T and T_g expressed in K. This provides us another way to predict the glass transition temperature of a polymer as along as we know its chemical structure, therefore its radial distribution function at different temperatures. The radial distribution function of a polymer at different temperatures can be obtained either from molecular dynamics simulation or from the neutron scattering experiments. In the neutron scattering experiments, the scattering function S(Q, w) can be linked to the radial distribution function by Fourier transformation using the so-called Van Hove function [Richter 2000; Frick and Richter 1995]. The prediction of glass transition temperature of polymer based on the simulated radial distribution function is also practically and scientifically

significant. Practically speaking it will help the design of polymers with the desired glass transition temperature; scientifically, this method will provide a molecular level understanding of the glass transition phenomenon. This method is still under investigation to test its validity for other polymers.

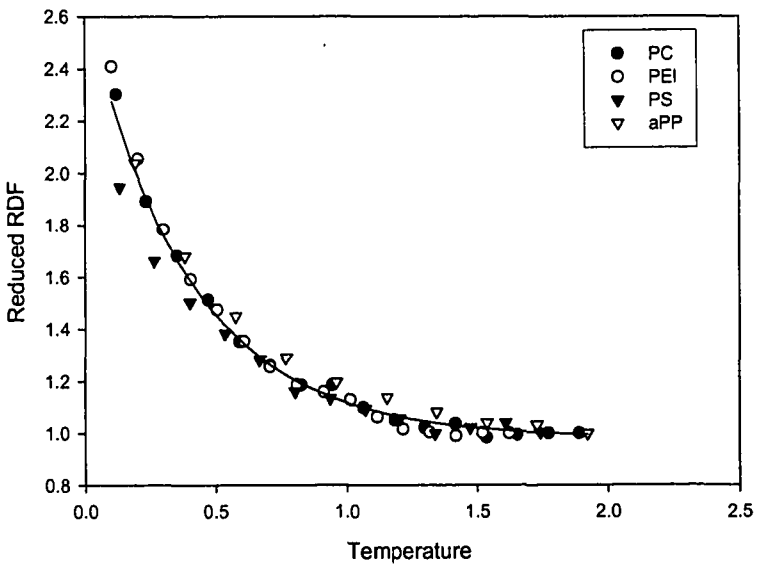

Figure 7.25: Reduced RDF versus reduced temperature

7.4 Summary

NPT MD simulations using the COMPASS force field were carried out for full atomistic models of polycarbonate, poly (ether imide), polystyrene and atactic polypropylene to determine their glass transition temperatures. In this study, two methods were used to predict the glass transition temperature based on the MD simulation results. The first one was the specific volume-temperature method, which is the most commonly used method in the literature. Our simulation results showed that computed specific volumes of aforementioned polymers above their experimental glass transition temperatures agreed very well with those from PVT measurements, indicating that the force field and the equilibration time used in the simulations were adequate for the polymers of interest. However, the computed specific volumes at low temperatures deviated significantly from the experimental values. Such overestimations in specific volumes led to predicted T_g's higher than the corresponding experimental values. We developed a new method based on the radial distribution function to predict the glass transition temperature. Compared with the specific volume-temperature method, the prediction greatly improved. The new method yields T_g's that agree more closely with experimental values, especially when conformations used in the low temperature MD simulations deviate significantly from those of the real materials. This is because the local specific volume determined from the radial distribution function is well equilibrated during the simulation. A master curve was found to relate the reduced temperature and the reduced intensity of the first peak of the radial distribution function. Energy analysis showed that different energy component responsible for glass transition for different polymers. For PC and aPP, both non-bonded energy and torsional energy showed a kink

around the glass transition temperature; while for PEI and PS, only non-bonded energy was found to be responsible for the glass transition.

7.5 References

Adachi, K. (1990) A molecular-model for Cooperative Local Motions in Amorphous Polymers, *Macromolecules*, 23(6): 1816-1821.

Anderson, H.C. (1980) Molecular Dynamics Simulations at Constant Pressure and/or Temperature, *J. Chem. Phys.*, 72(4): 2384-2393.

Angell, C.A. (1997) Entropy and Fragility in Supercooling Liquids, *J. Res. Natl. Inst. Stand. Tech.*, 102(2):171-185.

Bahar, I.; Erman, B.and Monnerie, L. (1990) Effect of Surrounding Medium on Intramolecular Conformational-Changes in Probe Molecules, *Macromolecules*, 23(16): 3805-3811.

Bengtzelius, U. (1986) Dynamics of A Lennard-Jones System Close to the Glass-Transition, *Phys. Rev. A*, 34(6): 5059-5069.

Bennemann, C.; Donati, C.; Baschagel, J. and Glotzer, S.C. (1999) Growing Range of Correlated Motion in a Polymer Melt on Cooling Towards the Glass Transition, *Nature*, 399, 246-249.

Bennemann, C.; Baschnagel, J. and Paul, W. (1999) Molecular Dynamics Simulation of a Glassy Polymer Melt: Incoherent Scattering Function, *Euro. Phys. J. B*, 10(2):323-334.

Binder, K.; Baschnagel, J. and Paul, W. (2003) Glass Transition of Polymer Melts: Test of Theoretical Concepts by Computer Simulation, *Prog. Polym. Sci.* 28(1):115-172.

Binder, K.; Baschnagel, J. and Paul, W. (2002) *In Bridging the Time Scales: Molecular Simulations of the Next Decade*; Nielaba, P; Mareschal, M. and Ciccotti, G., Eds; Springer: New York, 199-228.

Boyd, R.H. (1996) Glass Transition temperatures from Molecular Dynamics Simulations, *Trends in Poly. Sci.* 4(1): 12-17.

Buchholz, J.; Paul, W.P.; Varnik, F. and Binder, K. (2002) Cooling Rate Dependence of the Glass Transition Temperature of Polymer Melts: Molecular Dynamics Study, *J. Chem. Phys.*, 117(15): 7364-7372.

Colucci, D.M.; McKenna, G.B., Filliben, J.J.; Lee, A.; Curliss, D.B.; Bowman, K.B. and Russell, J.D. (1997) Isochoric and Isobaric Glass Transitions: Similarities and Differences, *J. Poly. Sci.: Poly. Phys.*, 35(10): 1561-1573.

Deazle, A.S.; Hamerton, I.; Heald, C.R. and Howlin, B.J. (1996) Molecular Modeling of High Performance Polymers, *Poly. Int.*, 41(2): 151-157.

Fan, C.F.; Cagin, T.; Shi, W. and Smith, K.A. (1997) Local Chain Dynamics of a Model Polycarbonate Near Glass Transition Temperature: A molecular Dynamics Simulation, *Macromol. Theory Simul.* 6(1): 83-102.

Fox, T.G. and Flory, P.J. (1950) 2nd –order Transition Temperatures and Related Properties of Polystyrene. 1. Influence of Molecular Weight, *J. Appl. Phys.*, 21(6): 581-591.

Frick, B. and Richter, D. (1995) The Microscopic Basis of the Glass Transition in Polymers from Neutron Scattering Studies, *Science*, 267: 1939-1945.

Fried, J.R. and Ren, P. (1999) Molecular Simulation of the Glass Transition of Polyphosphazenes, *Comp. Theo. Poly. Sci.*, 9: 111-116.

Fried, J.R. and Li, B. (2001) Atomic Simulation of the Glass Transition of Di-substituted Polysilanes, *Comp. Theo. Poly. Sci.* 11: 273-281.

Gibbs, J.H. and Dimarzio, E.A. (1958) Nature of the Glass Transition and the Glassy State, *J. Chem. Phys.*, 28(3):373-383.

Gotze, W. and Sjogren, L. (1992) Relaxation Processes in Supercooled Liquids, *Rep. Prog. Phys.*, 55(3): 241-376.

Han, J.; Gee, R.H. and Boyd, R.H. (1994) Glass Transition Temperatures of Polymers from Molecular Dynamics Simulations, *Macromolecules*, 27(26): 7781-7784.

Haward, R.N. (1973) *The Physics of Glassy Polymers*, Wiley, New York.

Jackle, J. (1986) Models of the Glass Transition, *Rep. Prog. Phys.* 49(2): 171-231.

Kaufman, H.S. and Falcetta, J.J. (1977) *Introduction to Polymer Science and Technology: An SPE Textbook*, Wiley, New York.

Kilburn, D.; Bamford, D.; Dlubek, G.; Pionteck, J. and Alam, M.A. (2003) The Size and Number of Local Free Volumes in Polypropylenes: A Positron Lifetime and PVT Study, *J. Poly. Sci.: B: Poly. Phys.* 41:3089-3093.

Leutheusser, E. (1984) Dynamical Model of the Liquid-Glass Transition, *Phys. Rev. A*, 29(5): 2765-2773.

Lobe, B. and Baschnagel, J. (1994) Monte Carlo Simulation of the Glass Transition in Two and Three-Dimensional Polymer Melts: Influence of the Spatial Dimension, *J. Chem. Phys.* 101(20: 1616-1624.

Lyulin, A.V.and Michels, M.A.J. (2002a) Large-scale Computer Simulation of Local Segmental Dynamics in Amorphous Atactic Polystyrene, *Comp. Phys. Comm.* 147(1-2): 298-302.

Lyulin, A.V.and Michels, M.A.J. (2002b) Molecular Dynamics Simulation of Bulk Atactic Polystyrene in the Vicinity of T_g, *Macromolecules*, 35(4):1463-1472.

Lyulin, A.V.; Balabaev, N.K. and Michels, M.A.J. (2002c) Correlated Segmental Dynamics in Amorphous Atactic Polystyrene: A Molecular Dynamics Simulation Study, *Macromolecules*, 35(25): 9595-9604.

Lyulin, A.V.; Balabaev, N.K. and Michels, M.A.J. (2003) Molecular-weight and Cooling Rate Dependence of Simulated T_g for Amorphous Polystyrene, *Macromolecules*, 36(22): 8574-8575.

McQuarrie, D.A. (1976) *Statistical Mechanics*, Harper & Row, New York.

Ngai, K.L. (1993) Comparisons Between Coupling Model and Molecular Dynamics Simulation for Local Chain Motions in Bulk Amorphous Polymers, *J. Chem. Phys.*, 98(9): 7588-7592.

Nose, S. (1984) A United Formulation of the Constant Temperature Molecular Dynamics Methods, *J. Chem. Phys.* 81 (1): 511-519

Pant, P.V.K.; Han, J.; Smith, G.D. and Boyd, R.H. (1993) A Molecular-Dynamics Simulation of Polyethylene, *J. Chem. Phys.* 99(1): 597-604.

Pezzin, G.; Ziliogra, F. and Sanmarti, P. (1970) Dependence of Glass Transition Temperature on Molecular Weight for Polyvinylchloride, *Eur. Polym. J.*, 6(7): 1053-1061.

Pozuelo, J. and Baselga, J. (2002) Glass Transition Temperature of Low Molecular Weight Poly(3-aminopropyl methyl siloxane): A Molecular Dynamics Study, *Polymer*, 43(22): 6049-6055.

Richter, D. (2000) Neutron Scattering in Polymer Physics, *Physica B*, 276-278: 22-29.

Rigby, D. and Roe, R.J. (1987) Molecular Dynamics Simulation of Polymer Liquid and Glass, 1. Glass Transition, *J. Chem. Phys.*, 87:7285-7292.

Robertson, R.E. (1992) In: *Computational Modeling of Polymers*, Bicerano, J. Eds.; Marcel Dekker: New York, 297-361.

Roe, R.J. (1994) Short-time Dynamics of Polymer Liquid and Glass Studied by Molecular-Dynamics Simulation, *J. Chem. Phys.*, 100(2): 1610-1619.

Rubinstein, M. and Colby, R.H. (2003*) Polymer Physics*, Oxford University Press, New York.

Santen, L. and Krauth, W. (2000) Absence of Thermodynamic Phase Transition in a Model Glass Former, *Nature*, 405(6786): 550-551.

Sciortino, F.; Gallo, P.; Tartaglia, P. and Chen, S.H. (1996) Supercooled Water and the Kinetics Glass Transition, *Phys. Rev. E*, 54(6): 6331-6343.

Siegmann, A. and Geil, R.H. (1970) Crystallization of Polycarbonate from Glassy State, 1. Thin Films Cast from Solution, J. Macro. Sci. B: Phys., 4(2) 239-272.

Soldera, A. (1998) Comparison Between the Glass Transition Temperatures of the Two PMMA Tacticities: A Molecular Dynamics Simulation Point of View, *Macromol. Symp.*, 133: 21-32.

Vollmayr, K.; Kob, K. and Binder, K. (1996) Cooling–rate Effects in Amorphous Silica: A Computer Simulation Study, *Phys. Rev. B*, 54(22): 16808-15827.

Wolfgardt, M.; Baschnagel, J.; Paul, W. and Binder, K. (1996) Entropy of Glassy Polymer Melts: Comparison between Gibbs-DiMarzio Theory and Simulation, *Phys. Rev. E*, 54(2): 1535-1543.

Yang, L.; Srolovitz, D.J. and Yee, A.F. (1999) Molecular Dynamics Study of isobaric and Isochoric Glass Transition in a Model Amorphous Polymer, *J. Chem. Phys.*, 110(14): 7058-7069.

Yip, S.; Sylvester, M.F. and Argon, A.S. (2000) Atomic Investigation of Segmental Mobility in Atactic Poly(propylene), *Comp. Theo. Poly. Sci.*, 10: 235-247.

Yoshioka, S.; Aso, Y. and Kojima, S. (2003) Prediction of Glass Transition Temperature of Freeze-Dried Formulations by Molecular Dynamics Simulation, *Pharmaceutical Res.* 20(6): 873-878.

Yu, K.Q.; Li, Z.S. and Sun, J.Z. (2001) Polymer Structures and Glass Transition: A Molecular Dynamics Simulation Study, *Macromol. Theo. Simul.* 10: 624-633.

Zhang, M.Z.; Choi, P. and Sundararaj, U. (2003) Molecular Dynamics and Thermal Analysis Study of Anomalous Thermodynamic Behavior of Poly(ether imide)/Polycarbonate Blends, *Polymer*, 44(6): 1979-1986.

Zoller, P. and Walsh, D. (1995) *Standard Pressure-Volume-Temperature Data for Polymers*, Tech. Pub. Co., Lancaster

Chapter 8

Conclusions and Future work

8.1 Miscibility of polymer blends

Although molecular dynamics simulation has been used for the study of polymer blends for more than two decades, this work represents the first attempt to use this method for the study of polymer-polymer miscibility of the engineering thermoplastics blends containing polymers with complex structures. In particular, the method was applied to three different engineering polymer blend pairs: PEI/PC blend, PEI/PBT blend and PC/PBT blend.

For the PEI/PC blend, both thermal analysis and TEM results showed that it is immiscible at all the studied concentrations; however, DSC measurements showed that there is some compatible of PC in the PEI rich phase at high PEI concentrations. TEM results also showed that the dispersed phase size is almost constant below 70 wt% PEI, and phase inversion occurs at about 50% PEI. The dispersed particle size decreases dramatically at higher PEI concentrations, and the shape of the dispersed phase is more stretched than that in PC rich blends. MD simulation results showed similar concentration dependence of Flory-Huggins interaction parameter to that of the T_g of PEI measurements versus concentration. Energy analysis showed that the variation of Flory-Huggins interaction parameter with concentration was mainly due to intermolecular interactions.

For the PEI/PBT blend, both MD simulation and TEM study have demonstrated that it is completely miscible in the melt state. While annealing the blend at 200 ^{0}C, crystallization of PBT occurred and was observed in the TEM micrograph and confirmed by an emerging melting peak in DSC measurements. Phase separation also occurred during the annealing process. MD simulation results suggested that the intramolecular interactions of the pure polymers were not affected by blending with other polymers. Miscibility between PEI and PBT is mainly due to favourable van der Waals interactions. This is in agreement with speculations of other researchers that miscibility of binary miscible blends containing PEI is due mainly to matched dispersion forces [Hunag and Woo, 2000; Woo and Tseng, 2000].

For the PC/PBT blend, different conclusions about its miscibility have been reported in the literature, and miscibility has been attributed to transesterification that may occur during melt blending. The MD simulation was applied to this blend to clarify whether or not the blend is miscible without transesterification. The calculated enthalpies of mixing and Flory-Huggins interaction parameters at various concentrations suggest that PC/PBT blends are completely immiscible in the melt state when there is no transesterification between the two polymers. Detailed analysis of the MD simulation results indicates that the observed immiscibility is caused by unfavorable intermolecular interactions.

It should be noted that for all the above mentioned three blend pairs, their miscibility ranged from completely miscible to immiscible. The trend for the Flory-Huggins interaction parameters obtained from the simulations are qualitatively in agreement with experimental results. Generally speaking, values of the simulated

interaction parameters are higher than the experimentally determined ones. Several factors can be attributed to such disagreement. First of all, in the original Flory-Huggins theory, the mean field approximation was used; however, in the MD simulation, the local concentrations and chemical details of the polymers were included. This is the main advantage of MD simulation. Secondly, choice of reference volume could affect the absolute value of the Flory-Huggins interaction parameter as such choices are somewhat arbitrary. The same problem arose for interaction parameters obtained from inverse gas chromatography (IGC). As a result, Zhao [2002] introduced a common reference volume to define the size of the lattice. Thirdly, the interaction parameter obtained from the MD simulation corresponds to the interactions of the constituent polymers in the melt state, while the experimentally measured values are in the solid state, the crystallization of one of the components may affect the experimental results. It was found that the accuracy of the force field used also has an effect on the MD simulation results.

Despite the fact that there is discrepancy between simulation and experimental results, the MD simulation approach provides us with valuable insight into the molecular origin of miscibility in engineering polymer blends.

8.2 Glass transition temperature prediction

NPT MD simulations of four polymers, PC, PEI, PS and aPP at a wide range of temperatures were performed. The predicted glass transition temperatures of these four polymers using the specific volume-temperature plots are in higher compared with the experimentally determined value. A new method based on the radial distribution function to predict the glass transition of polymers has been proposed. In this approach, a plot of the inverse of the peak intensity in the radial distribution function obtained from MD

simulation versus temperature is used to predict the glass transition temperature. The prediction was significantly improved using this method compared with traditionally used specific volume versus temperature method. Our simulation results showed that the specific volume could be accurately predicted at temperatures well above the glass transition temperature when the COMPASS force field was used; while at temperatures below the glass transition region, the simulations overestimated the specific volume. The RDF method works because the simulation time is not enough for the bulk specific volume to reach equilibrium; however, this time is sufficient for the local specific volume, to relax. The local specific volume is characterized by the RDF, By normalizing both the intensity of the first peak of the RDF function and temperature, we found that reduced RDF versus reduced temperature falls on a master curve. The energy analysis indicated that for PC and aPP, the torsional energy and non-bonded energy were responsible for the glass transition, while only non-bonded energy was responsible for the glass transition of PEI and PS.

8.3 Recommendations for future work

As mentioned, although PEI and PC blends are more compatible in the PEI rich phase, TEM results showed that they are still immiscible at all concentrations. Our simulation and experimental results have shown that PEI/PBT blends are completely miscible in the melt state. In order to increase miscibility between PC and PEI as well as the mechanical properties their blends, di-block PC/PBT copolymer or random copolymer created from transesterification during melt blending can be added to the PEI/PC blends to increase miscibility between PC and PEI. By doing so, a PC/PBT copolymer needs to be synthesized. Our previous experimental results showed that the

amount of copolymer formed in the melt blending of PC/PBT blends is too small to be detected. Therefore, catalyst is needed to form PC/PBT copolymers. The characterization of the synthesized copolymer is also needed. After the copolymer is obtained, its effect on the miscibility, and consequently, the mechanical properties of PEI/PC blend need to be investigated.

Computer simulations constitute a powerful tool for studying the effect of copolymers on the miscibility of immiscible polymer blends [Gersappe *et al*, 1994]. Prior to the experimental study of PC/PBT copolymer on the miscibility of PEI/PC blends, simulation should be conducted. A block PC/PBT copolymer or random copolymer model can be easily constructed in the simulation. Their effects on the miscibility and their location and conformation in the mixture can be visualized in the simulation, which will provide guidance for the experimental work. Also, the mechanical properties can be investigated using MD simulation [Theodorou and Suter, 1986a; 1986b] and correlated with their chemical structures.

Our simulation results have showed that the miscibility of PEI/PBT blends was attributed to the favorable van der Waals interactions. Is this the reason for miscibility inother miscible PEI blends, such as PEI/PET, PEI/PTT and PEI/PEEK blends? MD simulation of these blends may give the answer. Knowing the molecular mechanisms of miscible blends can help in the design of future polymer blends.

As shown in this thesis, MD simulation has been successfully applied to predict the melt miscibility of engineering thermoplastics polymer blends, and the simulation results are supported by experimental observations. However, some factors were not explored to the full extent due to the limitation of computational resources. In this study,

the concentration effect on the miscibility has been studied. However, the temperature also has a significance effect on the miscibility of polymer blends. In the literature, the phase diagram is rarely reported for engineering thermoplastics polymer blends because the temperature range at which the polymer is liquid is bounded by the melting temperature or glass transition temperature and the temperature at which significant degradation of the polymer begins, makeing it difficult to study the phase behavior of polymer blend experimentally. MD simulation provides a useful tool to address the phase behavior of engineering thermoplastic polymer blends. In the future, MD simulation can be used to investigate engineering thermoplastic polymer blends at different temperatures and molecular weights to construct a phase diagram. The phase diagram constructed by MD simulation will be of great help to polymer blend processing.

In the previous chapter, the MD simulated radial distribution function method has been successfully used for the prediction of T_g for four polymers, ranging from commodity polymers to engineering thermoplastics. A universal master equation has been developed to describe the temperature dependence of the reduced intensity of radial distribution function. In the future, we need more simulation work on other polymers or neutron scattering experiments of different polymers to validate this method. In the long run, we hope to obtain better understanding of the molecular mechanism of the glass transition phenomenon, and explain the dramatic decrease of the structure relaxation time in the range of glass transition temperature while the structure does not change much in this region. We hope to answer questions like why different energy components are responsible for glass transition in different polymers, and what is the relationship between T_g and chemical structure.

8.4 References

Gersappe, D.; Irvine, D.; Balaza, A.C.; Liu, Y.; Sokolov, J.; Rafailovich, M.; Schwarz, S. and Peiffer, D.G. (1994) The Use of Graft Copolymers to Bind Immiscible Blends, *Science*, 265, 1072-1074.

Huang, B.S and Woo, E.M. (2000) Blends of a Novel High-temperature Poly(oxy-1,4'-diphenyleneoxy-1,4-phenylenecarbonyl-1,4-phenylene) with Poly(ether imide): Structure, Interaction , and Miscibility, *Colloid Polym. Sci.*, 278: 392-398.

Theodorou, D.N. and Suter, U.W. (1986) Atomistic modeling of mechanical properties of polymeric glasses, *Macromolecules*, 19 (1): 139-154.

Theodorou, D.N. and Suter, U.W. (1986) Local-Structure and the Mechanism of Response to Elastic-Deformation in a Glassy Polymer, *Macromolecules*, 19(2): \79-387.

Woo, E.M. and Tseng, Y.C. (2000) Analysis and Charaterization of Unusual Ternary Polymer Miscibility in Poly(ether diphenyl ether ketone), Poly(ether ethr ketone), and Poly(ethr imide), *Macromol. Chem. Phys.* 201(14): 1877-1886.

Zhao, L.Y. (2002) *A Thermodynamic Study of Polyolefin Blends*, Ph.D Thesis, University of Alberta.